INFORMATION TO USERS

The most advanced technology has been used to photograph and reproduce this manuscript from the microfilm master. UMI films the text directly from the original or copy submitted. Thus, some thesis and dissertation copies are in typewriter face, while others may be from any type of computer printer.

The quality of this reproduction is dependent upon the quality of the copy submitted. Broken or indistinct print, colored or poor quality illustrations and photographs, print bleedthrough, substandard margins, and improper alignment can adversely affect reproduction.

In the unlikely event that the author did not send UMI a complete manuscript and there are missing pages, these will be noted. Also, if unauthorized copyright material had to be removed, a note will indicate the deletion.

Oversize materials (e.g., maps, drawings, charts) are reproduced by sectioning the original, beginning at the upper left-hand corner and continuing from left to right in equal sections with small overlaps. Each original is also photographed in one exposure and is included in reduced form at the back of the book. These are also available as one exposure on a standard 35mm slide or as a 17" x 23" black and white photographic print for an additional charge.

Photographs included in the original manuscript have been reproduced xerographically in this copy. Higher quality 6" x 9" black and white photographic prints are available for any photographs or illustrations appearing in this copy for an additional charge. Contact UMI directly to order.

U·M·I

University Microfilms International
A Bell & Howell Information Company
300 North Zeeb Road, Ann Arbor, MI 48106-1346 USA
313/761-4700 800/521-0600

Order Number 9014920

An investigation of active and selective oxygen in vanadium phosphorus oxide catalysts for n-butane conversion to maleic anhydride

Lashier, Mark Edward, Ph.D.

Iowa State University, 1989

U·M·I
300 N. Zeeb Rd.
Ann Arbor, MI 48106

An investigation of active and selective oxygen in vanadium phosphorus oxide catalysts for n-butane conversion to maleic anhydride

by

Mark Edward Lashier

A Dissertation Submitted to the
Graduate Faculty in Partial Fulfillment of the
Requirements for the Degree of
DOCTOR OF PHILOSOPHY

Major: Chemical Engineering

Approved:

Signature was redacted for privacy.

In Charge of Major Work

Signature was redacted for privacy.

For the Major Department

Signature was redacted for privacy.

For the Graduate College

Iowa State University
Ames, Iowa
1989

TABLE OF CONTENTS

GENERAL INTRODUCTION

The functionalization of paraffinic hydrocarbons is a relatively new and exciting area of catalytic research. The ability to transform a relatively cheap, but rather inert, hydrocarbon to one that is a valuable and versatile chemical intermediate is very attractive. Currently, the only industrial process utilizing this type of chemistry is the catalytic selective oxidation of n-butane to maleic anhydride over vanadium phosphorus oxide (VPO) catalysts [1]. Maleic anhydride has a variety of uses, ranging from agricultural chemicals to food additives [2].

The heart of this process is the active and selective vanadium phosphorus oxide catalyst. The literature discusses a wide variety of VPO phases, but it is the general consensus that one phase in particular, vanadyl pyrophosphate, is the most important one. It seems that this particular phase, in one form or another , is involved in a type of Mars and van Krevelen [3] oxidation/reduction catalysis with the V(IV) of the pyrophosphate being oxidized to some form of V(V) [4]. As a result, the vanadyl pyrophosphate and its various oxidized forms, vanadyl phosphates, have been the subject of many investigations. Most of the work has focused on correlating activity and selectivity with various preparation and activation techniques and the resulting crystallochemistry of the various phases. Of particular interest has been catalyst morphology, P/V ratio and oxidation/reduction characteristics. This work is important and has led to better understanding and

improvement of the system, but a more fundamental approach is needed to understand the general phenomenon of paraffin activation and selective oxidation. Centi *et al.*[5] stated it well in a recent review article:

> "The evidence leading to speculations on the catalytic behavior of PVO catalysts based only on the crystal chemistry aspects may not be sufficient for analysis of the complex reaction of butane conversion. A discussion of the selectivity in oxidation reactions of mixed oxides must necessarily include a consideration of the dynamics of the process comprising a three phase system:
>
> **(i)** a gas phase,
>
> **(ii)** a solid phase,
>
> **(iii)** a two-dimensional surface region at the interface.
>
> . . . . A very specific surface structure is needed and it would seem that the binding of intermediates until product is formed is essential to high selectivities."

This dissertation presents research completed with the intention of adding to that base of knowledge described above. Specifically, the third "phase" described above was probed. The work focuses on the role of lattice oxygens in the activation of n-butane, the stabilization of reactive intermediates, the insertion of oxygen to form selective products and the nonselective cracking and combustion processes.

The following sections of this dissertation will present a detailed review of literature concerning this work and research completed in this area.

Literature Review

Mechanistic Aspects of n–Butane Oxidation to Maleic Anhydride Over VPO Catalysts

This subsection will outline the present literature concerning particular aspects of the mechanism of the conversion of n–butane to maleic anhydride over vanadium phosphorus oxide catalysts. Particularly, that work concerning the activation of the paraffin molecule and the subsequent formation of intermediates will be reviewed.

Activation of n–butane Saturated hydrocarbons, such as n–butane, are relatively stable compounds. As a result, they have found little use other than as fuels. Due to the relative abundance of these species, they are an attractive source of "hydrocarbon backbone" or building blocks for other materials. The problem is to activate this relatively inert molecule in such a manner as to avoid combustion. Use of a catalyst system such as VPO can accomplish that. Activation of n–butane can be broken down into two types: C–H bond activation and C–C bond activation. Since C–C bond activation would lead to cracking and nonselective products, most work to date deals with the activation of the C–H bond.

Cavani *et al.* [6] point out that for successful activation of the C–H bond, the catalyst must provide a hydrogen abstraction center and an electron "sponge" to remove the electron involved in the bond. The specific nature of possible sites will be discussed in the "Active Sites" subsection. Therefore, for catalytic activation to occur, the n–butane molecule must be adsorbed on a site with the characteristics described by Cavani, the bond must be activated, and for the activation to be successfully selective, the resulting species must be stabilized.

Pepera *et al.* [4] suggest that the activated species is indeed stabilized at the

site of original contact and no species are desorbed until the final product (maleic anhydride or carbon oxides) is formed. They propose that V (IV) sites are responsible for the chemisorption of oxygen and the activation of n-butane.

Deuterated n-butane experiments by the Pepera group show that the activation of n-butane occurs through the removal of one of four methylene hydrogens. They further postulate that both the selective and nonselective routes are initiated through this mode of activation. Recent work by Gleaves *et al.*, using time resolved pulse techniques, provides evidence for two routes to combustion products, a fast route and a relatively slow route [7] . They conclude that these two routes represent two different modes of activation. It seems that highly active adsorbed oxygen species are responsible for the "fast" route, while the "slow" route could be accounted for by a mechanism such as suggested by Pepera *et al.* [4]. They conclude that since (at least to some extent) butane proceeding both to maleic anhydride and combustion products goes through the same rate determining step (activation), the selectivity of this process is determined after initial C-H bond activation and factors affecting selectivity cannot be determined by studying the kinetics of n-butane consumption alone. The alternate activation route of C-C bond scission was not considered as a route to combustion products; thus, this possibility cannot be ruled out. This work does indicate, though, that the oxygen insertion steps are very important to the selectivity of the process and further investigation is needed in this area.

Centi and Trifiro [1] take the conclusions of Pepera one step further. They claim that the activation of n-butane involves the contemporaneous removal of two of the four methylene hydrogens to form a 2-butene type species stabilized by the catalyst surface. Their conclusion is based on the kinetic study of various C_1-C_7

hydrocarbon oxidations over $(VO)_2P_2O_7$. The rates of reaction of the various hydrocarbons (with various numbers and reactivities of methylene hydrogens or lack of methylene hydrogens) fit well with this assumption. The proposed scheme of interaction is presented in Figure 1. It consists of the concerted removal of two hydrogens at an acid/base site. The rest of the proposed mechanism will be discussed in the "Intermediates" subsection of this review.

Intermediates proposed for n-butane to maleic anhydride While successful activation of the paraffin is a major step towards the selective oxidation of n-butane to maleic anhydride, it is really only the first step of a very complicated process. Several more hydrogens must be removed while three oxygens must be inserted. Several mechanisms have been proposed [8–18] from the fairly simple in Figure 2 to the fairly complex in Figure 3, the most common being

n-butane⟶1-butene⟶1,3-butadiene ⟶furan⟶maleic anhydride [19–23].

Many of these conclusions were based on the comparison of n-butane oxidation and oxidation of the corresponding olefins over VPO catalysts. Thus, no direct evidence confirming the presence of these proposed intermediates was used to confirm this hypothesis.

Recent work by several groups has attempted to confirm or deny the presence of these intermediates. Wenig and Schrader [9, 24, 25] used *in situ* FTIR to study industrial VPO catalyst under actual operating conditions. With n-butane as the reactant, no furan or 1,3-butadiene was observed. Only adsorbed n-butane, maleic anhydride, carbon monoxide, carbon dioxide, water, an adsorbed olefin species and maleic acid were observed. Maleic acid was considered a side product resulting from the reaction of maleic anhydride with water. Their 1-butene and 1,3-butadiene

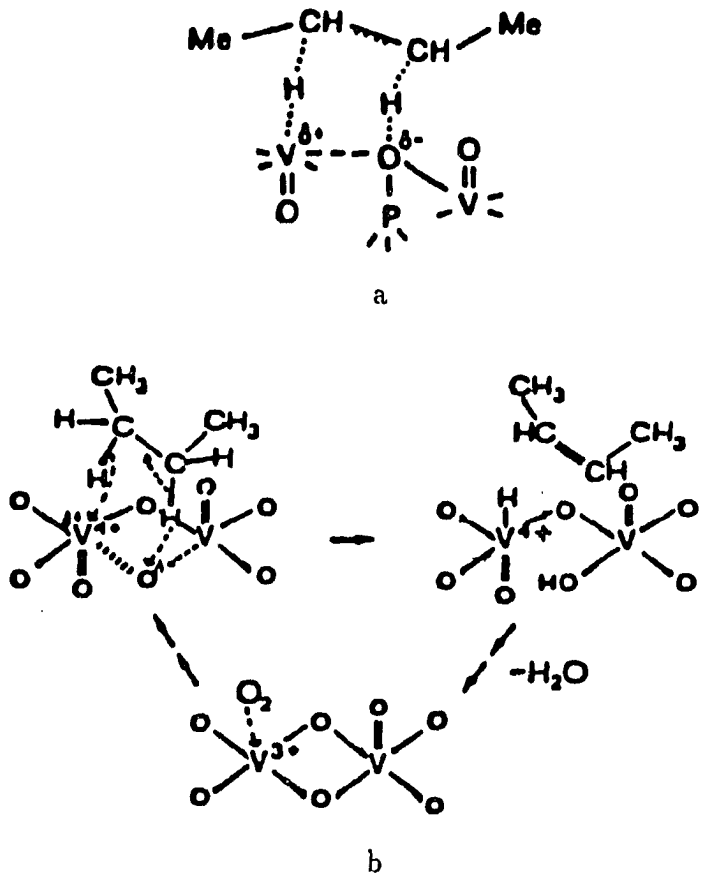

Figure 1: Proposed scheme of concerted mechanism of n-butane activation: (a)n-butane adsorption (b)oxidation/reduction cycle on catalyst surface [1]

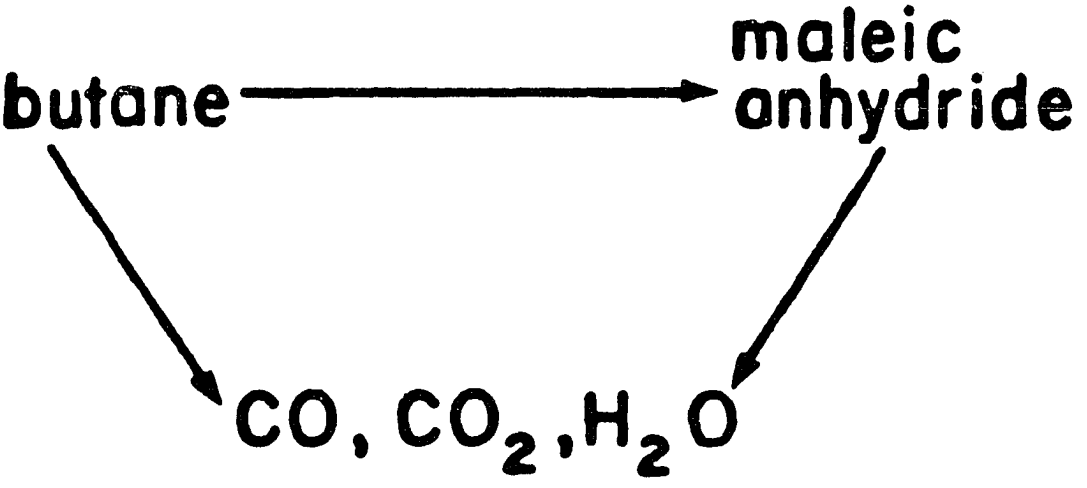

Figure 2: Simple reaction mechanism

studies reveal that 1-butene is converted to 1,3-butadiene which is then converted to maleic anhydride. No furan was observed. Side products formed on the catalyst surface included 2-butene, crotonaldehyde and maleic acid, while some type of conjugated olefin surface species was detected and postulated as an intermediate.

In situ IR work was also done by Puttock and Rochester [27] on vanadyl pyrophosphate. On this fairly low surface area (10 m^2/g) catalyst they studied the adsorption of 1-butene, 1,3-butadiene, furan and maleic anhydride. In all cases, they noted the formation of a strongly held carboxylate. They suggested that this was a precursor to combustion products. In contrast to the Wenig observations, they note the formation of furan from 1-butene and 1,3-butadiene on the catalyst surface.

Szakacs *et al.* [28] studied the oxidation of hydrocarbons of various oxidation levels (n-butane, 1-butene, 1,3-butadiene and furan) over α and β $VOPO_4$ in the absence of gas phase oxygen. Their results indicate that the products formed change as the oxygen level in the catalyst is depleted. Initially, n-butane forms only maleic anhydride and carbon oxides, but as less oxygen is available, butadiene and furan are formed. The results for 1-butene, 1,3-butadiene and furan show similar trends.

Kruchinin *et al.* [29] studied the oxidation of n-butane over a VPO catalyst containing cobalt oxide in a closed system, recirculating reactor. Based on comparison of results of carbon oxide formation when maleic anhydride was allowed to recirculate and when maleic anhydride was "frozen" out in a trap, they conclude that selective and nonselective oxidation occur by different paths. At the very least, this proves that once maleic anhydride leaves the surface it is not likely to be combusted; yet prior that initial desorption, this work can make no conclusions.

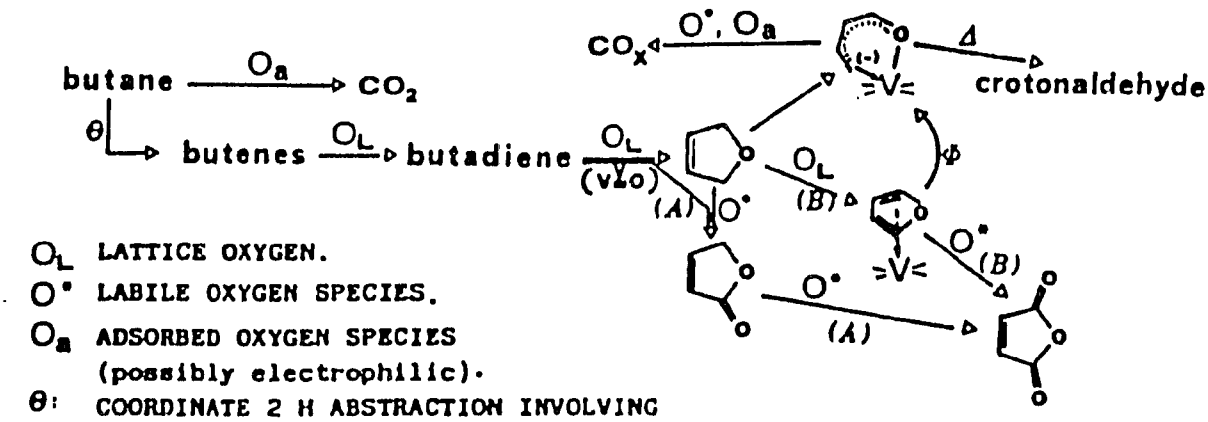

Figure 3: Complex reaction mechanism [29]

In more recent work, Centi and Trifiro [1] propose the fairly detailed mechanism presented below.

n-butane→ [1-butene→1,3-butadiene →dihydrofuran→furan] →maleic anhydride

This is the result of the contemporaneous removal of two hydrogens in the activation step, as discussed in the "Activation" sub-subsection. It is pointed out that, based on kinetics, it is highly unlikely that these intermediates will be detected in any appreciable quantities, as they are consumed immediately. They also report the formation of phthalic anhydride and indicate that it is formed from the same intermediate as maleic anhydride.

To circumvent the problem of nondetectability of intermediates, Gleaves *et al.* have developed a novel technique known as TAP (temporal analysis of products)[7]. Additional species were revealed in addition to the intermediates postulated by Centi and Trifiro [1]. The results of their collaborative work (Centi *et al.* [26]) is presented in Figure 3. Thus, they postulate parallel pathways to maleic anhydride, through either furan or γ-butyrolactone, with the same mode of activation. They also conclude that the furan route is slower than the lactone route, indicating that perhaps different oxygen species are involved in each pathway. They also note a strongly adsorbed species similar to the carboxylate mentioned by Puttock and Rochester [27]. It is desorbed as crotonaldehyde at 773 K and believed to be a precursor to carbon oxides. This topic will be discussed in depth in the "Oxygen Species" subsection.

Active Sites

As discussed in the introduction, the oxidation of n-butane to maleic anhydride is a "structure sensitive" reaction. The activity and selectivity of the

catalyst depends on its history (preparation, reaction atmosphere), morphology, P/V ratio and so on. But from a fundamental viewpoint, structure and morphology alone cannot explain the activity and selectivity of VPO catalysts. One must look at the active sites present at the surface of the catalyst and the role each of these plays in the activation and oxidation of n-butane. Then, the presence or absence and the behavior of these sites in relationship to preparation, morphology, P/V ratio and so forth can be put into context. Thus, this subsection of the literature review deals with research investigating the active surface of VPO catalysts. Particularly, surface acidity and oxygen species will be discussed.

Surface Acid/Base Properties Strictly speaking, the topic of surface acid and base properties should not be separated from the topics of oxygen species and hydroxls; thus, there will be some overlap with ensuing subsections. This part of the review will deal strictly with recent investigations probing acid/base properties of the catalyst.

Busca *et al.* [30] investigated the surface acidity of two $(VO)_2P_2O_7$ catalysts prepared according to different methods by ammonia, pyridine, acetonitrile, carbon monoxide and carbon dioxide adsorption, by ammonia temperature programmed desorption (TPD) and by 2-propanol oxidation. Their results indicate strong Brønsted as well as medium strong Lewis sites exist. TPD of ammonia indicates that three types of acid sites for ammonia adsorption exist: α , a weakly adsorbed species and β and γ, two types of chemisorbed ammonia of increasing acid strength. Both types of catalyst gave similar results when normalized for surface area. The α site was considered a Lewis acid site, while β and γ were considered Brønsted sites.

Puttock and Rochester [31] used *in situ* infrared of adsorbed water and

pyridine to study surface acidity of vanadyl pyrophosphate. They found that the surface of $(VO)_2P_2O_7$ is Brønsted acidic after heat treatment and typical reaction temperatures; thus, Brønsted sites could be involved in the catalysis. Characteristic IR bands for pyridine adsorbed on Lewis acid sites revealed the existence of Lewis sites, while an IR band at 1540 cm^{-1} revealed the presence of Brønsted sites. Puttock and Rochester postulated that the Lewis site was most likely an exposed V(IV) species. They also noted that the Lewis sites could be converted to Brønsted sites by treatment with water vapor.

In a second paper, Puttock and Rochester [27] studied the adsorption of butenes and 1,3-butadiene. They noted that the presence of Brønsted acid sites allowed the isomerization of the butenes and 1,3-butadiene.

Centi and Trifiro [1] postulate that their "contemporaneous" abstraction of two methylene hydrogens occurs at a pair of vanadyl octahedra as shown in Figure 4. Electrophillic attack on a C-H bond results in an acidic C-H which is then attacked by a weakly basic site like V-O-V (or V-O$\backslash_P$-V).

In a further investigation, Centi *et al.* [32] investigated the role of various sites by selectively blocking these sites with potassium, ammonia or sulfur dioxide. It was found that sulfur dioxide poisons maleic anhydride combustion sites, while ammonia and potassium inhibit n-butane activation and oxygen insertion, but not the conversion of 1-butene to 1,3-butadiene. This suggests that Brønsted sites are responsible for the formation and/or stabilization of surface adsorbates and are therefore a key in the mechanism of maleic anhydride synthesis.

Sulfur dioxide was assumed to associate with V(V) sites and thus it was concluded that these sites were responsible for combustion of maleic anhydride. Since maleic anhydride was produced in the presence of sulfur dioxide, it was also

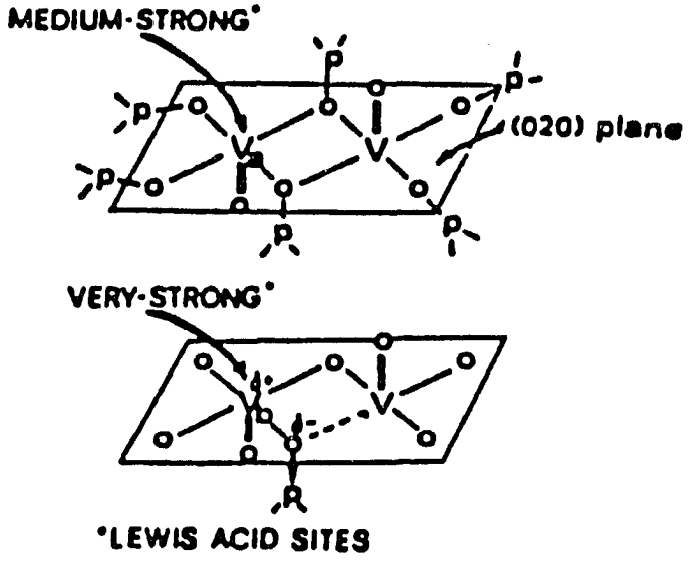

Figure 4: Possible $(VO)_2P_2O_7$ active sites [5]

concluded that the oxidation to maleic anhydride occurs at a different site than carbon dioxide, and therefore by a different mechanism.

Since ammonia and potassium should associate with Brønsted sites, the effect of these species on the catalytic activity and selectivity was attributed to changes in these sites.

Oxygens The obvious role of a selective oxidation catalyst is to oxidize a particular molecule to another form. The function of vanadium-phosphorus-oxide catalysts is to oxidize n-butane by the removal of hydrogens from and the insertion of oxygens onto the four carbon chain. Thus, to completely understand these catalysts, one must understand the types of oxygens involved in the system, what the role of each is and how various factors affect them. The subsection on surface acidity included some references to oxygen species. This subsection is intended to give an overall impression of work done towards identifying and characterizing the active, selective and nonselective oxygen species in the selective oxidation of n-butane to maleic anhydride over VPO catalysts.

Wenig and Schrader [33] found, while studying the characteristics and kinetics of industrial VPO catalysts, that multiple oxidation states of oxygen exist on the surface of these catalysts. The oxygen 1s x-ray photoelectron spectrum exhibited one or more shoulder bands, revealing this variety.

Kruchinin *et al.* [29] demonstrated that crystal lattice oxygens are involved in the production of carbon monoxide, carbon dioxide and maleic anhydride from n-butane over a VPO catalyst. This was accomplished by following the incorporation of ^{18}O from the gas phase into the products in a closed recirculating system. The incorporation was gradual, indicating that oxygen from the lattice was

being incorporated into the products, followed by gas phase oxygen incorporation into the lattice.

Pepera *et al.* [4] made a similar observation, but went on to qualify it further. Based on their results, they concluded that the reaction of n-butane over vanadium phosphorus oxides $(VO)_2P_2O_7$ is a special case of the Mars-van Krevelen [3] type oxidation/reduction catalytic reaction. Classic Mars-van Krevelen reactions involve the bulk oxidation and reduction of the catalyst. In this particular case, the oxidation and reduction is limited to the near surface layers of the catalyst. The work of Pepera *et al.*, involved equilibrating the surface of $(VO)_2P_2O_7$ with ^{18}O and then reacting n-butane over the catalyst. They monitored the incorporation of ^{18}O into carbon dioxide. Based on their observations and the consideration of several models and scenarios, they concluded that surface oxygens are in rapid exchange and that n-butane is irreversibly adsorbed in such a manner that oxygens are shuttled to and hydrogens away from the adsorbed molecule. They present evidence for a strongly adsorbed species that leads to the formation of carbon oxides. It is also important to note that upon treating catalyst which had been equilibrated under oxygen-16 with ^{18}O, no exchange could be detected. Thus, the oxygen species formed seem to be fairly stable, yet mobile on the surface. They did not investigate the incorporation of ^{18}O into either maleic anhydride or water.

Haber and Serwicka [34] discuss the nature of lattice oxygen species and the propensity of these species towards specific reactions. In general they state that catalytic oxidation occurs in one of two ways:

1. electrophillic oxidation proceeding through the activation of molecular oxygen (*i.e.*, O^{2-}, O_2^{2-}, O^- or an electrophillic lattice species) or

2. nucleophillic oxidation in which insertion of a nucleophillic oxygen species into a previously activated organic molecule occurs.

Electrophillic oxygens would tend to attack carbon-carbon bonds and result in nonselective activation and cracking. Conversly, nucleophillic oxygen species would attack carbon-hydrogen bonds, retaining the original hydrocarbon backbone, maintaining the possibility of selective oxidation. In metal-oxygen double bonds, such as Mo=O (and V=O)), the metal tends to withdraw electrons, rendering the site acidic and hence electrophillic. On the other hand, species which allow oxygen to retain a lone pair of electrons, such as Mo-O-Mo, V-O-P or V-O-V are basic and thus nucleophillic. Additionally, the strength of the acidity and basicity depends upon the atoms bound to the oxygens.

Evidence in support of these assertions comes from Haber and Serwicka's experience with MoO_3. In propene selective oxidation over MoO_3, terminal Mo=O are not involved in the reaction and hence are maintained, while bridging Mo-O-Mo oxygens are consumed. They state that it is likely that sites responsible for activation of oxygen to the electrophillic form are themselves quite electrophillic and could also contribute to cracking and combustion. Additionally, they point out that lower valent transition metal cations exposed at the surface of an oxide may function as active centers for supplying electrons for the adsorption of oxygen in the form of molecular or atomic radicals O^{2-} and O^{-}.

In a recent review article, Centi *et al.* [5] state, in reference to n-butane oxidation over $(VO)_2P_2O_7$:

> "It seems probable that different active sites and types of oxygen species are implicated in the polyfunctional behavior of the vanadyl pyrophosphate catalyst."

Indeed, several types of oxygen species can exist at the surface of vanadyl pyrophosphate as shown in Figure 5. Of these, the V–O–P bond is the most abundant [6].

In addition to lattice species, the possibility of highly reactive adsorbed oxygen species exists. Some disagreement exists in the literature concerning the role of each type of oxygen. Several studies [4, 20, 28, 35–38] indicate that lattice oxygen is sufficient for all steps in the oxidation of n–butane to maleic anhydride. On the other hand, recent work by Gleaves *et al.*, suggests that both lattice and surface activated adsorbed oxygen are necessary for the entire conversion to occur [7] . Their unique TAP reactor system, in which small pulses of reactant gas are passed through a catalyst bed held in high vacuum then to a quadrupole mass spectrometer, was used to study this system. They believe that under these conditions, they can detect otherwise undetectable intermediates and provide a time–resolved view of the catalytic process on the order of milliseconds. Based on such experiments feeding various combinations of oxygen, n–butane, 1–butene, 1,3–butadiene and furan, they make several conclusions. Their work suggests that a highly mobile yet irreversibly adsorbed oxygen species is responsible for n–butane activation and the oxidation of furan to maleic anhydride. This strongly adsorbed, yet mobile species is thought to be a V(V)–O type species formed by strong chemisorption of an electrophillic dioxygen molecule.

The TAP experiments indicate that intermediate oxidation steps (1–butene to furan) are accomplished by surface lattice oxygens. These surface lattice oxygens are responsible for allylic oxydehydrogenation and oxygen insertion with ring closure to form furan. Pulse ^{18}O experiments back this argument indicating that furan formed from butene or butadiene utilizes lattice oxygens from the surface

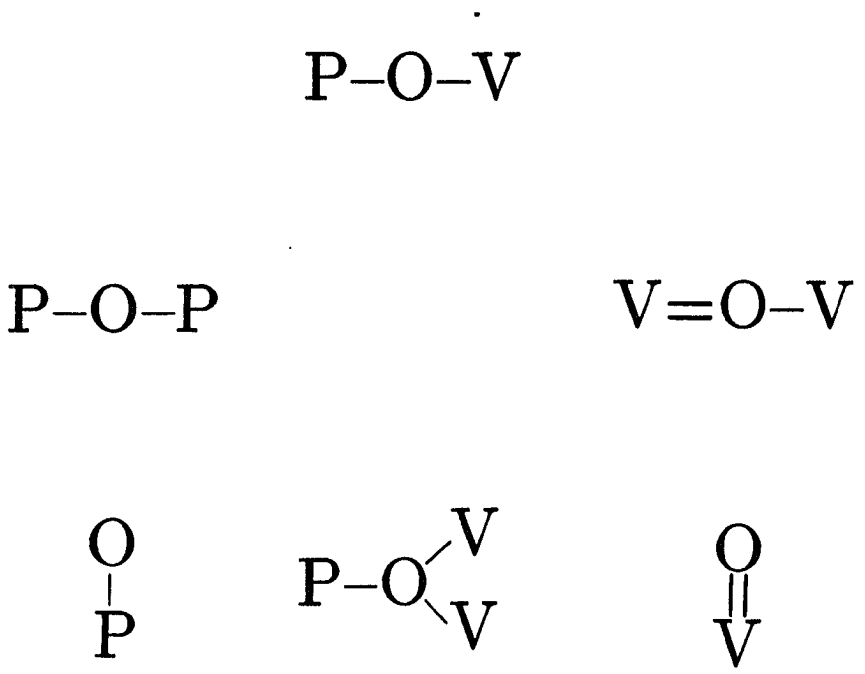

Figure 5: Oxygen species at the surface of vanadyl pyrophosphate [6]

layers only. They assert that if insufficient oxygen of the proper type is available at the surface, intermediates can be desorbed and react at other sites. When sufficient oxygen is available, a one site mechanism prevails (Figure 3).

As mentioned earlier, TAP experiments indicate two sources of oxygen exist for the formation of carbon dioxide. A source characterized as the "fast" source is identified as a highly reactive chemisorbed oxygen. The "slow" source is attributed to carbon dioxide formed from lattice oxygens. Work in support of these conclusions was presented by Centi *et al.* [32]. They found that carbon dioxide formation in the same system was not inhibited by the site blocking effects of ammonia present in the system. This indicates that an adsorbed di-oxygen molecule is responsible for a major portion of the carbon dioxide production. In the same paper, they present their version of the $(VO)_2P_2O_7$ active site, as shown in Figure 4.

Though TAP experiments indicate a strongly adsorbed oxygen species is responsible for n-butane activation, several authors claim weakly adsorbed oxygens or those at defects are responsible [28, 39, 40] . Yet others claim these weakly adsorbed and activated oxygens are very electrophillic and result in nonselective cracking [41, 42]. Finally, Centi and Trifiro [43] ascribe a weakly electrophillic nature to V=O species. They believe V(V)=O is responsible for oxygen insertion, while V(IV)=O or V(IV)-O-P, which would be less electrophillic than V(IV)=O's, are responsible for hydrogen abstraction.

Work done by Contractor and Sleight [44] on the oxidation of n-butane to maleic anhydride has led to a possible improvement of the industrial process for this reaction. They concluded that oxygen from the near surface lattice is involved in the selective oxidation process, and that at the surface, V(IV) to V(V) redox processes take place. The presence of the strong oxidizing agents O^{2-} or O^{-}

adsorbed on the surface was found to be detrimental, and selectivity losses were attributed to these species. To take advantage of the selective oxidation properties of $(VO)_2P_2O_7$ and yet limit the existence of detrimental species, they devised a process where the catalyst becomes a selective oxidation reagent. This was accomplished using an attrition resistant catalyst in the recirculating solids reactor shown in Figure 6. This system separates the oxidation and reduction functions of the catalyst and consequently increases selectivities and yields. This is a prime example of how knowledge of the nature of oxygen species can enhance the utility of the selective oxidation of n-butane and other paraffins.

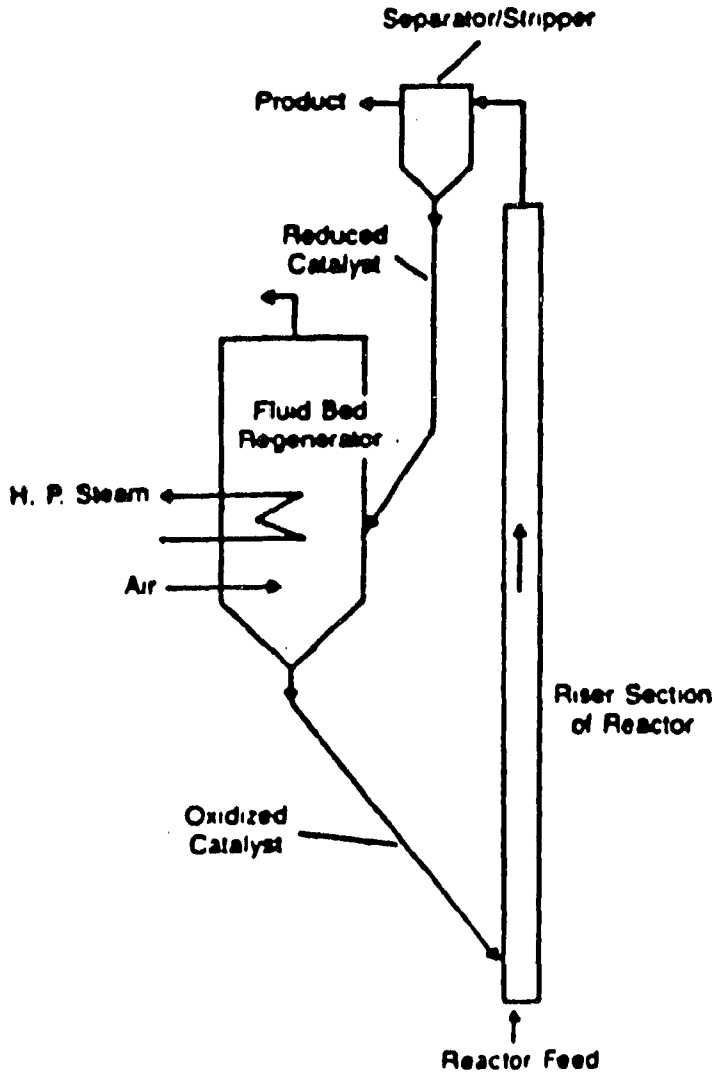

Figure 6: Recirculating solids reactor [44]

Research Objectives

It is the objective of this research to investigate the interaction of surface lattice oxygens of vanadium phosphorus oxide catalysts with various hydrocarbons postulated as intermediates in the conversion of n-butane to maleic anhydride. This investigation will attempt to identify those lattice oxygens responsible for the various steps in the reaction mechanism. The investigation will involve both vanadyl phosphate and vanadyl pyrophosphate catalysts. Fundamental insight into the activation of n-butane, stabilization of reactive intermediates on the catalyst surface, oxygen insertion and ring formation and nonselective combustion is the ultimate goal of this research, to be reached by the identification of those lattice oxygens species discussed.

Explanation of Dissertation Format

This dissertation contains three sections, each written in a form suitable for publication in a technical journal. A general introduction has been included to orient the reader to the scientific and industrial relevance of this work. A reference list is provided at the end of each section. References cited in the general introduction are given at the end of the dissertation. The research presented in each section represents original work conducted by the author.

PART I.

INVESTIGATION OF THE ACTIVE AND SELECTIVE LATTICE OXYGENS IN VPO CATALYSTS

ABSTRACT

An ^{18}O-enriched β-$VOPO_4$ catalyst was synthesized by the conversion of $(VO)_2P_2O_7$ to β-$VOPO_4$ in the presence of $^{18}O_2$. Characterization of the O-enriched β-$VOPO_4$ phase by laser Raman spectroscopy indicated the isotopic label was incorporated into specific tetrahedral lattice positions.

On-line mass spectrometry of the products of n-butane and 1-butene reaction over the labeled catalyst (in the absence of gas phase oxygen) demonstrated that selective oxidation and combustion occurred at different sites. *In situ* Raman experiments indicated that the initial high activity of the catalyst was not associated with bulk catalyst reduction; over extended time periods, extensive reduction did occur.

INTRODUCTION

Commercial interest in vanadium–phosphorus–oxygen (V–P–O) catalysts has resulted from the high activity and selectivity these materials have for C_4 hydrocarbon oxidation to maleic anhydride. Several studies have linked catalytic activity and selectivity to specific V–P–O phases [1–4] or to P to V ratios used in catalyst formulations [5–8]. The active centers of V–P–O catalysts have been primarily characterized by surface acidity [9] and texture [9–11]. The identification of active sites responsible for paraffin activation, oxygen incorporation, and complete combustion have yet to be identified.

Participation of lattice oxygen during the selective oxidation of hydrocarbons is a general characteristic of many metal oxide catalysts. Lattice oxygen for V–P–O catalysts appears to be utilized in both n-butane [12–14] and 1-butene [14] selective oxidation; gas phase oxygen is required for catalyst reoxidation [13]. Labeled (^{18}O) catalyst studies have proven valuable in the identification of active oxygen sites for the conversion of propylene to acrolein. Studies utilizing $^{18}O_2$ in the feed mixture [15–19] or ^{18}O-enriched bismuth molybdate catalysts [15, 20, 21] have established other extensive participation of lattice oxygen in the conversion of propylene to acrolein. Selective reduction of a bismuth molybdate catalyst with probe molecules such as propylene, 1-butene, methanol, and ammonia (followed by reoxidation with $^{18}O_2$) has been performed to examine the active sites responsible for α–H

abstraction and oxygen insertion [22]. Laser Raman spectroscopy has revealed that bridging Bi–O–Mo oxygen centers are responsible for α–H abstraction while oxygen incorporation into the allylic intermediate occurs at Mo–O centers. Similar structural identification of the active sites for C_4 hydrocarbon oxidation by V–P–O catalysts has not been reported.

In the present study, examination of the lattice oxygen involved in functions such as paraffin activation, oxygen incorporation, and complete combustion has been performed using *in situ* Raman spectroscopy of a β–$VOPO_4$ catalyst and using mass spectrometry to analyze reaction products. Fundamental information regarding the active sites for n–butane (paraffin) and 1–butene (olefin) selective oxidation has been obtained.

EXPERIMENTAL PROCEDURE

Synthesis of ^{18}O–Enriched β–$VOPO_4$

^{18}O–enriched β–$VOPO_4$ was prepared by the solid state reaction of $(VO)_2P_2O_7$ with $^{18}O_2$. $^{18}O_2$ was obtained from Merck, Sharp and Dohme with an atom enrichment of 97.8%. The synthesis of $(VO)_2P_2O_7$ has been described previously [1]. Powdered $(VO)_2P_2O_7$ (0.50 g) was charged to a 9 mm O.D. Pyrex tube which was evacuated and back filled with a stoichiometric quantity of $^{18}O_2$ gas. The reaction tube was heated at 823 K for 24 h followed by cooling to 473 K at a rate of 50 K/h.

Laser Raman Spectroscopic Characterization

Laser Raman spectra were obtained using a Spex 1403 laser Raman spectrometer with the 514.3 nm line of a Spectra Physics Model 2020–05 argon ion laser operated at 100 mW at the source. A Nicolet 1180E computer system permitted accumulation of the spectra. Raman spectra reported for β–$VOPO_4$ and ^{18}O–enriched β–$VOPO_4$ represent a 40 scan accumulation at 2-cm^{-1} resolution with a central slit setting of 1000 μm and a scan drive of 6.25 cm^{-1}/s.

Reactor Studies

Reactions of n-butane and 1-butene using the ^{18}O-enriched catalyst were performed in a continuous flow microreactor system in the absence of gas phase oxygen. The microreactor was a 1/4" stainless steel tube passivated by calcination in O_2 after treatment with phosphoric acid. 0.3 g of pressed and sieved catalyst (10–20 mesh) was used in each experiment. The composition and flow rate of the gases fed to the microreactor were controlled by Tylan mass flow controllers (Model FC260). The feed gas was delivered at 50 cm^3/min (standard temperature and pressure, sccm) with a composition of 2% n-butane or 1-butene (Matheson, instrument grade) in He (Matheson, zero grade). A reduced copper catalyst (BASF) was used to remove residual oxygen. The reactor system with *in situ* mass spectrometric capabilities is shown in Figure 1.

Mass spectral analysis of the products of n-butane and 1-butene reaction over the ^{18}O-enriched catalyst was performed by a UTI 100C precision quadrupole mass analyzer controlled by a PDP 11/23 computer. The mass analyzer was interfaced with the microreactor system by a glass SGE single stage molecular jet separator.

The ^{18}O content of maleic anhydride, CO_2, and H_2O produced by the ^{18}O-enriched β-$VOPO_4$ catalyst was determined for the oxidation of n-butane and 1-butene. The ^{18}O content of maleic anhydride was calculated from the percent of maleic anhydride molecules with mass-to-charge ratios (m/e) of 98, 100, 102, and 104 as follows:

$$\%^{18}O_{MAN} = \frac{\sum I_{100} + 2\sum I_{102} + 3\sum I_{104}}{3(\sum I_{98} + \sum I_{100} + \sum I_{102} + \sum I_{104})}$$

For 1-butene, phthalic anhydride was formed as the catalyst became reduced. Phthalic anhydride also has a 104 m/e peak, and the maleic anhydride data were

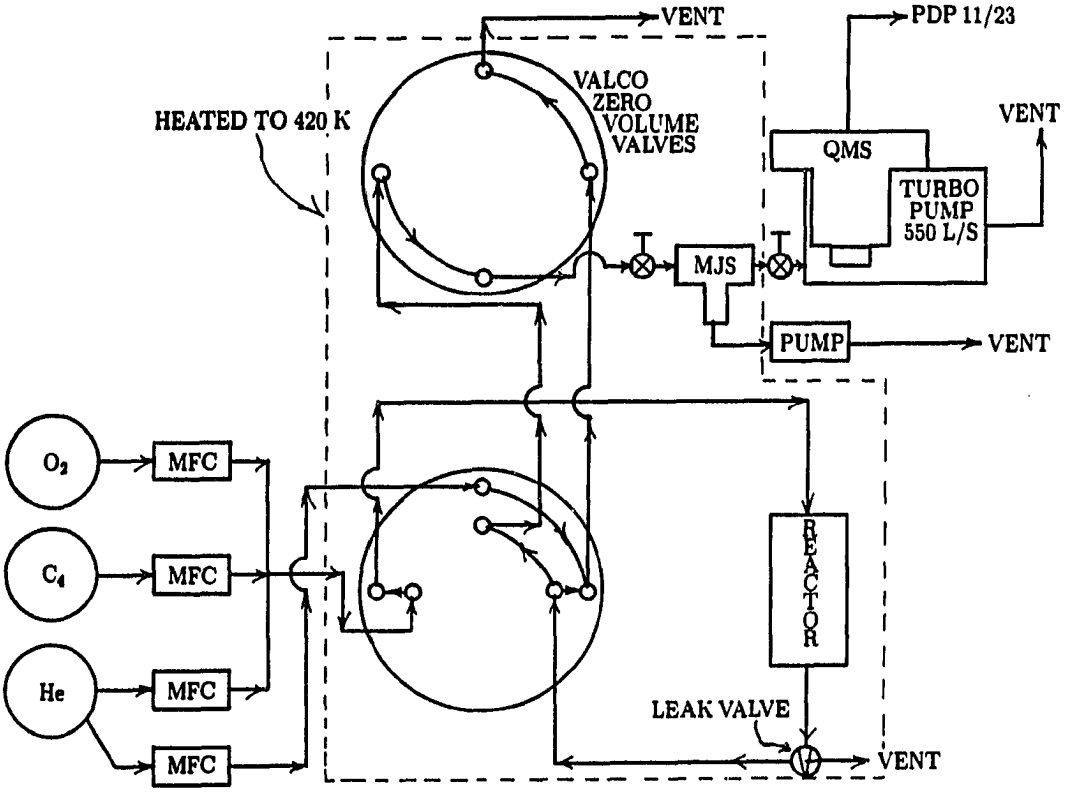

Figure 1: Reactor system

corrected by monitoring other phthalic anhydride peaks.

The ^{18}O content of carbon dioxide and water were determined in a similar manner.

The CO_2 data were corrected by subtracting the minor interferences at m/e 44 from n-butane or 1-butene fragmentation and background CO_2. The following formula was used to calculate the ^{18}O content in CO_2:

$$\%^{18}O_{CO_2} = \frac{\sum I_{46} + 2\sum I_{48}}{2(\sum I_{44} + \sum I_{46} + \sum I_{48}+)}$$

CO could also be observed, but the data were significantly complicated by interference form background N_2 and $C^{16}O$.

The ^{18}O content of water produced by both combustion and selective oxidation was estimated from mass spectral intensities corresponding to $H_2{}^{16}O$ (m/e 18) and $H_2{}^{18}O$(m/e 20). The content of the ^{18}O label was calculated as follows:

$$\%^{18}O_{H_2O} = \frac{\sum I_{20}}{\sum I_{18} + \sum I_{20}}$$

In Situ Laser Raman Spectroscopy

A Spex 1877 Triplemate laser Raman spectrometer was used with 14.3 nm line of a Spectra Physics Model 164 argon ion laser operated with 200mW at the source. No thermal or photochemical decomposition of the catalyst sample occurred under these conditions. An EG&G 1215 optical multichannel analyzer and an EG&G 1420 detector were used with the spectrometer. Typically, a 4-cm^{-1} resolution spectrum was acquired in 15-30 seconds. The spectrograph entrance slit was set at 50 μm for a 1200 gr/mm spectrograph grating.

In situ laser Raman spectra of the functioning catalyst were obtained using a tubular controlled atmosphere cell [14]. The cell incorporated Teflon gaskets for gas-tight sealing and was well insulated to remove temperature gradients. The thermocouple was attached to the quartz catalyst holder to be in direct contact with the catalyst bed. Identical catalyst loadings and flow rates were used in both the mass spectrometry and laser Raman experiments. The *in situ* Raman studies did not involve ^{18}O–enriched catalysts. n–Butane was reacted at 773 K, and 1–butene was reacted at 723 K.

EXPERIMENTAL RESULTS

Characterization of ^{18}O-Enriched β-$VOPO_4$

The Raman spectrum of ^{18}O-enriched β-$VOPO_4$ prepared by the solid state reaction of $(VO)_2P_2O_7$ with $^{18}O_2$ was compared to the Raman spectrum of similarly prepared β-$VOPO_4$ [1] using $^{16}O_2$ (Figure 2). Spectral features showing a specific incorporation of ^{18}O into the lattice of β-$VOPO_4$ could be observed. Raman band assignments for β-$VOPO_4$ have been discussed previously [1]. ^{18}O could be detected in the catalyst lattice by a P-^{18}O band at 886 cm^{-1}; the P-^{16}O stretch at 896 cm^{-1} had near equal intensity. Another P-^{18}O band was observed at 961 cm^{-1}. The intensity of this band, however, was rather weak (about 5% of the P-^{16}O band at 987 cm^{-1}). A slight broadening of the P-O band at 1072 cm^{-1} was also observed. Unreacted $(VO)_2P_2O_7$ was detected by a very weak band at 923 cm^{-1} in the spectrum of ^{18}O-enriched β-$VOPO_4$. The Raman spectrum of β-$VOPO_4$ prepared by the reaction of $(VO)_2P_2O_7$ with $^{16}O_2$ also indicated the presence of a small amount of unreacted $(VO)_2P_2O_7$.

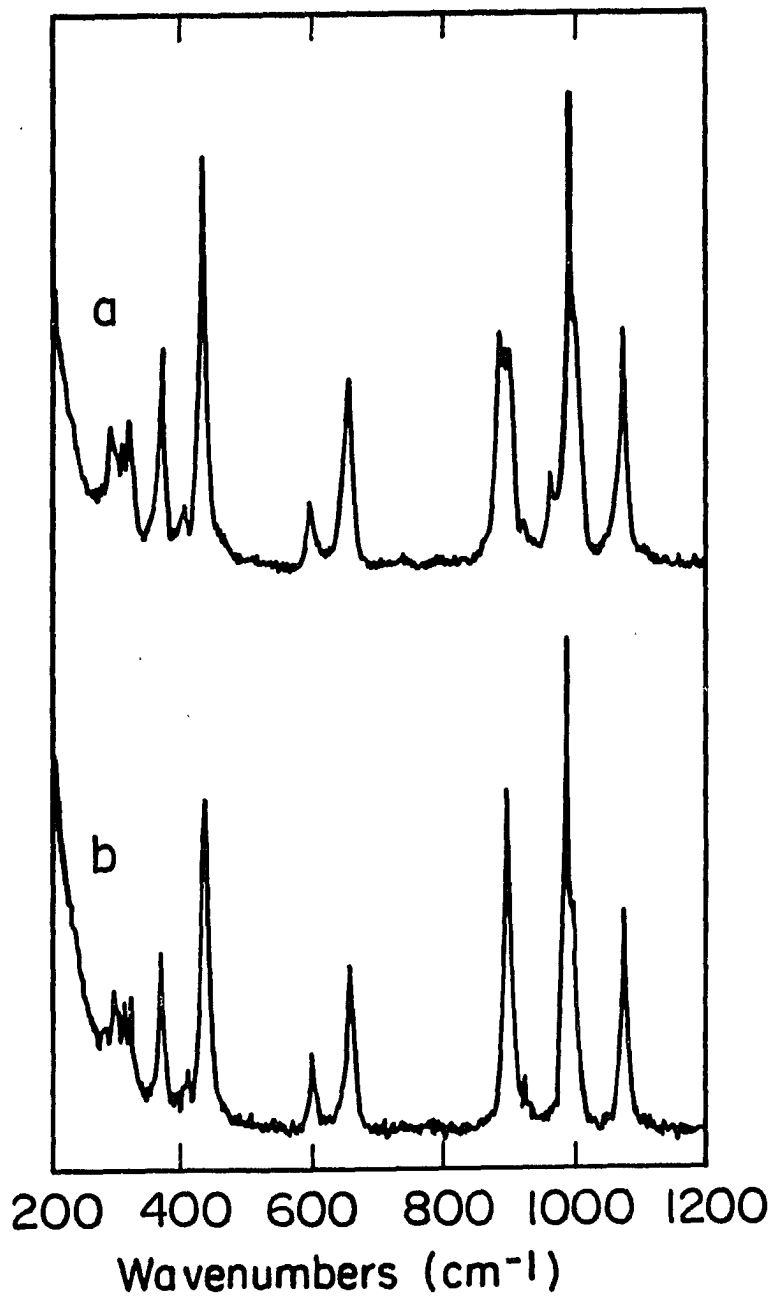

Figure 2: Raman spectra of (a) ^{18}O-enriched β-$VOPO_4$ prepared by reaction of $(VO)_2P_2O_7$ with $^{18}O_2$ and (b) β-$VOPO_4$ prepared by reaction of $(VO)_2P_2O_7$ with $^{16}O_2$

Mass Spectrometry Studies

^{18}O incorporation into the products of n-butane oxidation

The amounts of ^{18}O incorporation in maleic anhydride, CO_2 and H_2O and the n-butane conversion were studied by reaction of n-butane over the labeled catalyst in the absence of gas phase O_2. As the exposure to n-butane proceeded, the conversion decreased from about 5% to nearly 0%. Significant levels of maleic anhydride were produced for nearly 20 mins (Figure 3). As the catalyst was further exposed to n-butane, furan was detected.

The ^{18}O content of maleic anhydride, CO_2, and H_2O are presented in Figure 4. The ^{18}O content of the maleic anhydride ranged from an initial level of 11-12% to an ultimate level of about 13-14%. The ^{18}O content of the CO_2 produced was initially at the 7-8% level, dropped to a low of about 6% after about two minutes, and then leveled off at about 6%. The ^{18}O content in the H_2O produced in this reaction varied from an initial level of about 8% to a final level near 12%. The most striking feature is that maleic anhydride was produced containing ^{18}O at nearly twice the level of CO_2, while H_2O contained ^{18}O at an intermediate level.

^{18}O incorporation into the products of 1-butene oxidation

The amount of ^{18}O incorporated in maleic anhydride, CO_2, and H_2O and the 1-butene conversion were also studied by reaction of 1-butene over the labeled catalyst in the absence of gas phase O_2. As the catalyst was exposed to 1-butene, the conversion decreased from nearly 50% to around 0%. The production of maleic anhydride decreased rapidly to a low-but fairly steady-level after about 2 mins

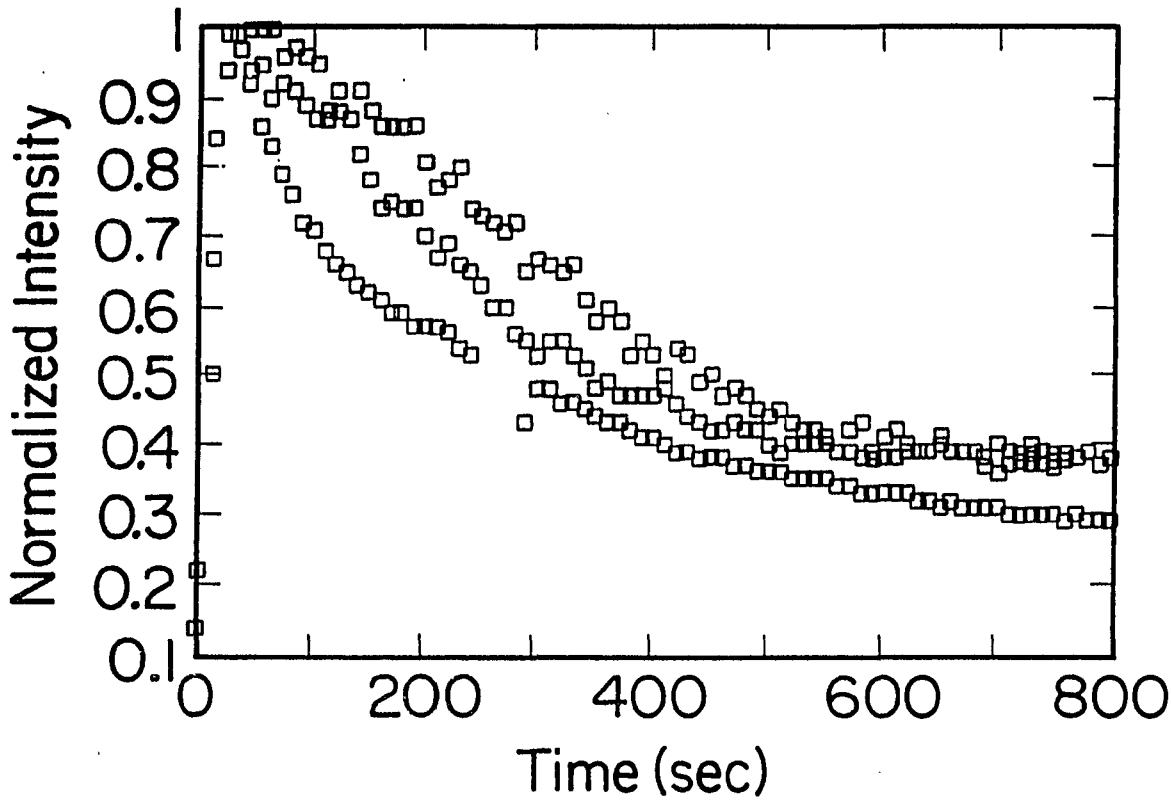

Figure 3: Maleic anhydride production from 2% n-butane over ^{18}O enriched β-$VOPO_4$ (773 K): m/e 98 normalized intensity

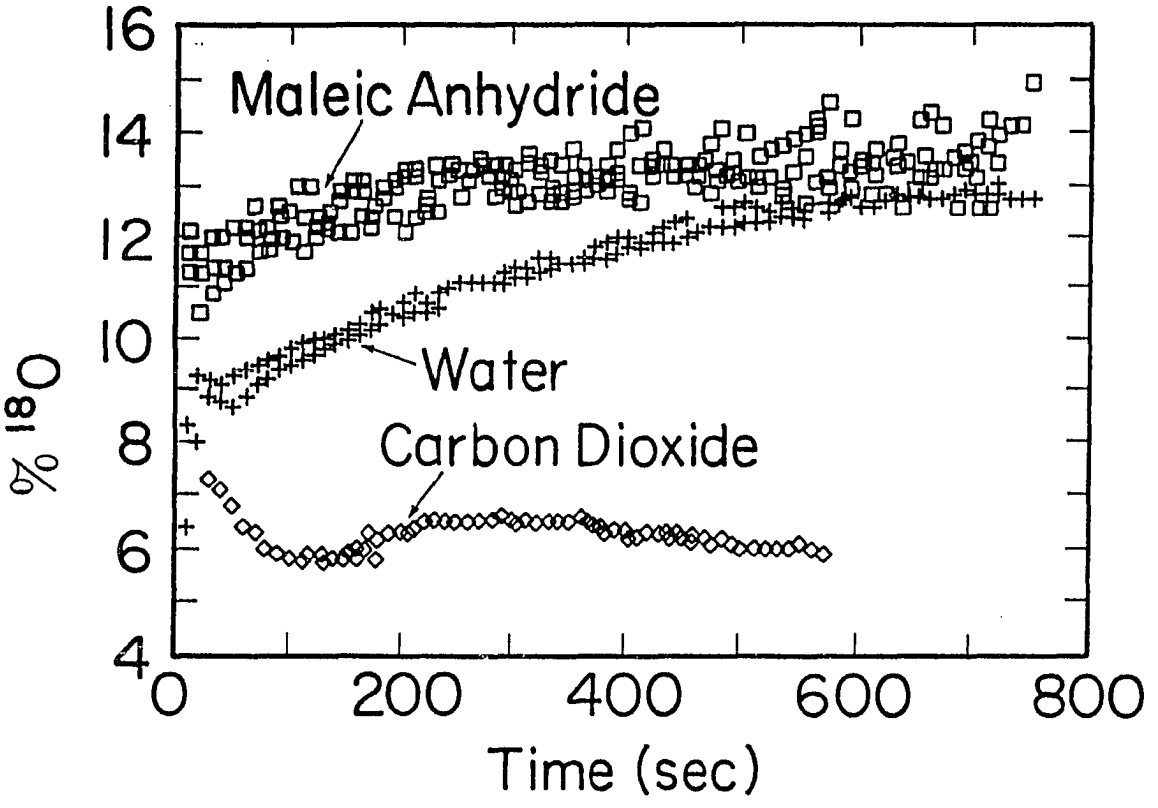

Figure 4: ^{18}O content of maleic anhydride, CO_2, and H_2O during 2% n-butane oxidation by ^{18}O-enriched β-$VOPO_4$ (773 K)

(Figure 5). Furan could be detected throughout the experiment, while phthalic anhydride could be detected at a longer time for exposure to 1-butene.

The levels of ^{18}O in maleic anhydride, CO_2, and H_2O are presented in Figure 6. ^{18}O levels in maleic anhydride ranged from an initial level of 12–13% to a final value of 14–15%. The ^{18}O level in CO_2 started at about 7–8%, rose to a maximum of about 10% at about 90 sec, and then decreased to the 4–6% level. As with n-butane, the maleic anhydride ^{18}O level and CO_2 ^{18}O level produced from 1-butene were significantly different. The level of ^{18}O incorporation into maleic anhydride for each feed gas was similar with 1-butene producing slightly higher levels. This was probably due to the difference in catalyst selectivity for these feeds. The ^{18}O content of H_2O produced in this reaction was initially about 6%, and increased to about 10%.

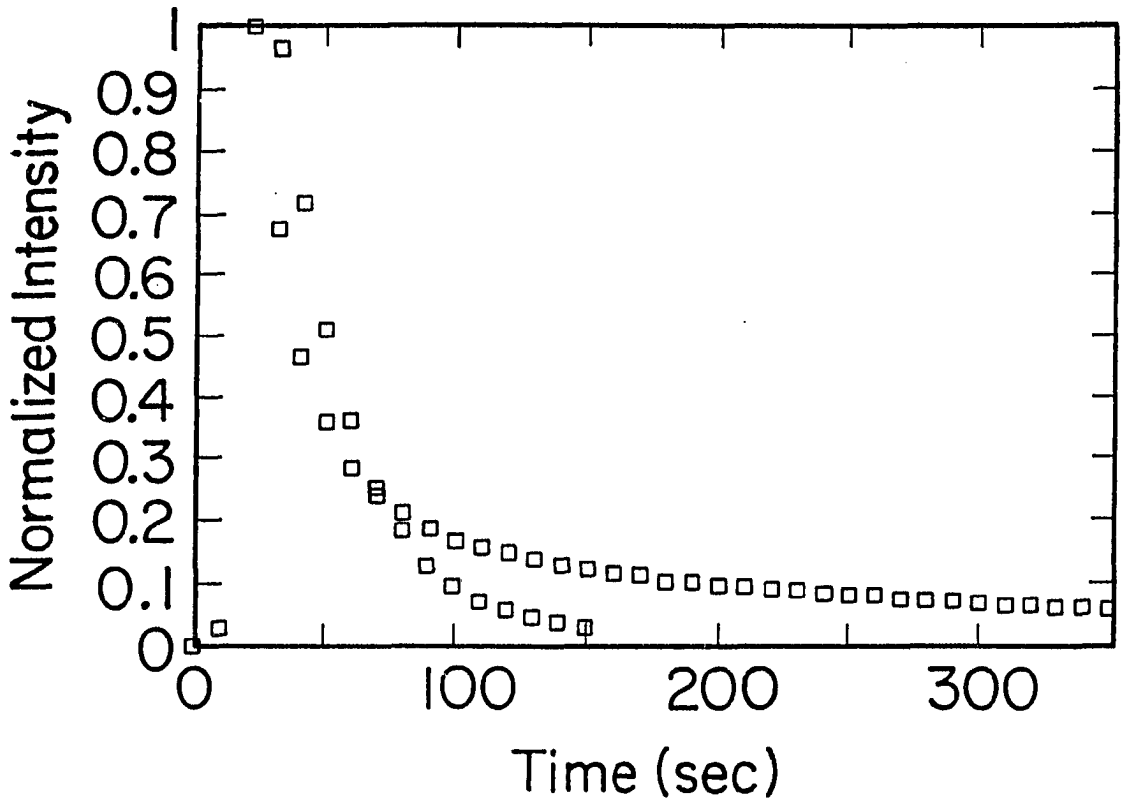

Figure 5: Maleic anhydride production from 2% 1-butene over ^{18}O-enriched β-$VOPO_4$ (723 K): m/e 98 normalized intensity

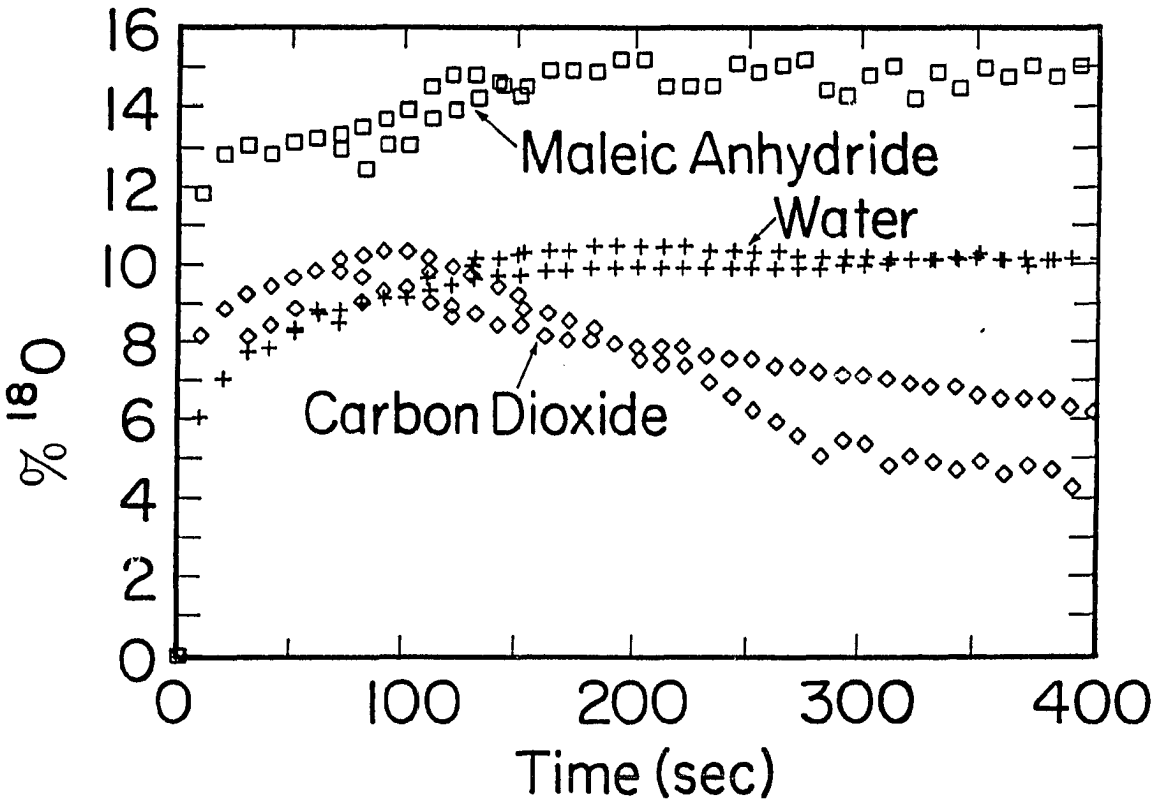

Figure 6: ^{18}O content in maleic anhydride, CO_2, and H_2O during 2% 1-butene oxidation over ^{18}O-enriched β-$VOPO_4$ (723 K)

In Situ Laser Raman Spectroscopy

Characterization during n–butane oxidation

In situ Raman spectra of β–$VOPO_4$ under conditions of n–butane oxidation at 773 K are presented in Figure 7. Comparison of the room temperature spectrum and the reaction temperature spectrum illustrates temperature effects: thermal broadening and slight peak shifts occurred, but no bulk thermal reduction was evident. As the reaction of 2% n–butane in He with the catalyst began, no reduction was apparent until nearly 30 mins when a $(VO)_2P_2O_7$ band at 970 cm^{-1} began to appear. During this time period, however, there was a reduction in intensity of the Raman scattering form the β–$VOPO_4$ phase which could be due to reduction or other effects.

Characterization during 1–butene oxidation

In situ Raman spectra of β–$VOPO_4$ under conditions of exposure to 1–butene at 723 K are presented in Figure 8. As for the previous n–butane studies at 773 K, thermal broadening and an intensity loss occurred upon heating, but these effects were not as severe at 723 K. As the reaction of 2% 1–butene commenced, all peak intensities decreased continuously. $(VO)_2P_2O_7$ was formed after about six minutes, as evidenced by the appearance of a band at 930 cm^{-1}. The intensity of this band increased continuously, accompanied by a decrease in the β–$VOPO_4$ bands.

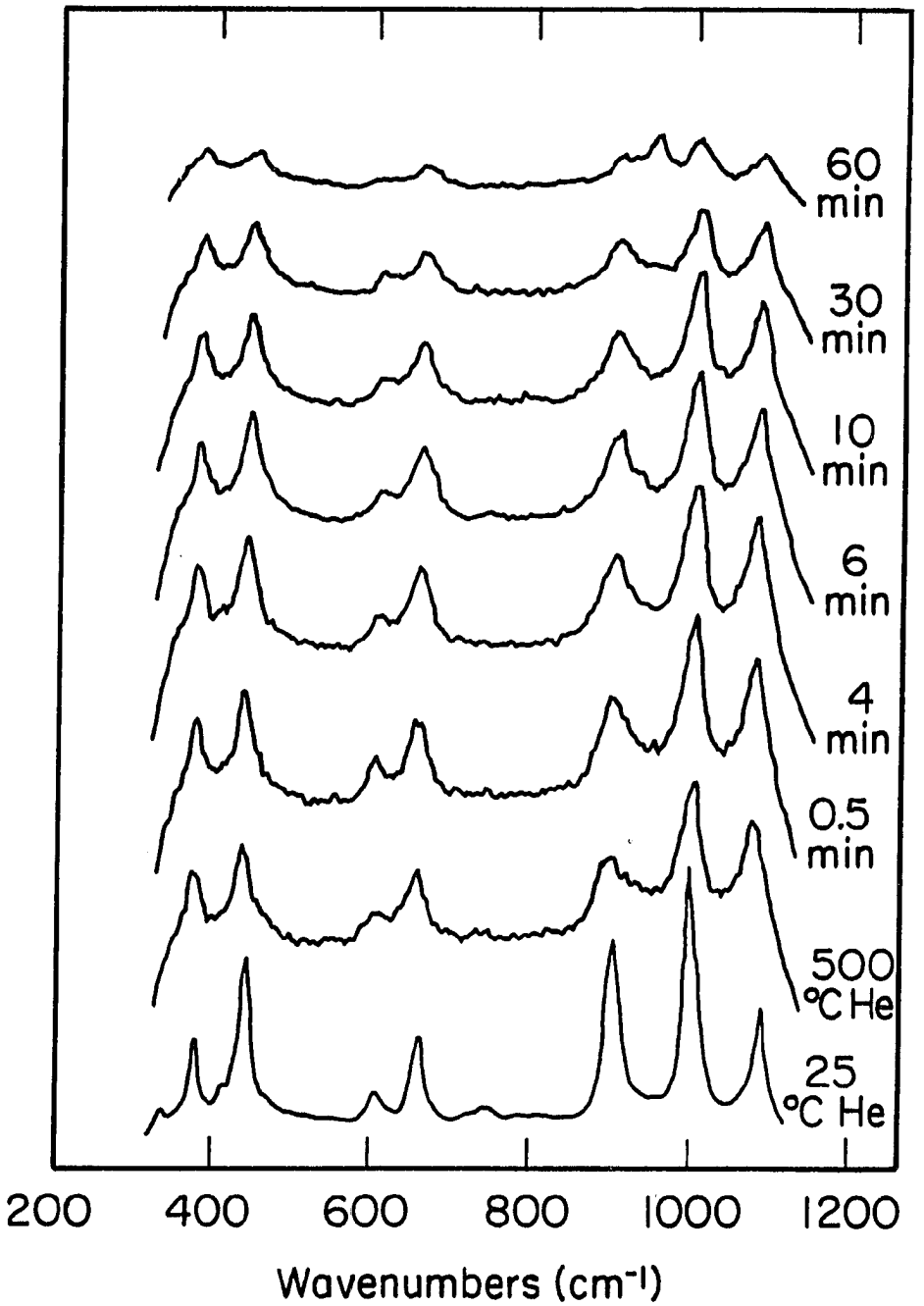

Figure 7: Raman spectra of β–$VOPO_4$ during n-butane oxidation (773 K)

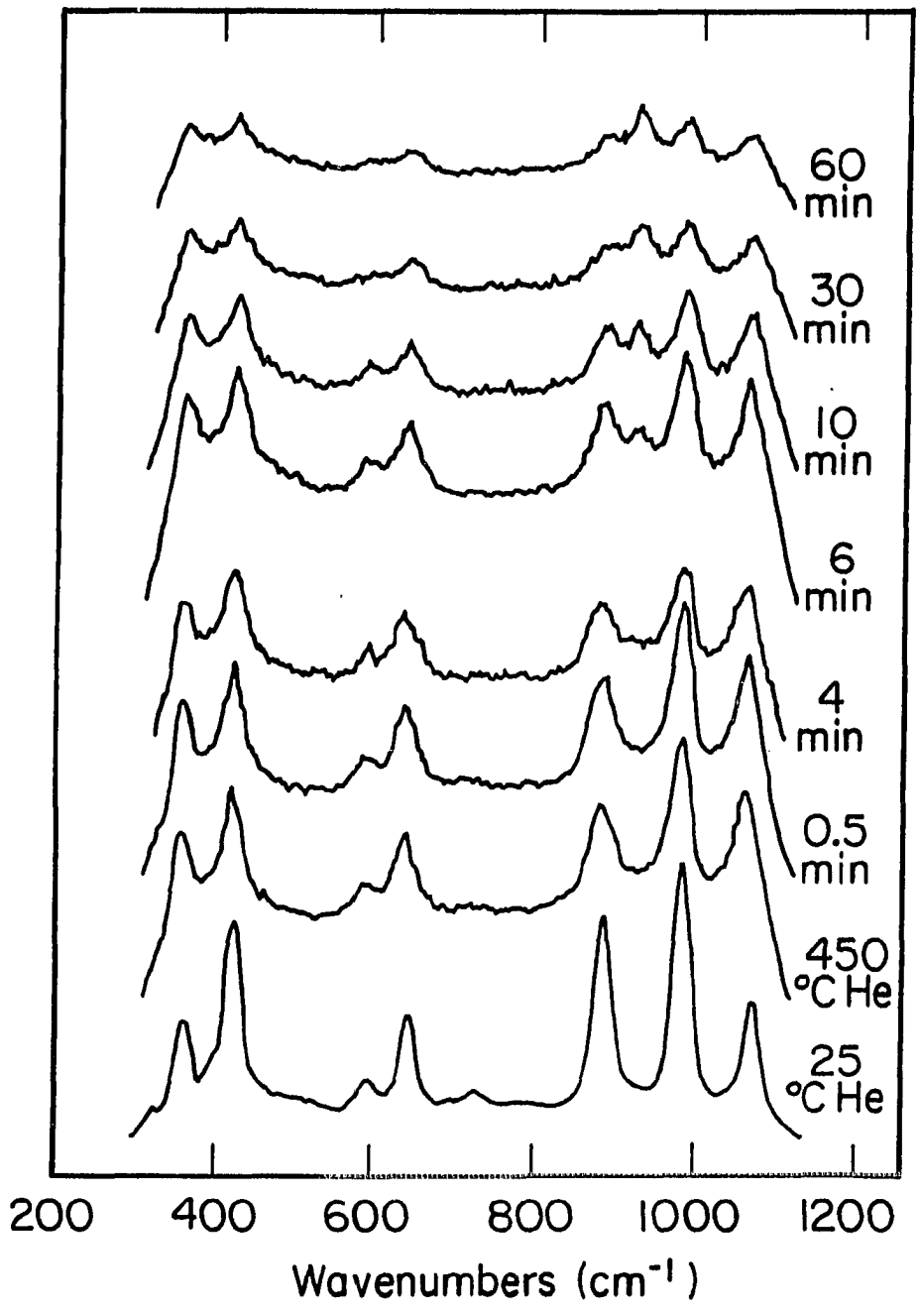

Figure 8: Raman spectra of *3*–$VOPO_4$ during 1-butene oxidation (753 K)

DISCUSSION OF RESULTS

The β–$VOPO_4$ structure consists of irregular VO_6 octahedra which form corner-sharing chains through V=O–V bonding [23]. Sheets of these chains exist in the β–$VOPO_4$ phase. The PO_4 tetrahedra share oxygen atoms with four separate VO_6 octahedra in three separate chains. Only the equatorial oxygens in the VO_6 octahedron are shared with a phosphorus atom. Adjacent sheets of VO_6 octahedra are bridged by corner sharing of two equivalent oxygen atoms of the PO_4 group with VO_6 groups positioned above and below. The PO_4 group also shares corners with two octahedra in the same octahedral chain. These latter two oxygen atoms are crystallographically distinct as a result of the displacement of the vanadium atom from the center of the octahedron.

The crystal structure of $(VO)_2P_2O_7$ is also characterized by infinite octahedral chains formed by corner sharing VO_6 octahedra [24]. However, the VO_6 octahedra are linked in pairs through a common equatorial edge, forming double octahedral chains. Each tetrahedron of the pyrophosphate group is involved in a tridentate bridge between three different octahedral chains.

The Raman spectra of the isotopically enriched catalysts provided information about the nature of the $(VO)_2P_2O_7$ to β–$VOPO_4$ phase transformation. The solid state reaction of $(VO)_2P_2O_7$ with $^{18}O_2$ produced an ^{18}O–enriched phase according to specific stoichiometry: one mole of $(VO)_2P_2O_7$ reacted with one–half mole of

$^{18}O_2$ to form the ^{18}O-enriched β-$VOPO_4$ phase. The Raman results indicated that incorporation of the ^{18}O occurred in specific lattice sites. The Raman spectrum of ^{18}O-enriched β-$VOPO_4$ had an isotopically shifted P-^{18}O band at 886 cm^{-1} which was of nearly equal intensity as the related P-^{16}O band at 896 cm^{-1}. ^{18}O was also incorporated to a much lesser extent at other P-O positions as indicated by a band at 987 cm^{-1}. The incorporation of ^{18}O into the PO_4 groups of β-$VOPO_4$ therefore occurs very specifically; random distribution of ^{18}O in the β-$VOPO_4$ phase clearly was not observed. In addition, complete incorporation of ^{18}O into a limited region or portion of the material was not detected.

$$(VO)_2P_2O_7 + 1/2\ ^{18}O_2 \longrightarrow 2\beta\text{-}VOPO_{7/2}{}^{18}O_{1/2}$$

The structures of the catalysts suggest that the β-$VOPO_4$ to $(VO)_2P_2O_7$ transformation involves the cooperative movement of VO_6 octahedra to form double octahedral chains characteristic of $(VO)_2P_2O_7$ [3]. Concurrently, pyrophosphate structures are formed from neighboring (above and below) phosphate tetrahedra of β-$VOPO_4$.

Because of the specific incorporation of ^{18}O into the lattice of the catalytically active β-$VOPO_4$ phase, it was possible to relate the production of oxygenated products with the reactivity of the oxygen sites. Of particular interest was the identification of sites that are responsible for partial oxidation (production of maleic anhydride) and complete combustion (production of CO_2). The oxidation of n-butane by ^{18}O-labeled β-$VOPO_4$ resulted in the preferential incorporation of ^{18}O into maleic anhydride as compared to CO_2 and H_2O. For example, the initial ^{18}O content of maleic anhydride was approximately two times greater than for CO_2

for n-butane reaction at 773 K. Similar results were observed for 1-butene at 723 K. According to the Raman spectrum of ^{18}O-labeled β-$VOPO_4$, the P-^{18}O stretch at 886 cm^{-1} and the complementary P-^{16}O stretch at 896 cm^{-1} had relative intensities indicating that approximately 40% of the oxygen associated with this stretching vibration were labeled with ^{18}O. A small degree of ^{18}O incorporation into another P-O lattice position was detected: the intensity of a P-^{18}O band at 961 cm^{-1} was approximately 5% compared to the related P-^{16}O stretch at 987 cm^{-1}.

Due to the stoichiometric nature of the preparation, only 10% of the total oxygen in the catalyst can be ^{18}O. Based on the Raman characterization, all of the ^{18}O is incorporated at P-O positions. For both n-butane and 1-butene feeds, maleic anhydride was produced which contained nearly 13% ^{18}O. To account for this selective incorporation, a "pool" of 13% ^{18}O in the catalyst must exist. If all oxygen atoms associated with P-O bonding were considered to be equivalent, such a pool of 13% ^{18}O would exist. The Raman data would appear to indicate, however, that ^{18}O tends to be associated with two of the three P-O oxygen stretches. It is quite, however, possible that these oxygen positions are structurally more similar at the catalyst surface than in the catalyst bulk.

The ^{18}O levels found in carbon dioxide indicate that total oxidation likely occurs through more than one pathway. Direct combustion of maleic anhydride to carbon dioxide is known to occur over β-$VOPO_4$ [25]. However, if complete oxidation of maleic anhydride occurred randomly at all available oxygen sites, the ^{18}O found in carbon dioxide would be higher than the 6-8% observed. Similarly, if combustion occurred only at unlabeled sites, the ^{18}O content of the carbon dioxide should be lower than the observed values. An additional route (or routes) to

complete combustion products must also exist involving utilization of some oxygen from labeled sites. This reaction pathway could proceed by an initial electrophillic attack on the C–C bonds of n-butane or other C_4 hydrocarbon intermediates. The V=O site has been identified as being electrophillic [26] and therefore is likely to be involved in this nonselective activation. Such "cracking" reactions would produce highly activated C_1–C_3 species which could interact with any available oxygen site to produce carbon dioxide. It is possible that combustion could proceed exclusively on the V=O sites, but the Raman spectra indicate that no ^{18}O is incorporated at these positions. The C_1–C_3 reactive intermediates are likely also to undergo reaction at other oxygen sites, including the ^{18}O–labeled P–O sites (also involved in maleic anhydride production).

Shown in Figure 9(a) is a depiction of the location of the ^{18}O labeled sites as identified by the laser Raman studies. Also shown in Figure 9(b) is the activation of n-butane and the insertion of oxygen at P–O sites, resulting in the production of maleic anhydride. Combustion of C_4 hydrocarbons and maleic anhydride involving C_1–C_3 reactive intermediates is depicted in Figure 9(c).

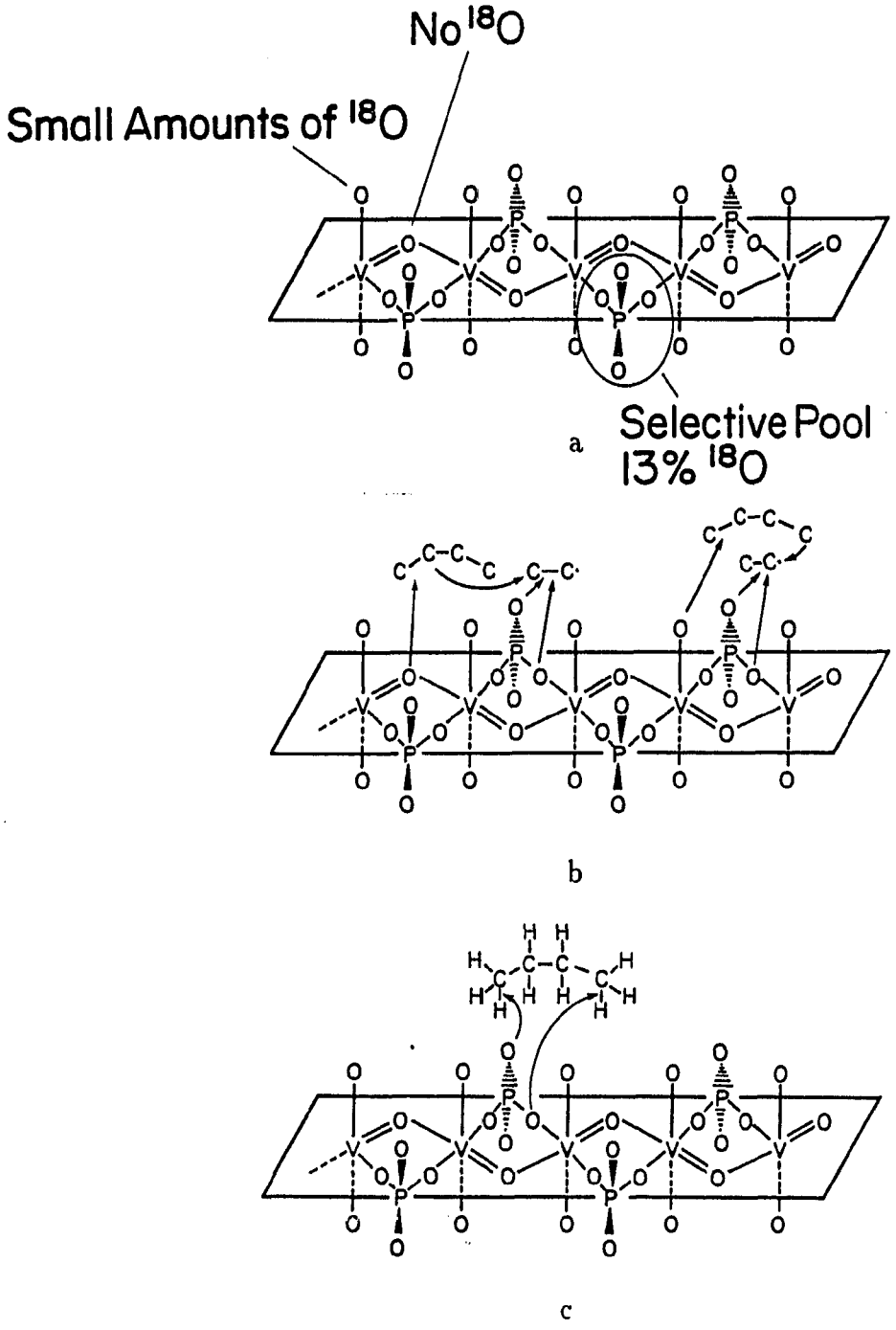

Figure 9: Plausible reaction surface: (a) location of ^{18}O as determined by laser Raman spectroscopy, (b) activation of n-butane and oxygen insertion to produce maleic anhydride, (c) example of complete combustion of hydrocarbons and maleic anhydride involving several oxygen sites

CONCLUSIONS

The incorporation of ^{18}O into maleic anhydride (about 13%) is very similar for both n-butane and 1-butene feeds, although the reaction rates differ significantly. The reaction pathways for the selective oxidation of these species would appear to be similar after the initial activation. The source of these selective oxygen atoms was identified as being associated with P-O structures. CO_2 formation occurs through at least two possible pathways. The ^{18}O levels observed indicate that in addition to the route from the combustion of maleic anhydride, CO_2 is formed from highly reactive species produced by cracking of carbon-carbon bonds by electrophillic V=O species.

ACKNOWLEDGMENT

This work was performed at Ames Laboratory under contract No. W-7405-eng-82 with the U. S. Department of Energy. The United States government has assigned the DOE Report number IS-T 1411 to this thesis.

REFERENCES CITED

1. Moser, T. P.; Schrader, G. L. Journal of Catalysis (1985) **92**, 216.
2. Morselli, L.; Trifiro, F.; and Urban, L. Journal of Catalysis (1982) **75**, 112.
3. Bordes, E.; Courtine, P. Journal of the Chemical Society, Chemical Communications (1985), 294.
4. Bordes, E.; Courtine, P. Journal of Catalysis (1979) **57**, 236.
5. Wenig, R. W.; Schrader, G. L. Industrial Engineering Chemistry Fundamentals (1986) **25**, 612.
6. Garbassi, F.; Bart, B.; Tassinari, R.; Vlaic, G.; and Lagarde; P. Journal of Catalysis (1986) **98**, 317.
7. Hodnett, B.; Delmon, B. Journal of Catalysis (1984) **88**, 43.
8. Hodnett, B.; Permanne, Ph.; Delmon, B. Applied Catalysis (1983) **6**, 231.
9. Busca, G.; Centi, G.; and Trifiro, .F. Journal of the American Chemical Society (1985) **107**, 7758.
10. Busca, G.; Cavani, F.; Centi, G.; Trifiro, F. Journal of Catalysis (1986) **49**, 400.
11. Cavanni, F.; Centi, G.; Trifiro, F. Journal of the Chemical Society, Chemical Communicaions (1985), 492.
12. Pepera, M. A.; Callahan, J. L.; Desmond, M. J.; Milberger, E. C.; Blum, P. R.; Bremer, N. J. Journal of the American Chemical Society (1985) **107**, 4883.
13. Kurchinin, Yu.; Mishchenko, Yu.; Nechiporuk, P.; Gel'bshtein, A. Kinetica i Kataliz (1984) **25(2)**, 369.
14. Moser, T.P.; Schrader, G.L. Journal of Catalysis (1987) **104**, 99.
15. Wragg, R.; Ashmore, P.; Hockey, J. Journal of Catalysis (1971) **22**, 49.

16. Keulks, G. Journal of Catalysis (1970) **19**, 232.

17. Krenzke, D.; Keulks, G. Journal of Catalysis (1980) **61**, 316.

18. Sancier, K.; Wentrcek, P.; Wise, H. Journal of Catalysis (1975) **39**, 141.

19. Hoefs, E.; Monnier, J.; Keulks, G. Journal of Catalysis (1979) **57**, 331.

20. Otsubo, T.; Miura, H.; Morikawa, Y.; Shirasaki, T. Journal of Catalysis (1975) **36**, 240.

21. Miura, H.; Otsubo, T.; Shirasaki, T.; Morikawa, Y. Journal of Catalysis (1979) **56**, 84.

22. Glaeser, L.; Brazdil, J.; Hazele, M.; Mehic, M.; Grasselli, R. Journal of the Chemical Society, Faraday Transactions (1985) **1(79)**, 2903.

23. Gopal, R.; Calvo, C. Journal of Solid State Chemistry (1972) **5**, 432.

24. Gorbunova, Yu.; Linde, S. Soviet Physics-Doklady (1979) **24(3)**, 138.

25. Moser, T.P.; Wenig, R.W.; Schrader, G.L. Applied Catalysis (1987) **34**, 39.

26. Haber, J.; Serwicka, E. M. Reaction Kinetics and Catalysis Letters (1987) **35(1-2)**, 369.

PART II.

THE ROLE OF LATTICE OXYGENS IN C_4 OXIDATION OVER *3*–$VOPO_4$

ABSTRACT

The role of lattice oxygens of β–$VOPO_4$ in the oxidation of C_4 hydrocarbons has been investigated using a catalyst specifically labeled with ^{18}O. Labeled and unlabeled lattice oxygens were identified by laser Raman spectroscopy, while ^{18}O incorporation into products was monitored by mass spectrometry. The results of this study indicate that the initial interaction of n–butane with β–$VOPO_4$ is fundamentally different than that for olefins and oxygenated species. Specific lattice oxygens could be identified as responsible for mechanistic steps under anaerobic conditions. Additionally, it was shown that, under the conditions of this work, maleic anhydride was combusted only at unlabeled sites.

INTRODUCTION

Vanadium phosphorus oxides (VPO) are unique and complex catalysts. It is well known that VPOs can be used to activate and selectively oxidize n–butane and other paraffins [1] to maleic anhydride. The oxidation of n–butane to maleic anhydride is a 14 electron process with a complicated reaction mechanism, as evidenced in the literature concerning the possible mechanisms [2–17]. Several closely related mechanisms have been proposed, usually involving adsorbed or free olefins (butenes and butadiene) and partially oxidized species (furan, tetrahydrofuran, and γ–butyrolactone).

Investigations involving VPO catalysts and the selective activation and oxidation of n–butane to maleic anhydride have resulted in the correlation of many catalyst characteristics (phase, morphology, P/V ratio, surface acididty) [2, 16, 18–27] to activity and selectivity of the catalyst. Recently, the focus has turned to identifying and characterizing specific active sites in the catalyst [28–32]. The role of various oxygen species was investigated by Gleaves *et al.*. They postulate that at least two different oxygen species, either lattice or strongly adsorbed, are utilized in the activation and selective oxidation process. At least one of these oxygens is postulated to have a major role in CO_x formation [32].

In an attempt to limit the presence of highly reactive adsorbed oxygen species, Contractor and Sleight developed a recirculating solids reactor, which separates the

steps of hydrocarbon oxidation over the catalyst and catalyst reoxidation [33]. Thus it is apparent that a fundamental understanding of all oxygen species present in this system is crucial to the understanding of the mechanism of selective activation and oxidation of n-butane on VPO catalysts.

We have shown previously [34] that, for β-$VOPO_4$, under anaerobic conditions, different lattice oxygens are responsible for the roles of selective oxidation (P-O-V) and nonselective oxidation (V=O, V-O-V, and P-O-V). This was accomplished by labeling specific catalytic sites with ^{18}O and monitoring the anaerobic oxidation of n-butane with mass spectrometry. The logical extension of this work is to relate the postulated mechanistic steps to specific lattice oxygens, as this present work attempts to do.

EXPERIMENTAL PROCEDURE

Synthesis of ^{18}O–Enriched β–$VOPO_4$

^{18}O–enriched β–$VOPO_4$ was prepared by the solid state reaction of $(VO)_2P_2O_7$ with $^{18}O_2$ as described previously [34].

Laser Raman Spectroscopic Characterization

Laser Raman spectra were obtained using a Spex 1403 laser Raman spectrometer with the 514.3 nm line of a Spectra Physics Model 2020–05 argon ion laser operated at 100 mW at the source. A Nicolet 1180E computer system permitted accumulation of the spectra. Pre– and post– reaction spectra reported represent a 40 scan accumulation at 2–cm^{-1} resolution with a central slit setting of 1000 μm and a scan drive of 6.25 cm^{-1}/s.

Reactor Studies

Reactions of n–butane, 1–butene, 1,3–butadiene, furan, γ–butyrolactone, and maleic anhydride using the ^{18}O–enriched catalyst were performed, without the presence of gas phase oxygen, in the pulse microreactor system shown in Figure 1. The microreactor was a 1/4 in. stainless steel tube passivated by calcination in O_2 after treatment with phosphoric acid. Two-tenths of a gram of pressed and sieved

catalyst (10–20 mesh) were used in each experiment. The catalyst was held in place by plugs of pyrex wool, which had been washed and calcined in O_2. Treated reactors and glass wool showed negligible combustion activity for all feeds at the reaction temperature.

The reactor was continuously purged with helium flowing at 50 cm^3/min (at standard temperature and pressure, sccm). A ten port Valco valve equipped with 0.5 ml loops was used to introduce hydrocarbon pulses. The valve and loops were maintained at 425 K. The composition and flow rate of the gases fed to the sample loop and the microreactor were controlled by Tylan mass flow controllers (Model FC260). Pure n-butane, 1-butene and 1,3-butadiene (Matheson, instrument grade) were diluted with helium (Matheson, zero grade) to 2 % hydrocarbon and fed to the loop. To provide low (less than 1 %) concentrations of furan (Kodak), γ-butyrolactone (Alfa), and maleic anhydride (Kodak), helium was fed to a saturator [35] maintained at a temperature which provided a vapor pressure of less than 10 torr for that particular species. A reduced copper catalyst (BASF) was used to remove residual oxygen from the helium. For furan, the heater was replaced by a styrofoam box (2 in walls) and the saturator was placed in a dry ice/acetone bath. The system was maintained at 195 K, providing a furan vapor pressure of about 1 torr, or about 0.1 mol %. The saturator was maintained at 330 K for γ-butyrolactone, providing a feed of about 1 % hydrocarbon. The saturator was maintained at 340 K for maleic anhydride, providing a feed of slightly less than 1 mol % hydrocarbon.

Loaded reactors were purged with helium for longer that 3 h, then heated from room temperature to reaction temperature (773 K for n-butane, 723 K for other feeds) and held at reaction temperature for 1 h. Pulsing of the desired feed was then

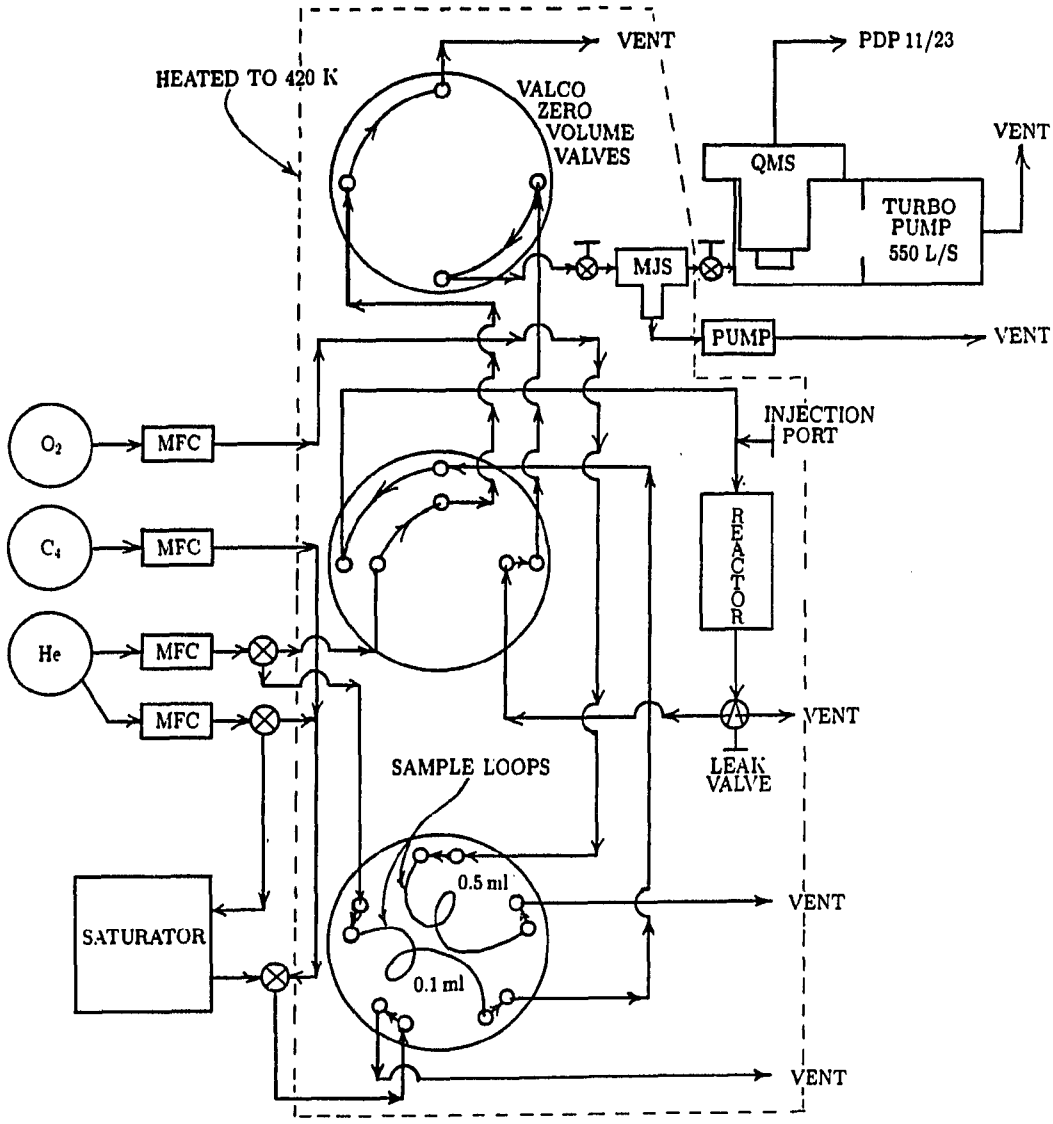

Figure 1: Reactor system

commenced at a rate of one pulse per minute. Each experiment consisted of at least 75 pulses.

Mass spectral analysis of the products of n-butane, 1-butene, 1,3-butadiene, furan, γ-butyrolactone and maleic anhydride reaction over the ^{18}O-enriched catalyst was performed by a UTI 100C precision quadrupole mass analyzer controlled by a PDP 11/23 computer [36]. The mass analyzer was interfaced with the microreactor system by a glass SGE single stage molecular jet separator.

The ^{18}O content of maleic anhydride, CO_2, furan and, when applicable, γ-butyrolactone, was determined for the oxidation of n-butane, 1-butene, 1,3-butadiene, furan, γ-butyrolactone and maleic anhydride. As a result of the pulse nature of these experiments, it was not possible to accurately monitor the entire spectral region of interest for all pulses. Therefore, the mass spectrum was divided into 5 small ranges, which would be monitored, one range per pulse. The ranges and the species in those ranges are presented in Table 1. Typical peaks were 3-5 seconds wide, depending on the species observed. Survey scans covering the entire spectral range were made using unlabeled catalyst to ensure that all species present were accounted for.

Mass spectral data were collected for all feed species on both labeled and unlabeled catalysts. All species present were then accounted for and any interferences (spectral overlaps) of crucial mass to charge ratios (m/e) noted. A sample set of peaks for maleic anhydride produced from n-butane is presented in Figure 2. The peaks were integrated by summing the intensities of each scan from the beginning of the peak to the end. Early, low level scans were used as background, normalized to the same number of scans as the integration, and then subtracted from the integrated intensity. This was done for all peaks of interest.

Table 1: Mass spectral ranges scanned every fifth pulse and species of interest in those ranges

Range (m/e)	Species	Number of Scans/Peak
42–50	CO_2	80
17–22	H_2O	80
67–90	furan & γ–butyrolactone	20
95–110	maleic anhydride	30
50–60	n–butane, 1–butene, 1,3–butadiene	40

Occasionally, fragments from species present would give m/e peaks coincident with m/es of interest. This necessitated the use of correction factors for that m/e based on another m/e of the offending species. These factors were based on the accumulation of large numbers of scans of the mass spectrum of the offending species. The factors used are presented in Table 2.

The ^{18}O present in each species was then accounted for and calculated as a percentage of total oxygen present in that species. The percent ^{18}O in maleic anhydride was calculated according to the following formula:

$$\%^{18}O_{MAN} = \frac{\sum I_{100} + 2\sum I_{102} + 3\sum I_{104}}{3(\sum I_{98} + \sum I_{100} + \sum I_{102} + \sum I_{104})}$$

For 1–butene and 1,3–butadiene, phthalic anhydride was formed and the intensity at m/e 104 had to be corrected for this contribution.

The percent ^{18}O in furan was calculated according to the following formula:

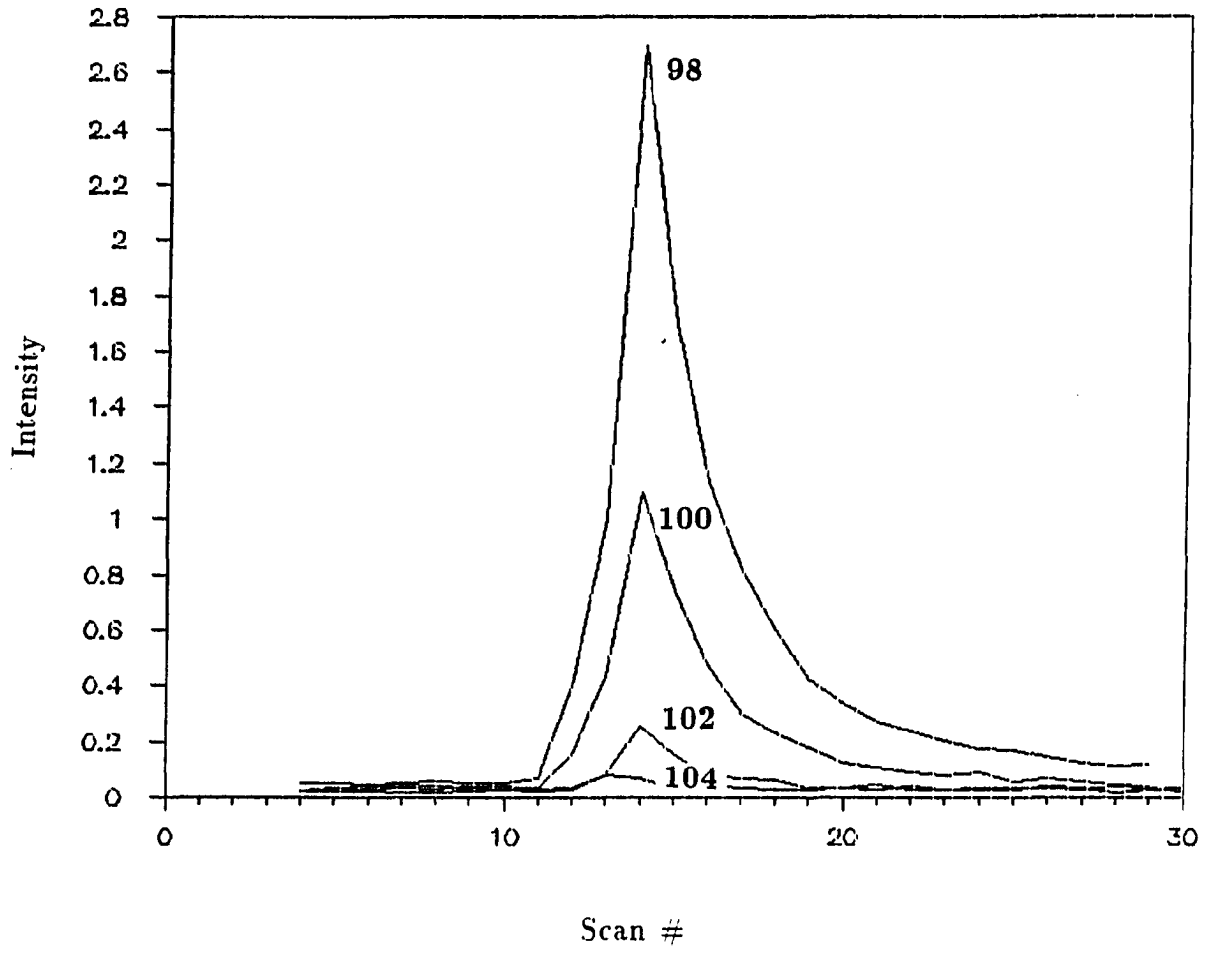

Figure 2: Sample mass spectral data: maleic anhydride produced from a 2% n-butane pulse over β-$VOPO_{7/2}{}^{18}O_{1/2}$

Table 2: Mass spectral data correction factors

m/e Peak	Interfering Species	Interfered Species	Reference m/e	Correction Factor (f)[a]
44	n-butane	CO_2	43	0.03
70	maleic anhydride	^{18}O labeled furan	82	0.9
104	phthalic anhydride	^{18}O x 3 labeled maleic anhydride	105	12.6

[a] $I_{cor} = I_{raw} - f \times I_{ref}$ All corrections are typically less than 15% of total I_{raw} peak.

$$\%^{18}O_{FUR} = \frac{\Sigma I_{70}}{\Sigma I_{68} + \Sigma I_{70}}$$

Corrections were made for interference at m/e 70 from a minor maleic anhydride fragment.

The percent ^{18}O in CO_2 was calculated according to the following formula:

$$\%^{18}O_{CO_2} = \frac{\Sigma I_{44} + 2\Sigma I_{48}}{2(\Sigma I_{44} + \Sigma I_{46} + \Sigma I_{48})}$$

Corrections were made by subtracting the minor interferences at m/e 44 from n-butane and background CO_2. CO could also be observed, but the data were significantly complicated by interference from background N_2 and $C^{16}O$.

EXPERIMENTAL RESULTS

Characterization of pre and post reaction catalysts

No change in Raman spectra occurred from pre to post reaction (up to 100 pulses). A complete discussion of the isotopically labeled bonds as indicated by laser Raman spectroscopy has been provided previously [34].

Mass Spectrometry Studies

The average ^{18}O content observed in all products for each species fed is summarized in Table 3 while the relative production of each product per pulse is presented in Table 4.

^{18}O incorporation into the products of n–butane oxidation

Maleic anhydride, furan and CO_2 were produced from all n–butane pulses. While the level of production of each species changed (less than 50%), the ^{18}O levels in those products remained nearly constant. Twelve percent of the total oxygen in the maleic anhydride produced from n-butane over β–$VOPO_{7/2}{}^{18}O_{1/2}$ was ^{18}O. ^{18}O was observed at the 5% level in the CO_2 produced in the same reaction. Furan was formed containing ^{18}O at the 28% level.

Table 3: Summary of ^{18}O content in all products for each species fed to β-$VOPO_{7/2}{}^{18}O_{1/2}$ in the absence of gas phase oxygen

	Maleic Anhydride	Furan	CO_2	γ-Butyrolactone
n-Butane	12%	28%	4.5%	-
1-Butene	14%	13%	9.5%	-
1,3-Butadiene	14%	14%	8%	-
Furan	9.5%	0%	7%	-
γ-butyrolactone	12%	22%	5%	3-4%
Maleic anhydride	5.5%	9-16%	1%	-

Table 4: Summary of relative production per pulse of various products from species fed to β-$VOPO_{7/2}{}^{18}O_{1/2}$ in the absence of gas phase oxygen

	Maleic Anhydride	Furan	CO_2
n-Butane[a]	1	1	1
1-Butene	5	30	20
1,3-Butadiene	100	30	30
Furan	2	2	4
γ-butyrolactone	1	2	10
Maleic anhydride	0.1	20	10

[a]The production level per pulse is normalized to the production level observed for that product from n-butane.

^{18}O incorporation into the products of 1-butene oxidation

Maleic anhydride, furan and CO_2 were produced from all 1-butene pulses. 1-butene pulses (2% in helium) produced over thirty times as much maleic anhydride, five times as much furan and twenty times as much CO_2 per pulse as n-butane produced. Maleic anhydride and CO_2 production levels fell 90% from pulse one to pulse 75, yet the ^{18}O content of the products remained nearly constant. Furan production levels remained constant throughout the experiment. After about 5 pulses, phthalic anhydride was observed, creating a fragment at m/e 104. Maleic anhydride produced from 1-butene pulses over β-$VOPO_{7/2}{}^{18}O_{1/2}$ contained oxygen which was 14% ^{18}O. Furan produced in this reaction contained oxygen which was 12% ^{18}O, while CO_2 was produced containing oxygen which was 10 % ^{18}O.

^{18}O incorporation into products of 1,3-butadiene oxidation

Maleic anhydride, furan, CO_2 and phthalic anhydride were produced from all 1,3-butadiene pulses. 1,3-butadiene pulses (2% in helium) produced over thirty times as much maleic anhydride, 100 times as much furan and over 30 times as much CO_2 per pulse as n-butane produced. Production of maleic anhydride per pulse fell 95%, CO_2 production per pulse fell 80%, while furan production remained unchanged from pulse 1 to pulse 75. ^{18}O content of these species remained at the same level throughout the experiments. Maleic anhydride was produced from 1,3-butadiene over β-$VOPO_{7/2}{}^{18}O_{1/2}$ with an oxygen content of 14.5% ^{18}O. Furan was produced in the same reaction with an oxygen content of 13% ^{18}O. Carbon dioxide was produced from 1,3-butadiene with an oxygen content of 8.5% ^{18}O.

^{18}O incorporation into products of furan oxidation

Maleic anhydride and CO_2 were produced from nearly all furan pulses. Furan pulses (0.1% in helium) eventually produced twice as much maleic anhydride and four times as much CO_2 per pulse as did the n-butane pulses. Maleic anhydride was not detected on the first furan pulse in any experiment, but from pulse two to pulse 75, the production level increased 2000%, while CO_2 production per pulse remained nearly constant. ^{18}O content of these species remained nearly constant throughout the experiment. Maleic anhydride was produced from furan pulses over β-$VOPO_{7/2}{}^{18}O_{1/2}$ containing oxygen which was about 9.5% ^{18}O. CO_2 was produced in the same reaction containing oxygen which was about 7% ^{18}O. No evidence for oxygen exchange between furan and ^{18}O from the catalyst was observed.

^{18}O incorporation into products of γ-butyrolactone oxidation

Maleic anhydride, furan and CO_2 were produced from all pulses of γ-butyrolactone (less than 1% in helium) over β-$VOPO_{7/2}{}^{18}O_{1/2}$. The production of maleic anhydride from γ-butyrolactone pulses began at very low levels and increased with pulse number by greater than 60%. The final level was approximately twice that produced from n-butane pulses. CO_2 was produced at a level 10 times greater per pulse than that of n-butane. The production of CO_2 fell by 50% from pulse 1 to pulse 75. Initially, furan was produced from γ-butyrolactone pulses at low levels, but the production per pulse increased by over 70% to the same level observed in the n-butane experiments. Maleic anhydride produced from γ-butyrolactone contained oxygen which was nearly 12% ^{18}O. Furan produced from γ-butyrolactone pulses contained about 22.5% ^{18}O. CO_2 produced

from γ–butyrolactone pulses contained oxygen which was about 6% ^{18}O. Effluent γ–butyrolactone contained oxygen which was 3–4% ^{18}O.

^{18}O incorporation into products of maleic anhydride oxidation

Furan and CO_2 were produced from all maleic anhydride pulses (less than 1 % in helium) over β–$VOPO_{7/2}{}^{18}O_{1/2}$. Maleic anhydride pulses produced furan at about one–tenth the level and CO_2 at about ten times the level per pulse as n–butane. ^{18}O content of these species remained nearly constant throughout the experiment. Furan was produced from maleic anhydride over β–$VOPO_{7/2}{}^{18}O_{1/2}$ containing oxygen which was about 13% ^{18}O. CO_2 was produced in the same experiment containing oxygen which was less than 2% ^{18}O. Effluent maleic anhydride contained oxygen which was 5–6% ^{18}O. This level did not change when the partial pressure of maleic anhydride fed to the reactor was reduced by about 30%.

DISCUSSION

Structural Considerations

The β–$VOPO_4$ structure consists of irregular VO_6 octahedra which form corner sharing chains through V=O–V bonding [37]. Sheets of these chains exist in the β–$VOPO_4$ phase. The PO_4 tetrahedra share oxygen atoms with four separate VO_6 octahedra in three separate chains. Adjacent sheets of VO_6 octahedra are bridged by corner sharing of two equivalent oxygen atoms of the PO_4 group with VO_6 groups positioned above and below. These P–O–V oxygens will be referred to as bridging (B) oxygens in this discussion. The PO_4 group also shares corners with two octahedra in the same octahedral chain. These latter two oxygen atoms are crystallographically distinct as a result of the displacement of the vanadium atom from the center of the octahedron. These P–O–V species are in the equatorial plane of the VO_6 octahedron and will be referred to as E_1 and E_2 oxygens.

These crystallographically distinct oxygens (B, E_1, and E_2) give rise to distinct peaks in the Raman spectrum of β–$VOPO_4$ [2]. As shown previously [34], when β–$VOPO_4$ is enriched with ^{18}O by the following reaction

$$(VO)_2P_2O_7 + 1/2\ {}^{18}O_2 \longrightarrow 2\ \beta\text{-}VOPO_{7/2}{}^{18}O_{1/2}$$

Table 5: ^{18}O distribution in β-$VOPO_{7/2}{}^{18}O_{1/2}$

Lattice Oxygen Species	Designation	^{18}O Content
V=O-V		0%
V-O-P[a]	E_1	0%
V-O-P[b]	B	5%
V-O-P[c]	E_2	40%
		All V-O-Ps: 12.5% Overall: 10%

[a] 1 per PO_4 group.
[b] 2 per PO_4 group.
[c] 1 per PO_4 group.

the ^{18}O goes into specific lattice positions. It was shown that V=O and E_1 oxygens were not enriched with ^{18}O, while B oxygens became 5 % enriched. E_2 oxygens gained the most ^{18}O, becoming 40 % ^{18}O. This results in an overall oxygen content of 10 % ^{18}O. The ^{18}O distribution is depicted in Figure 3 and summarized in Table 5.

Maleic anhydride produced from n-butane and 1-butene in the absence of gas phase oxygen over catalyst labeled in this manner contains oxygen which is 13 % ^{18}O, while CO_2 oxygen contains considerably less ^{18}O [34]. The present work refines and extends the previous work. Similar experiments (n-butane and 1-butene) were performed in pulse rather than continuous mode. Identical results were obtained for ^{18}O content in maleic anhydride and CO_2. Additionally, furan produced in these reactions was monitored for ^{18}O incorporation. Similar experiments performed with 1,3-butadiene, furan, γ-butyrolactone and maleic

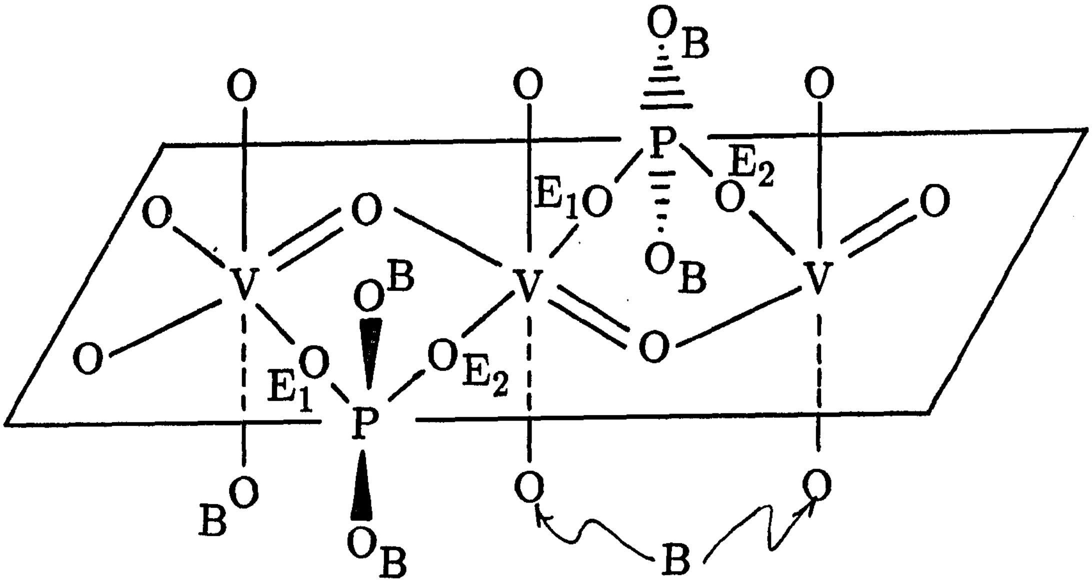

Figure 3: ^{18}O distribution in β-$VOPO_{7/2}{}^{18}O_{1/2}$

anhydride provided information regarding the interaction of these species with the various lattice oxygens and the potential of these species as intermediates in the reaction forming maleic anhydride from n-butane over β-$VOPO_4$.

^{18}O Levels in the Products of C_4 Oxidation

^{18}O levels in maleic anhydride

A comparison of ^{18}O levels in maleic anhydride for all species fed is presented in Figure 4. The formation of maleic anhydride from n-butane, 1-butene and 1,3-butadiene over β-$VOPO_{7/2}{}^{18}O_{1/2}$ appears to occur in a similar manner for all three cases. The ^{18}O levels observed for maleic anhydride produced from these three species indicated that oxygen used to produce maleic anhydride comes from a lattice "pool" composed of approximately 13 % ^{18}O. This indicates that some combination of the three different types of P-O-V oxygens are involved. Similarly, the ^{18}O levels observed in maleic anhydride when furan is fed to the system indicate that:

1. The original oxygen in furan is not exchanged
2. The two additional oxygens come from a pool of oxygen which is about 13 % ^{18}O, perhaps the same pool which was utilized by n-butane, 1-butene and 1,3-butadiene.

Unlike furan, γ-butyrolactone, which contains two oxygens, forms maleic anhydride containing oxygen which is 12 % ^{18}O. This indicates that furan and γ-butyrolactone are not likely consecutive intermediates in the formation of maleic anhydride from n-butane over this catalyst. The simplest explanation for the observed level of ^{18}O in maleic anhydride formed from γ-butyrolactone is, in addition to the observed exchange, a majority of the third oxygen inserted

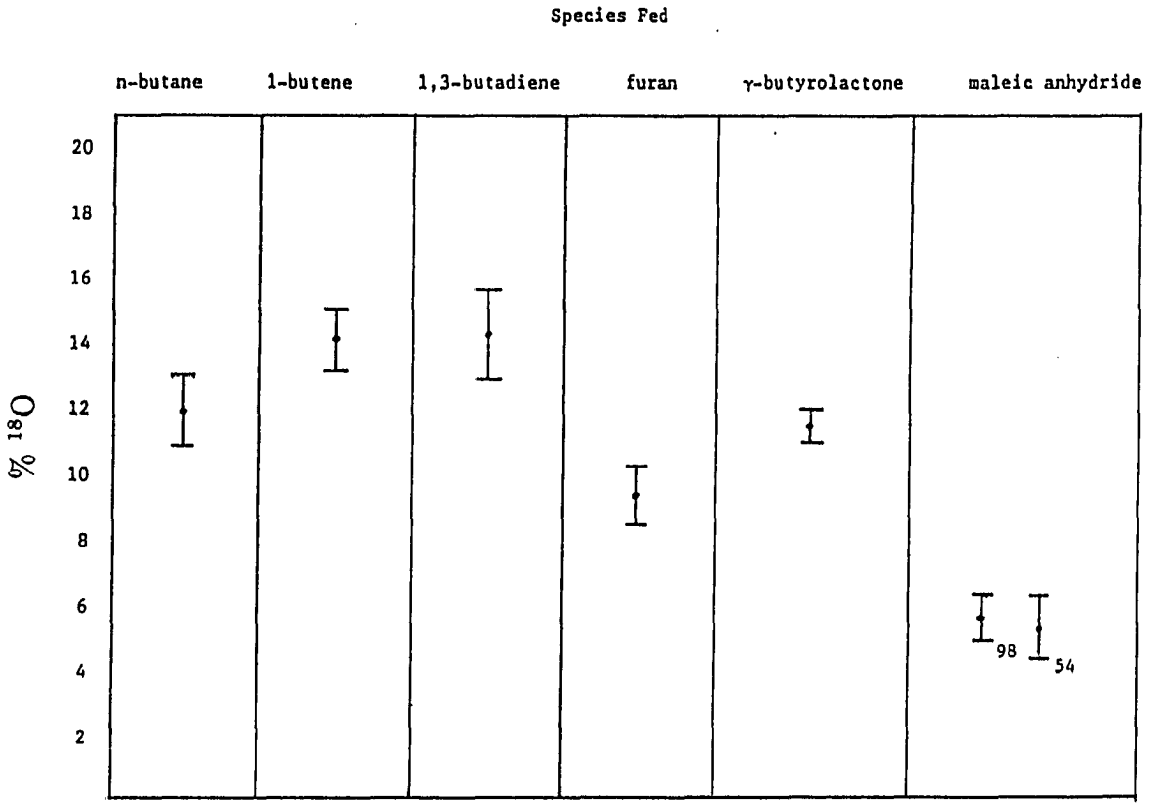

Figure 4: Comparison of ^{18}O content in maleic anhydride produced from various feeds over β-$VOPO_{7/2}{}^{18}O_{1/2}$

originates from a site containing high levels of ^{18}O (E_2), with some coming from sites with lower levels of ^{18}O (B or E_1).

Maleic anhydride "produced" when maleic anhydride pulses were fed contained low levels of ^{18}O (5 %). This indicates that maleic anhydride can interact reversibly with selective sites. The exchange could be the result of the formation of maleic acid then subsequent dehydration to maleic anhydride. Maleic anhydride combustion experiments [35] indicate that maleic acid is formed at low levels under these conditions. The 5 % enrichment is observed for the 54 m/e fragment of maleic anhydride, which contains only terminal maleic anhydride oxygens [38]. Thus all maleic anhydride oxygens are involved in the exchange, adding justification to an exchange mechanism which involves ring opening. To create the ^{18}O levels observed, the fourth oxygen added would have to be about 20 % ^{18}O.

^{18}O levels in CO_2

A comparison of ^{18}O levels in CO_2 from all species fed is shown in Figure 5. The trend indicated by these data appears to be the result of two opposing forces:

1. The reactivity of the feed molecule
2. The "oxidation state" of the feed molecule.

n–Butane, the most difficult species of those fed to activate and oxidize, shows the lowest ^{18}O content of CO_2 of all feeds with the exception of maleic anhydride. This level doubles when 1–butene is the feed and decreases as the feed species becomes less saturated with hydrogen and has more oxygens inserted, until maleic anhydride, which exhibits very low levels of ^{18}O in the CO_2 produced from it, is fed. n–Butane and maleic anhydride, the feed and product of most interest, exhibit the most

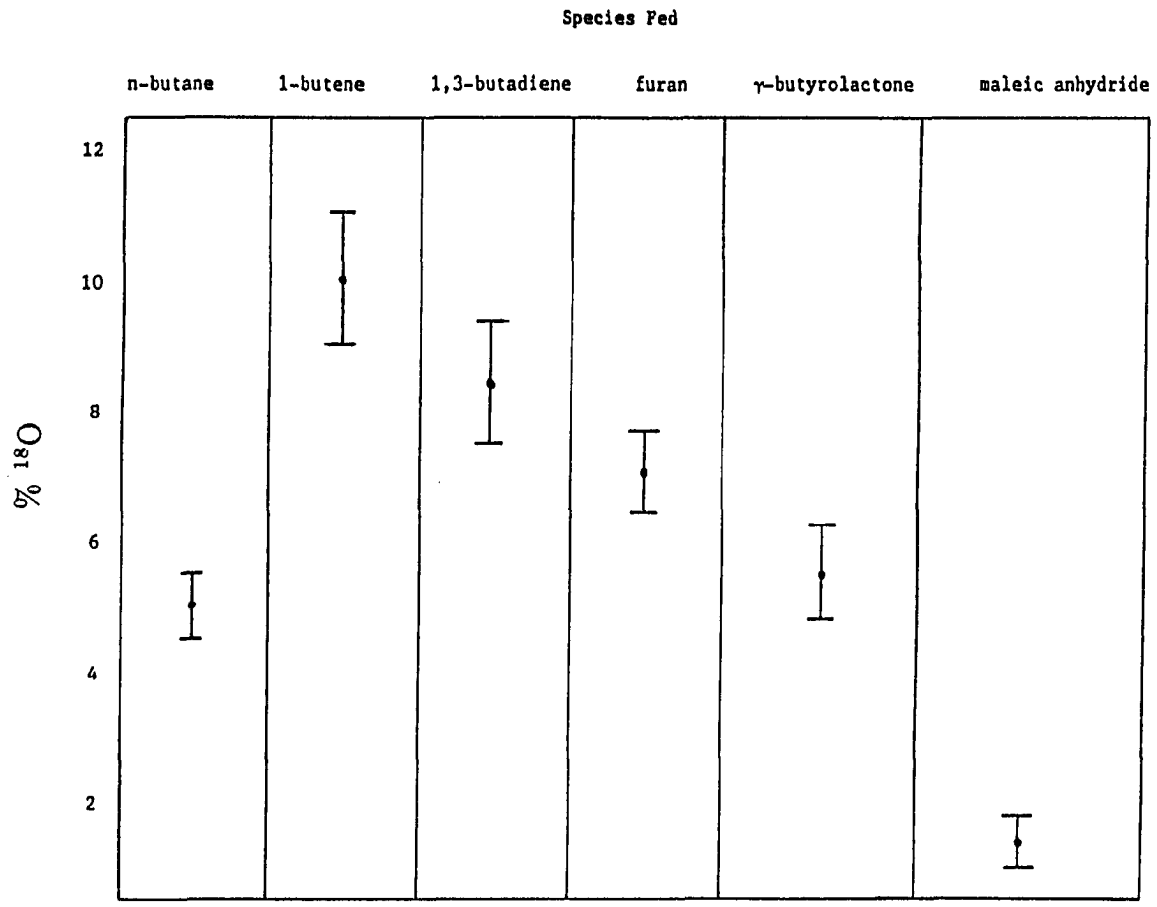

Figure 5: Comparison of ^{18}O content in CO_2 produced from various feeds over β-$VOPO_{7/2}{}^{18}O_{1/2}$

interesting behavior. Since all feeds produce maleic anhydride at one type of site with a particular level of ^{18}O, those species producing CO_2 with elevated levels of ^{18}O must be producing CO_2 at a greater variety of sites and at higher levels (as observed) than species producing CO_2 with ^{18}O at lower levels. Thus, of all species fed, n-butane and maleic anhydride show the most "selective" interaction with the catalyst. And more importantly, maleic anhydride is combusted mainly at sites which contain no ^{18}O. The same can be said for none of the other species fed. This clearly indicates that CO_2 is formed from n-butane by pathways not limited to only the consecutive combustion of maleic anhydride. A pathway which allows combustion at sites containing ^{18}O must be considered in view of these results.

^{18}O levels in furan

All species studied produced furan. The ^{18}O levels observed in furan formed from each species fed are shown in Figure 6. These results reveal much about the initial insertion of oxygen into n-butane derived intermediates and the initial interaction of the various species fed with catalytic sites. While n-butane, 1-butene and 1,3-butadiene produced maleic anhydride with similar levels of ^{18}O, such was not the case with furan produced from these species. The ^{18}O level observed in furan produced from n-butane is more than twice that observed for 1-butene and 1,3-butadiene. This indicates that, while the overall result is nearly the same (^{18}O level in maleic anhydride), the initial interaction and activation of the paraffin on this catalyst is fundamentally different from that of the olefins. It appears that the initial interaction of n-butane, which has been shown to irreversibly adsorb on VPO catalysts [28], is much more particular about which oxygens are inserted to form furan. While this does not rule out the possibility of strongly adsorbed olefins as

intermediates, it does suggest that free olefins have a limited, if any, role in the mechanism.

Mechanistic Ramifications

The information provided by the structure and labeling of β-$VOPO_{7/2}{}^{18}O_{1/2}$ and the evidence provided by species produced over this catalyst provides fundamental information on the mechanism of the oxidation of n-butane to maleic anhydride over β-$VOPO_4$. A comparison of the ^{18}O content of furan produced from n-butane and that produced from 1-butene and 1,3-butadiene shows that the initial activation of n-butane on this catalyst occurs in a manner such that the resulting strongly adsorbed intermediate can be oxidized to an adsorbed furan like species at only very specific sites. Under aneorobic conditions, small amounts of this species desorb as furan, containing high levels of ^{18}O. It is likely that a highly enriched P-O-V oxygen (E_2) is responsible for the majority of this oxygen insertion function. The ^{18}O levels observed in furan formed from 1-butene and 1,3-butadiene indicate that this furan is formed at random P-O-V sites (E_1, E_2 and B), a result of the greater reactivity of these olefins. Since no free olefins are observed when n-butane is fed and the resulting ^{18}O content of furan is so different than that of the olefins, free olefins can be ruled out as a major pathway from n-butane to maleic anhydride.

The ^{18}O content of maleic anhydride formed from the various species provides further mechanistic information. In the case of n-butane, maleic anhydride is formed by the insertion of two oxygens into an adsorbed furan like species. The adsorbed furan like species contains one oxygen which, on the average, is about 28 % ^{18}O. To produce maleic anhydride containing 13 % ^{18}O, these two additional

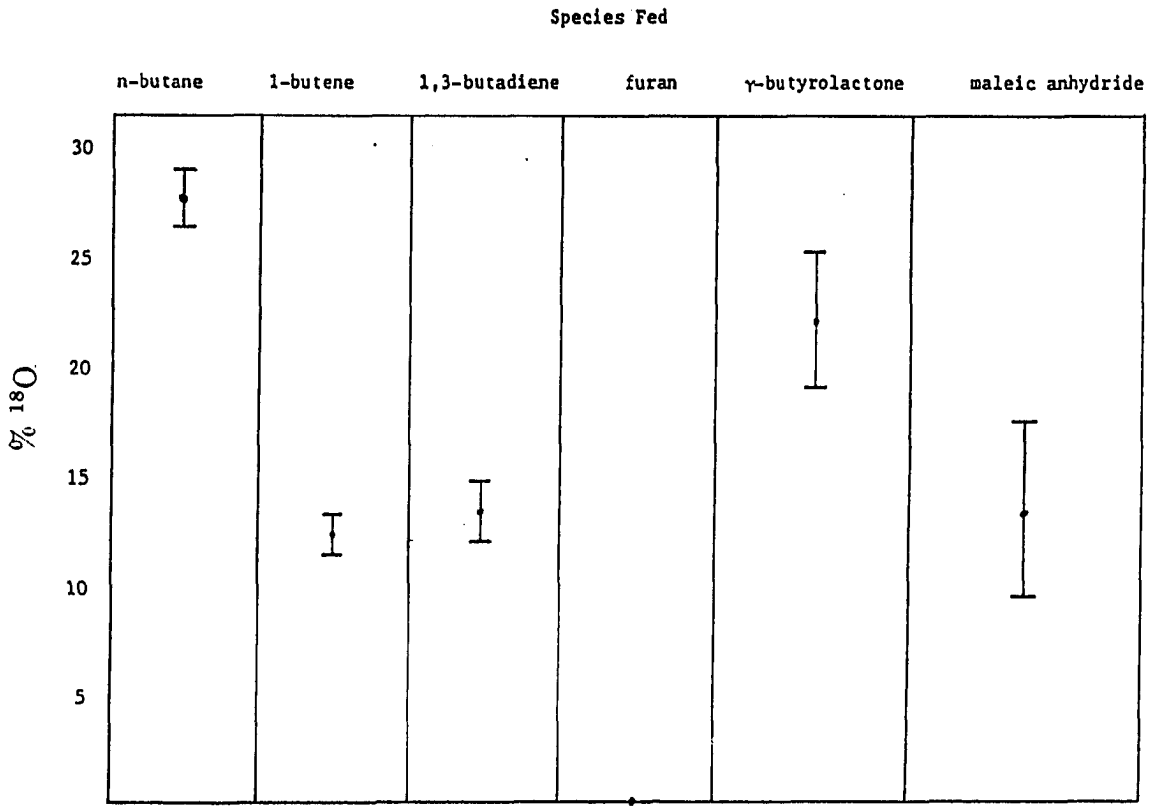

Figure 6: Comparison of ^{18}O content in furan produced from various feeds over β-$VOPO_{7/2}{}^{18}O_{1/2}$

oxygens would have to be approximately 5 % ^{18}O each. This corresponds well to the ^{18}O enrichment of site B. 1-butene and 1,3-butadiene form furan at all P-O-V sites and then utilize the same sites for maleic anhydride formation from this furan, as indicated by the ^{18}O levels observed.

Maleic anhydride production from a furan feed shows that all P-O-V sites are utilized for free furan conversion to maleic anhydride. This indicates that, for olefins, free furan may be a major pathway to maleic anhydride. Also, since furan is so easily combusted, this free furan could account for much of the nonselective oxidation observed for the olefins. Conversly, though a small amount of free furan is observed during anaerobic oxidation of n-butane, free furan cannot be a major pathway to maleic anhydride from n-butane. If free furan was a major pathway, furan from n-butane (28 % ^{18}O) would form maleic anhydride with greatly elevated ^{18}O levels (at least 17 %).

These mechanistic steps can be associated with specific lattice oxygens in β-$VOPO_4$. P-O-V E_1 and E_2 are crystallographically distinct and probably have slightly different reactivities. On the other hand, they occupy very similar positions in the crystal structure. Thus, as the level of ^{18}O observed in furan from n-butane is 28 % (intermediate to the 40 % observed in E_2 and the 0 % observed in E_1) and the next two oxygens inserted are enriched with ^{18}O at the 5 % level (as observed in P-O-V B), it is proposed here that upon initial activation, n-butane forms a strongly adsorbed olefinic species which is constrained in such a manner that it can form an adsorbed furan like species at only P-O-V E_2 or E_1. E_2 is more reactive (longer bonds [37]) than E_1; thus the observed ^{18}O content of furan formed at these sites is skewed towards the 40 % level. Specifically, the numbers observed indicate that 80 % of the adsorbed furan like species is formed at site E_2, while 20 % is

formed at E_1. This species then reacts (in the same ratio) with the two P–O–V's available (5 % ^{18}O) to result in maleic anhydride containing 13 % ^{18}O, as observed. This explanation takes into account all available structural information and all observed mass spectral information. Several other scenarios can be conceived, but none explain all the observed data as this one does.

All ^{18}O levels observed for species produced from γ–butyrolactone indicate that this species exhibits behavior considerably different from all other feeds studied, thus it is highly unlikely that γ–butyrolactone is a major intermediate in the oxidation of n–butane to maleic anhydride over β–$VOPO_4$.

CONCLUSIONS

n–Butane is adsorbed and activated on β–$VOPO_4$ in an irreversible and very particular manner which results in a highly constrained adsorbed olefinic species. This species can then react with adjacent P–O–V sites E_1 or E_2, depending on the adsorbed species orientation. Site E_2 reacts roughly 4 times as fast as site E_1, resulting in adsorbed furan like species, 80 % containing E_2 oxygens, 20 % containing E_1 oxygens. The furan like species is then further oxidized by the adjacent B P–O–V oxygens (two per PO_4 tetrahedra) to form maleic anhydride, the majority of which then desorbs. Free olefins and free furan do not play a major role in this mechanism, nor does γ–butyrolactone of any type.

Conversly, free olefins, such as 1–butene and 1,3–butadiene are less selective about which oxygens are used to form furan. All P–O–V oxygens are utilized in this reaction. In turn, all P–O–V oxygens are used to complete the conversion to maleic anhydride. This is a direct result of the less selective manner in which the oxidation of olefins is initiated with respect to n–butane.

Free furan reacts in a manner consistent with the observed reaction of furan formed from olefins. Maleic anhydride formed from free furan utilizes all P–O–V oxygens.

Figure 7 depicts the selective oxidation of n–butane on a plausible reaction surface of β–$VOPO_4$.

Conversion of n–butane to carbon oxides cannot be attributed solely to the combustion of maleic anhydride. While this route may account for a significant portion of the conversion to carbon oxides, nonselective activation (cracking) and combustion of reactive intermediates also provide pathways to carbon oxides.

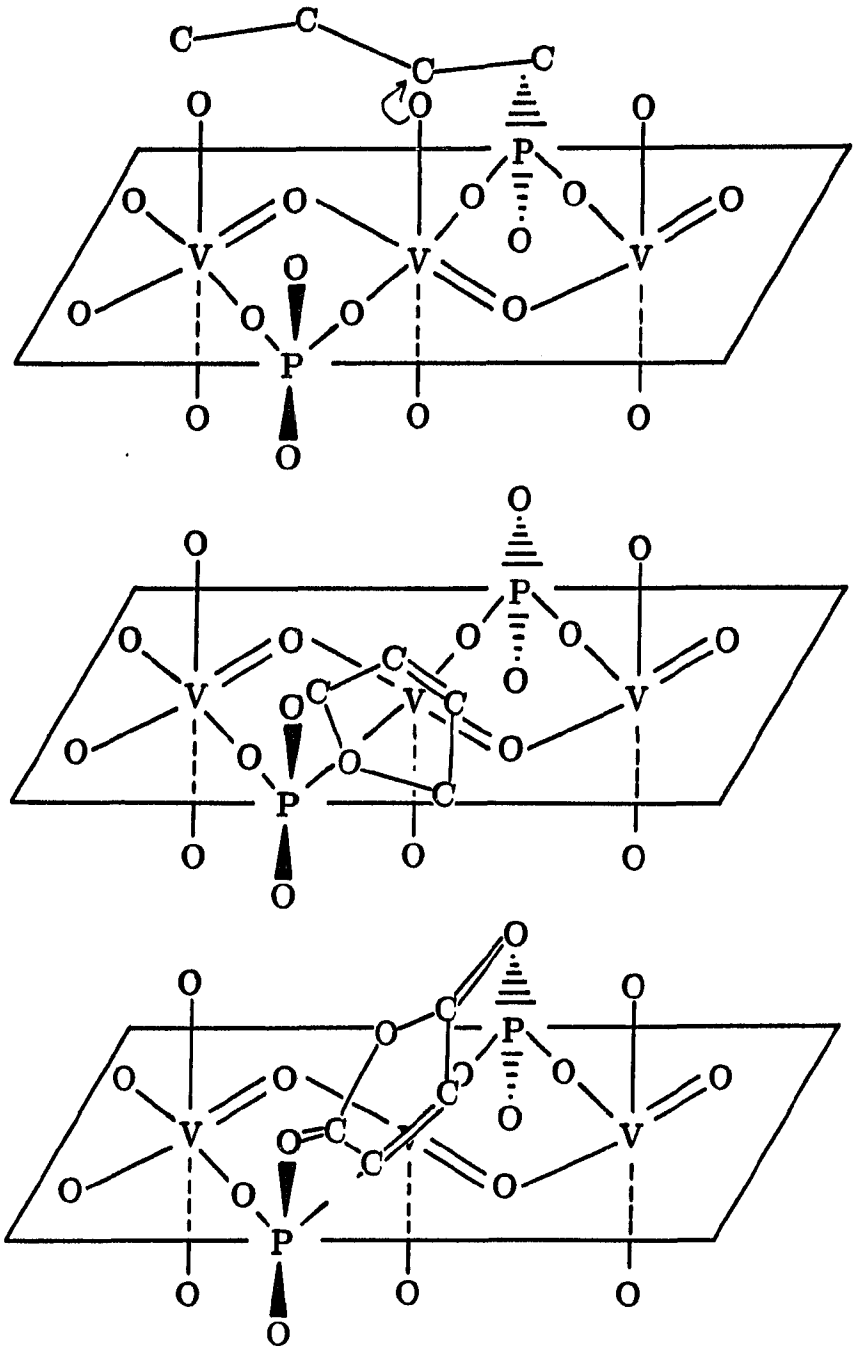

Figure 7: Selective oxidation of n-butane on a plausible reaction surface of β-$VOPO_4$: (a) activation, (b) formation of adsorbed furan-like species, (c) formation of maleic anhydride

ACKNOWLEDGMENT

This work was performed at Ames Laboratory under contract No. W-7405-eng-82 with the U. S. Department of Energy. The United States government has assigned the DOE Report number IS-T 1411 to this thesis.

REFERENCES CITED

1. Busca, G.; Centi, C.; Journal of the American Chemical Society (1989) **111**, 46.
2. Moser, T. P.; Schrader, G. L. Journal of Catalysis (1985) **92**, 216.
3. Wenig, R. W.; Schrader, G. L. Journal of Physical Chemistry (1986) **90**, 6480.
4. Ostroushko, V. I.; Kernos, Yu. D.; Ioffe, I. I. Neftekhimiya (1972) **12(3)**, 95.
5. Morselli, L.; Riva, A.; Trifiro, F.; Emig, G. La Chimica E L'Industria (1978) **60(10)**, 791.
6. Ai, M.; Bountry, P.; Montarnal, R. Bulletin de la Societe Chimique de France (1970) **8–9**, 2775.
7. Ai, M. Bulletin of the Chemical Society of Japan (1970) **43(1)**, 3490.
8. Varma, R. L.; Saraf, D. N. Journal of Catalysis (1978) **55**, 361.
9. Escardino, A.; Sola, C.; Ruiz, F. Aneles de Quimica (1973) **69**, 385.
10. Wohlfhart, K.; Hofmann, H. Chemie Ingenièur Technik (1980) **52(10)**, 811.
11. Hodnett, B. K.; Permanne, Ph.; Delmon, B. Applied Catalysis (1983) **6**, 231.
12. Wustneck, N.; Wolf, H.; Seeboth, H. Reaction Kinetics and Catalysis Letters (1982) **21(4)**, 497.
13. Centi, G.; Fornasari, G.; Trifiro, F. Journal of Catalysis (1984) **89**, 44.
14. Hodnett, B. K.; Delmon, B. Applied Catalysis (1985) **15**, 141.
15. Centi, G.; Manenti, I.; Riva, A.; Trifiro, F. Applied Catalysis (1984) **9**, 177.
16. Morselli, L.; Trifiro, F.; Urban, L. Journal of Catalysis (1982) **75**, 112.
17. Ai, M. Journal of Catalysis (1981) **67**, 110.

18. Puttock, S. J.; Rochester, C. H. Journal of the Chemical Society Faraday Transactions 1 (1986) **82**, 3033.

19. Busca, G.; Centi, G.; Trifiro, F.; Lorenzelli, V. Journal of Physical Chemistry (1986) **90**, 1337.

20. Puttock, S. J.; Rochester, C. H. Journal of the Chemical Society Faraday Transactions 1 (1986) **82**, 2773.

21. Centi, G.; Golinelli, G.; Trifiro, F. Bicentenary Catalysis (1988), 191.

22. Bordes, E.; Courtine, P. Journal of the Chemical Society, Chemical Communications (1985), 294.

23. Bordes, E.; Courtine, P. Journal of Catalysis (1979) **57**, 236.

24. Wenig, R. W.; Schrader, G. L. Industrial Engineering Chemistry Fundamentals (1986) **25**, 612.

25. Garbassi, F.; Bart, B.; Tassinari, R.; Vlaic, G.; and Lagarde; P. Journal of Catalysis (1986) **98**, 317.

26. Hodnett, B.; Delmon, B. Journal of Catalysis (1984) **88**, 43.

27. Busca, G.; Centi, G.; and Trifiro, F. Journal of the American Chemical Society (1985) **107**, 7758.

28. Pepera, M. A.; Callahan, J. L.; Desmond, M. J.; Milberger, E. C.; Blum, P. R.; Bremer, N. J. Journal of the American Chemical Society (1985) **107**, 4883.

29. Kurchinin, Yu.; Mishchenko, Yu.; Nechiporuk, P.; Gel'bshtein, A. Kinetica i Kataliz (1984) **25(2)**, 369.

30. Moser, T.P.; Schrader, G.L. Journal of Catalysis (1987) **104**, 99.

31. Centi, G.; Trifiro, F. Catalysis Today (1988) **3**, 151.

32. Gleaves, J. T.; Ebner, J. R.; Kuechler, T. C. Catalysis Reviews, Science and Engineering (1988) **30(1)**, 49.

33. Contractor, R. M.; Sleight, A. W. Catalysis Today (1988) **3**, 175.

34. Lashier, M. E.; Moser, T.P.; Schrader, G.L.; In *Studies in Surface Science and Catalysis: New Developments in Selective Oxidation*; Centi, G., Trifiro, F., eds. (Elsevier:Amsterdam, 1990).

35. Moser, T.P.; Wenig, R.W.; Schrader, G.L. Applied Catalysis (1987) **34**, 39.

36. McCarty, K.F. Dissertation, Iowa State University, Ames, IA (1985).

37. Gopal, R.; Calvo, C. Journal of Solid State Chemistry (1972) 5, 432.

38. Stenhagen, E.; Abrahamson, S.; McLafferty, F.W. eds.
Atlas of Mass Spectral Data (Interscience Publishers, New York, 1969).

PART III.

THE ROLE OF LATTICE OXYGENS IN THE OXIDATION OF C_4 HYDROCARBONS OVER $(VO)_2P_2O_7$

ABSTRACT

The role of the lattice oxygens of $(VO)_2P_2O_7$ in the oxidation of C_4 hydrocarbons has been investigated using a catalyst with specific oxygen sites labeled with ^{18}O. Labeled and unlabeled lattice oxygens were identified by laser Raman spectroscopy and Fourier transform infrared spectroscopy, while ^{18}O incorporation into the products of oxidation was monitored by mass spectrometry. The results of this study link specific lattice oxygens with specific mechanistic steps, including both selective and nonselective steps. Alternating pulses of $^{16}O_2$ and $^{18}O_2$ revealed that sites maintain their identity (selective verses nonselective) even upon reoxidation with gas phase oxygen. The oxidation of strongly adsorbed intermediates during $^{18}O_2$ pulses shows that these intermediates are highly oxygenated.

INTRODUCTION

The heart of any catalytic process is the catalytic active site. A fundamental understanding of the catalytic process requires a fundamental understanding of the active site. The selective oxidation of n-butane to maleic anhydride over VPO catalysts is no exception. This 14 electron process involves the activation of a paraffin, stabilization of reactive intermediates, removal of 8 hydrogen atoms and the insertion of 3 oxygen atoms. Several mechanisms for this reaction, usually involving adsorbed or free olefins (butene and butadiene) and oxygenated species (furan, tetrahydrofuran, and γ-butyrolactone), have been proposed [1-17].

A particular VPO phase, $(VO)_2P_2O_7$, has been identified as an especially active and selective catalyst for the conversion of n-butane to maleic anhydride. Though the most active and selective catalysts are complicated and difficult to characterize, the $(VO)_2P_2O_7$ phase has been identified as an essential component for active and selective catalysts. As a result, much research has focused on this phase, and its physical and chemical characteristics have been well characterized [2, 16, 18-27].

Recently, fundamental characteristics of the active sites have attracted attention. A particular focus has been placed on the various oxygen species present in the working catalyst. Gleaves and Ebner have investigated the role of various oxygen species in the selective oxidation of n-butane to maleic anhydride over

$(VO)_2P_2O_7$. They postulate that two routes to CO_x exist. The predominate route uses surface lattice oxygens while a secondary route uses adsorbed O_2 is a secondary route in the formation of CO_x. This surface lattice oxygen is also postulated to be responsible for furan formation, while an oxygen species they refer to as *O, which could be either a surface lattice or adsorbed species, is responsible for n-butane activation and maleic anhydride formation [28].

Centi *et al.* have investigated the role of surface oxygen species by selectively blocking sites with certain molecules such as SO_2, NH_3 and K. Their work indicates that different sites are responsible for selective and nonselective oxidation [29].

Practical application of this type of knowledge has been utilized by Contractor and Sleight in their development of a recirculating solids reactor for this reaction. This system utilizes an attrition resistant form of $(VO)_2P_2O_7$. The reactor design separates the oxidation and reduction of the catalyst by continuously recirculating the catalyst between two separate chambers. Thus the oxidation of the hydrocarbon is accomplished in the absence of gas phase O_2 [30]. The object of this system is to limit the number of highly reactive surface oxygen species, which lead to combustion, on the surface of the catalyst. It is clear that a fundamental understanding of the oxygen species associated with the active sites is valuable from an applied as well as a fundamental viewpoint.

We have shown previously that, for β-$VOPO_4$, specific lattice sites can be labeled with ^{18}O [31]. These sites were then identified as either selective or nonselective by monitoring the products of C_4 oxidation with a mass spectrometer. In addition, specific selective oxygens could be assigned to specific mechanistic steps. The present work will extend this to the $(VO)_2P_2O_7$ phase lattice oxygens.

EXPERIMENTAL PROCEDURE

Synthesis of ^{18}O Enriched $(VO)_2P_2O_7$

^{18}O-enriched $(VO)_2P_2O_7$ was prepared by the high temperature reduction of β-$VOPO_{7/2}{}^{18}O_{1/2}$. Synthesis of β-$VOPO_{7/2}{}^{18}O_{1/2}$ was described previously [31]. β-$VOPO_{7/2}{}^{18}O_{1/2}$ was placed in platinum lined quartz boats and placed in a quartz tube furnace. The quartz chamber was purged with oxygen free nitrogen (less than 5 ppm oxygen, Matheson) for 3 h; this flow was maintained during the following heating stages. The chamber was then heated from 473 K to 673 K over 2 h. After maintaining a temperature of 673 K for 2 h, the sample was heated to 1033 K over 1 h. The sample was held at this temperature for 36 h then cooled to 573 K over 9.2 h and then to room temperature. This method of reducing β-$VOPO_4$ to $(VO)_2P_2O_7$ is documented by Bordes [32].

Characterization of Catalyst Structure and Isotopic Enrichment

Laser Raman spectroscopy

Laser Raman spectra were obtained using a Spex 1403 laser Raman spectrometer with the 514.3 nm line of a Spectra Physics Model 2020-05 argon ion laser operated at 100 mW at the source. A Nicolet 1180E computer system permitted accumulation of the spectra. Spectra reported represent a 40 scan

accumulation at 2-cm^{-1} resolution with a central slit setting of 1000 μm and a scan drive of 6.25 cm^{-1}/s.

Fourier transform infrared spectroscopy

Transmission infrared spectra were recorded using a Nicolet 60-SX Fourier transform infrared spectrometer with single beam optics. Each spectrum represents the accumulation of 100 scans at 2 cm^{-1} resolution.

Thermal reduction

To determine the amount of ^{18}O in the enriched $(VO)_2P_2O_7$, it was necessary to characterize the ^{18}O content of the oxygen leaving the catalyst during the thermal reduction of β-$VOPO_{7/2}{}^{18}O_{1/2}$. To accomplish this, samples of β-$VOPO_{7/2}{}^{18}O_{1/2}$ were placed in 6 mm quartz tubes and connected to the system shown in Figure 1. The thermal reduction system consists of the quartz tube containing catalyst to be reduced, an Ultratorr (Omaha Valve) high vacuum connector connected to a high vacuum valve which isolates a quadrupole mass spectrometer and a 550 liter per minute turbomolecular pump (the same system used for the mass spectrometry studies). The tube was slowly evacuated to less than 10^{-7} torr and held overnight. The chamber was then heated from 473 K to 673 K over 2 h. After maintaining a temperature of 673 K for 2 h, the sample was heated to 1033 K over 1 h. The sample was held at this temperature until no more oxygen could be detected leaving the sample. The off gas was monitored with the mass spectrometer described in the Reactor Studies section.

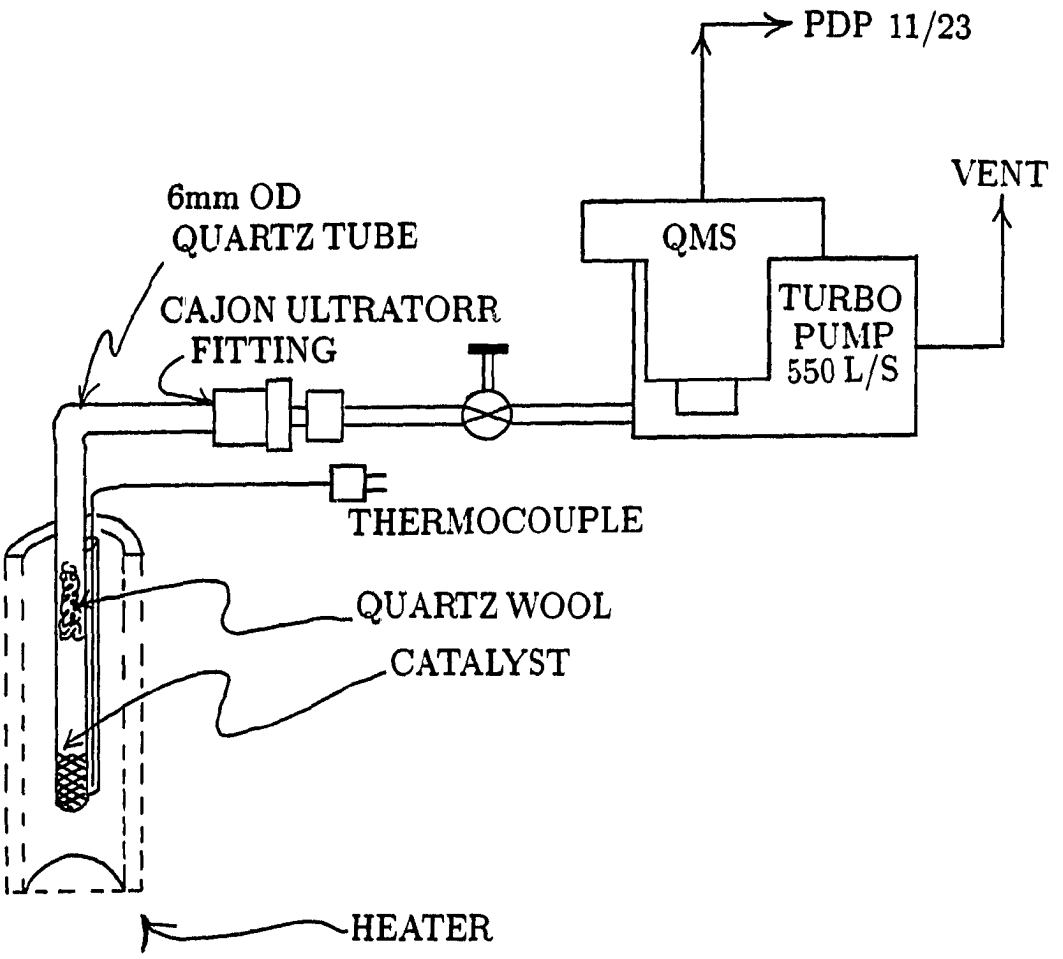

Figure 1: Thermal reduction with *in situ* mass spectral monitoring

Reactor Studies

Hydrocarbon pulses

Reactions of n–butane, 1–butene, 1,3–butadiene, furan, γ–butyrolactone and maleic anhydride using the ^{18}O-enriched and nonenriched catalysts were performed in the pulse microreactor system (Figure 2) in the absence of gas phase oxygen. Two tenths gram of pressed and sieved catalyst (10–20 mesh) was used in each experiment. The catalyst was held in place by plugs of pyrex wool which had been washed and calcined in O_2. The stainless steel reactors were pretreated with phosphoric acid and calcined in air to passivate the metal. Treated reactors and glass wool showed negligible combustion activity for all feeds at reaction temperature.

The reactor was continuously purged with helium flowing at 50 ml/min (at standard temperature and pressure). A reduced copper catalyst (BASF) was used to remove residual oxygen from the helium. A ten port Valco valve equipped with 0.5 ml loops was used to introduce hydrocarbon pulses. The valve and loops were maintained at 425 K. The composition and flow rate of the gases fed to the sample loop and the microreactor were controlled by Tylan mass flow controllers (Model FC260). Pure n–butane, 1–butene and 1,3–butadiene (Matheson, instrument grade) were diluted with helium (Matheson, zero grade) to 2% hydrocarbon and fed to the loop. To provide low (less than 1%) concentrations of furan (Kodak), γ–butyrolactone(Alfa) and maleic anhydride(Kodak), helium was fed to a saturator [33] maintained at a temperature which provided a vapor pressure of less than 10 torr for that particular species. For furan, the heater was replaced by a styrofoam box (2 in walls) and the saturator was placed in a dry ice/acetone bath. The system

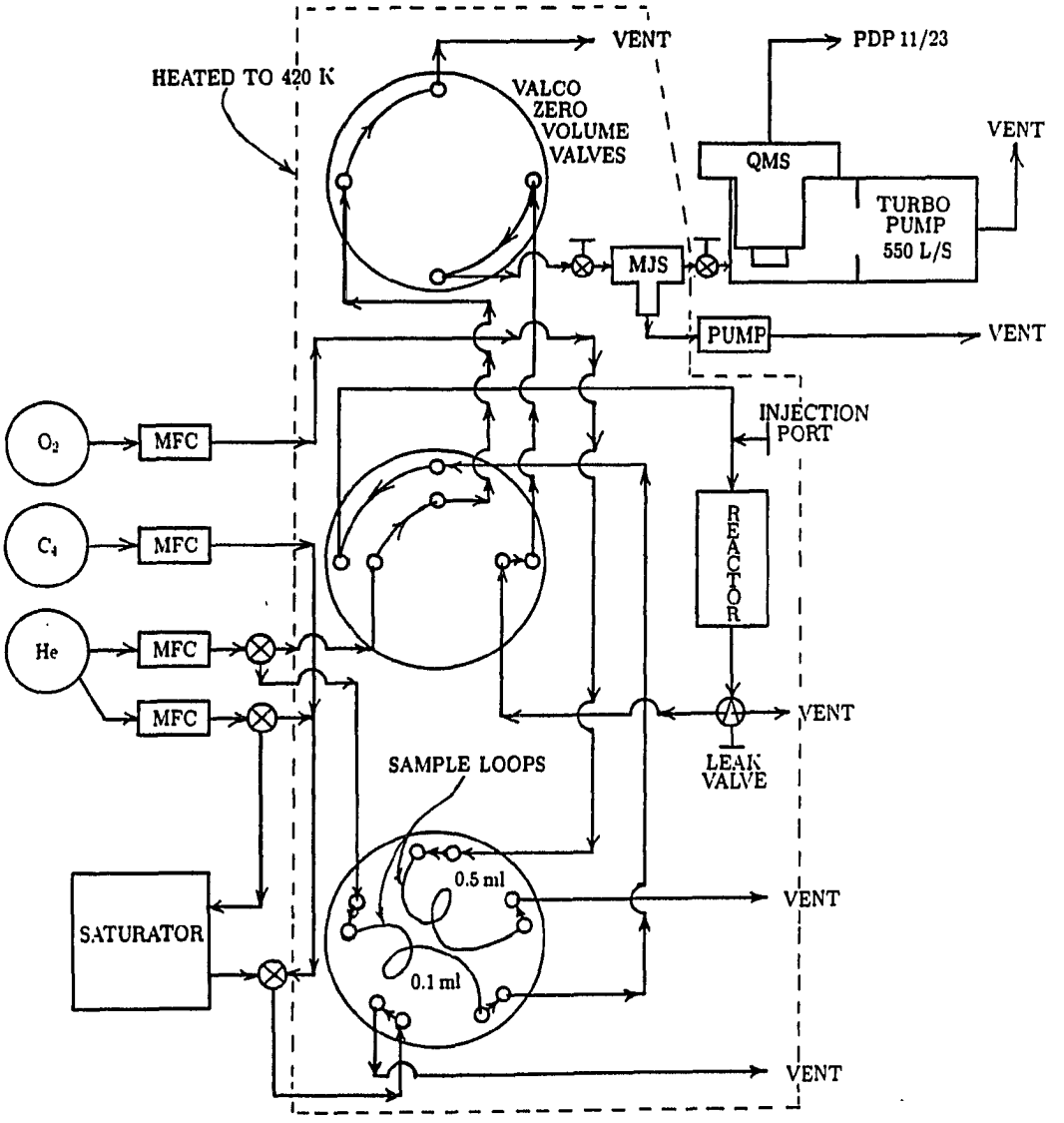

Figure 2: Reactor system

was maintained at 195 K, providing a furan vapor pressure of about 1 torr, or about 0.1 mol%. The saturator was maintained at 330 K for γ–butyrolactone, providing a feed of about 1% hydrocarbon. The saturator was maintained at 340 K for maleic anhydride, providing a feed of slightly less than 1 mol% hydrocarbon.

Loaded reactors were purged with helium for longer that 3 h, then heated from room temperature to reaction temperature (773 K for n–butane, 723 K for other feeds) and held at reaction temperature for 1 h. Pulsing of the desired feed was then commenced at a rate of one pulse per minute. Each experiment consisted of at least 75 pulses.

Alternate pulses of O_2 and hydrocarbon

Reactions of n–butane, 1–butene, 1,3–butadiene, furan, γ–butyrolactone and maleic anhydride were performed with alternating pulses of oxygen in the microreactor system shown in Figure 2. Treated reactors and glass wool showed negligible activity for both oxygen and hydrocarbon pulses at reaction temperature.

Reactors were loaded with 0.2 g of the appropriate catalyst and continuously purged with helium flowing at 50 sccm. A ten port Valco valve equipped with one 0.5 ml and one 0.1 ml loop was used to introduce alternating pulses of hydrocarbon and oxygen, respectively. When $^{18}O_2$ (MSD Isotopes) was used, it was introduced by syringe (0.2 ml, Precsion Sampling Corporation) through a septum as indicated in Figure 2.

The composition and flow rate of the gases fed were controlled as described earlier. The oxygen–to–hydrocarbon ratio for most species fed is similar to that which would occur in a continuous feed mixture of 2% hydrocarbon in air. Alternate oxygen and hydrocarbon pulses were introduced every 30 seconds. $^{16}O_2$

experiments were performed using enriched and nonenriched catalysts while $^{18}O_2$ experiments were performed with the enriched catalyst only.

Mass spectral analysis

Mass spectral analysis of the products of n-butane, 1-butene, 1,3-butadiene, furan, γ-butyrolactone and maleic anhydride reaction over the ^{18}O-enriched catalyst was performed by a UTI 100C precision quadrupole mass analyzer controlled by a PDP 11/23 computer [34]. The mass analyzer was interfaced with the microreactor system by a glass SGE single stage molecular jet separator.

The ^{18}O content of maleic anhydride, CO_2, furan and, when applicable, γ-butyrolactone, was determined for the oxidation of n-butane, 1-butene, 1,3-butadiene, furan, γ-butyrolactone and maleic anhydride. As a result of the pulse nature of these experiments, it was not possible to accurately monitor the entire spectral region of interest for all pulses. Therefore, the mass spectrum was divided into 5 small ranges, which could be monitored, one range per pulse. The ranges and the species in those ranges are presented in Table 1. Typical peaks were 3-5 seconds wide, depending on the species observed. Survey scans covering the entire spectral range were made using unlabeled catalyst to ensure that all species present were accounted for.

Mass spectral data was collected for all feed species on both labeled and unlabeled catalysts. All species present were then accounted for and any interferences (spectral overlaps) of crucial mass to charge ratios (m/e) noted. A sample set of peaks for maleic anhydride produced from n-butane is presented in Figure 3. The peaks were integrated by summing the intensities of each scan from the beginning of the peak to the end. Early, low level scans were used as

Table 1: Mass spectral ranges scanned every fifth pulse and species of interest in those ranges

Range (m/e)	Species	Number of Scans/Peak
42–50	CO_2	80
17–22	H_2O	80
67–90	furan & γ–butyrolactone	20
95–110	maleic anhydride	30
50–60	n–butane, 1–butene, 1,3–butadiene	40

background, normalized to the same number of scans as the integration, and then subtracted from the integrated intensity. This was done for all peaks of interest. Occasionally, fragments from species present would give m/e peaks coincident with m/e peaks of interest. This necessitated the use of correction factors for that m/e based on another m/e of the offending species. These factors were based on the accumulation of large numbers of scans of the mass spectrum of the offending species. The factors used are presented in Table 2.

The ^{18}O present in each species was then accounted for and calculated as a percentage of total oxygen present in that species. The percent ^{18}O in maleic anhydride was calculated according to the following formula:

$$\%^{18}O_{MAN} = \frac{\sum I_{100} + 2\sum I_{102} + 3\sum I_{104}}{3(\sum I_{98} + \sum I_{100} + \sum I_{102} + \sum I_{104})}$$

For 1–butene and 1,3–butadiene, phthalic anhydride was formed and the intensity at m/e 104 had to be corrected for this contribution.

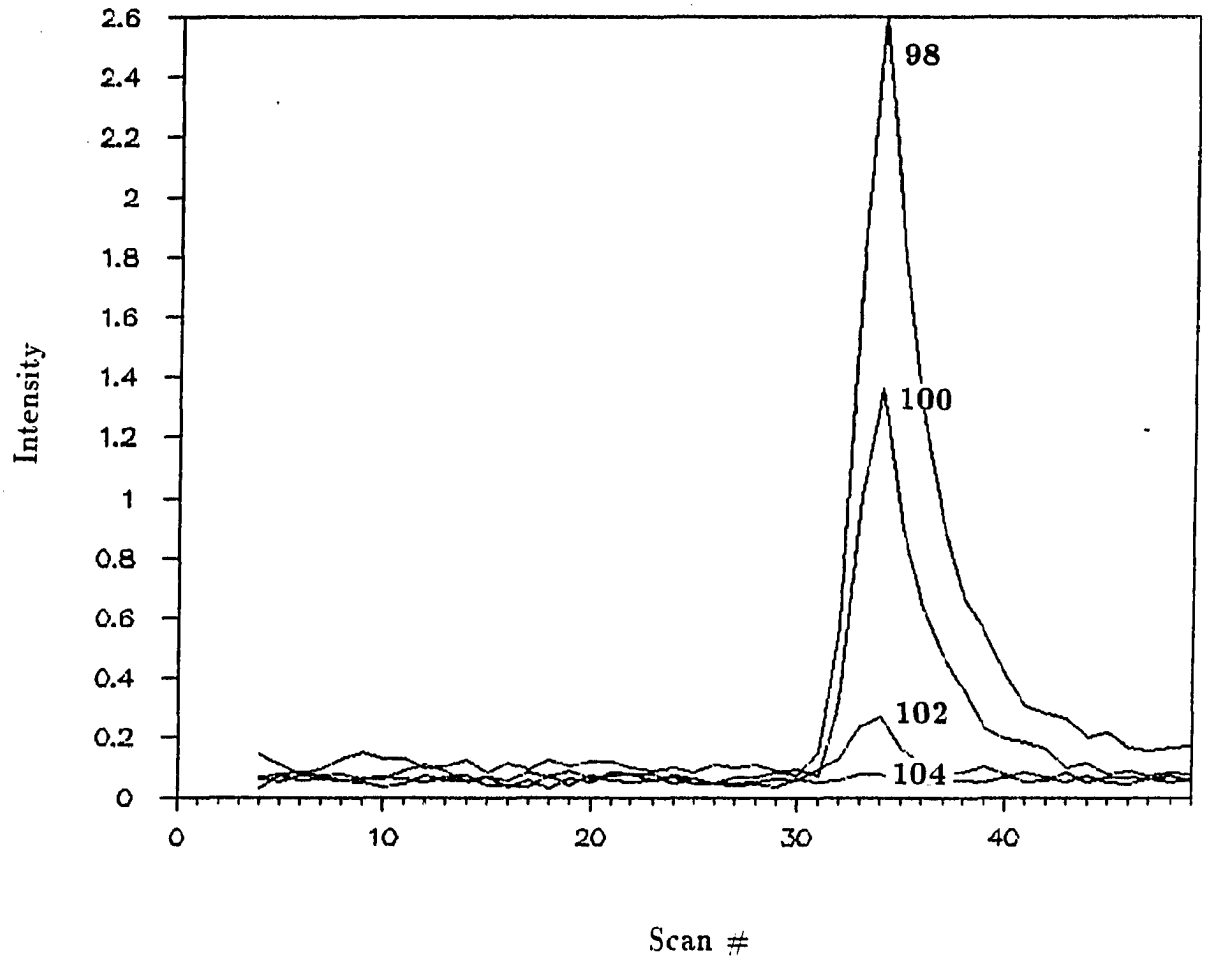

Figure 3: Sample mass spectral pulse data: maleic anhydride produced from a pulse of 2% n-butene over ^{18}O enriched $(VO)_2P_2O_7$ during $^{18}O_2$ alternate pulse experiment

Table 2: Mass spectral data correction factors

m/e Peak	Interfering Species	Interfered Species	Reference m/e	Correction Factor (f)[a]
44	n-butane	CO_2	43	0.03
70	maleic anhydride	^{18}O labeled furan	82	0.9
104	phthalic anhydride	^{18}O x 3 labeled maleic anhydride	105	12.6

[a] $I_{cor} = I_{raw} - f \times I_{ref}$ All corrections are typically less than 15% of total I_{raw} peak.

The percent ^{18}O in furan was calculated according to the following formula:

$$\%^{18}O_{FUR} = \frac{\sum I_{70}}{\sum I_{68} + \sum I_{70}}$$

Corrections were made for interference at m/e 70 from a minor maleic anhydride fragment.

The percent ^{18}O in CO_2 was calculated according to the following formula:

$$\%^{18}O_{CO_2} = \frac{\sum I_{46} + 2\sum I_{48}}{2(\sum I_{44} + \sum I_{46}\sum I_{48})}$$

Corrections were made by subtracting the minor interferences at m/e 44 from n-butane and background CO_2. CO could also be observed, but the data were significantly complicated by interference from background N_2 and $C^{16}O$.

EXPERIMENTAL RESULTS

Characterization of ^{18}O Enriched $(VO)_2P_2O_7$

Vibrational spectroscopy

The Raman spectrum of ^{18}O enriched $(VO)_2P_2O_7$ prepared by the solid state thermal reduction of β-$VOPO_{7/2}{}^{18}O_{1/2}$ [31] was compared to the Raman spectrum of similarly prepared $(VO)_2P_2O_7$ using β-$VOPO_4$ [2] (Figure 4). Spectral features showing a specific incorporation of ^{18}O into the lattice of $(VO)_2P_2O_7$ could be observed. Raman band assignments for $(VO)_2P_2O_7$ have been discussed previously [2]. ^{18}O could be detected in the catalyst by a P–^{18}O–P band at 910 cm^{-1}; the P–^{16}O–P band at 925 cm^{-1} had approximately twice the intensity. No other isotopically shifted bands were observed in the Raman spectrum. Unfortunately, the Raman bands representing V=O and PO_3 groups are very weak and nothing definite can be said about isotopic labeling in these positions. However, the IR bands corresponding to these particular bonds are quite strong and well resolved [2]. The Raman-active bands are also observable in the infrared spectrum. A comparison of the FTIR spectra for enriched and nonenriched catalyst is shown in Figure 5. A shift similar to that observed for the P–O–P bond in the Raman spectra is quite obvious at the 927 and 941 cm^{-1} IR bands. The 941 peak becomes less intense and shifts slightly to 936, and a less intense isotopically shifted peak at

919 cm^{-1} appears. The 927 cm^{-1} band reduces in intensity and shifts slightly to 924 cm^{-1} and an isotopically shifted band appears at 903 cm^{-1}. The V=O band at 991 cm^{-1} shows no indication of isotopic labeling at this site. The PO_3 asymetric stretches near 1061 cm^{-1}, on the other hand, shift to 1036 cm^{-1}, with shoulders at 1075, and 1057, revealing that an undetermined amount of ^{18}O is present at this type of site.

When the ^{18}O enriched $(VO)_2P_2O_7$ was reoxidized with stoichiometric amounts of $^{16}O_2$, the ^{18}O present was not scrambled to other sites, as shown in the Raman spectrum in Figure 6.

Though the ^{18}O levels have decreased, the ^{18}O is still present in the same sites as observed in the original β-$VOPO_{7/2}{}^{18}O_{1/2}$ [31]. This spectrum also indicates that the intensity of the P-^{18}O band at 895 cm^{-1} decreases by a much greater percentage than the intensity of the P-^{18}O band at 985 cm^{-1}. This indicates that proportionately more ^{18}O was lost from the 895 cm^{-1} P-O site than from the 985 cm^{-1} site.

Thermal reduction

Monitoring the reduction of β-$VOPO_{7/2}{}^{18}O_{1/2}$ by the method described earlier revealed that oxygen leaves the catalyst in the form of O_2. The ^{18}O content of this oxygen was 14% to 15%. Nearly all of the ^{18}O leaving the catalyst was in the form of $^{18}O^{16}O$. The reduction was complete, under these conditions, in approximately 1 h.

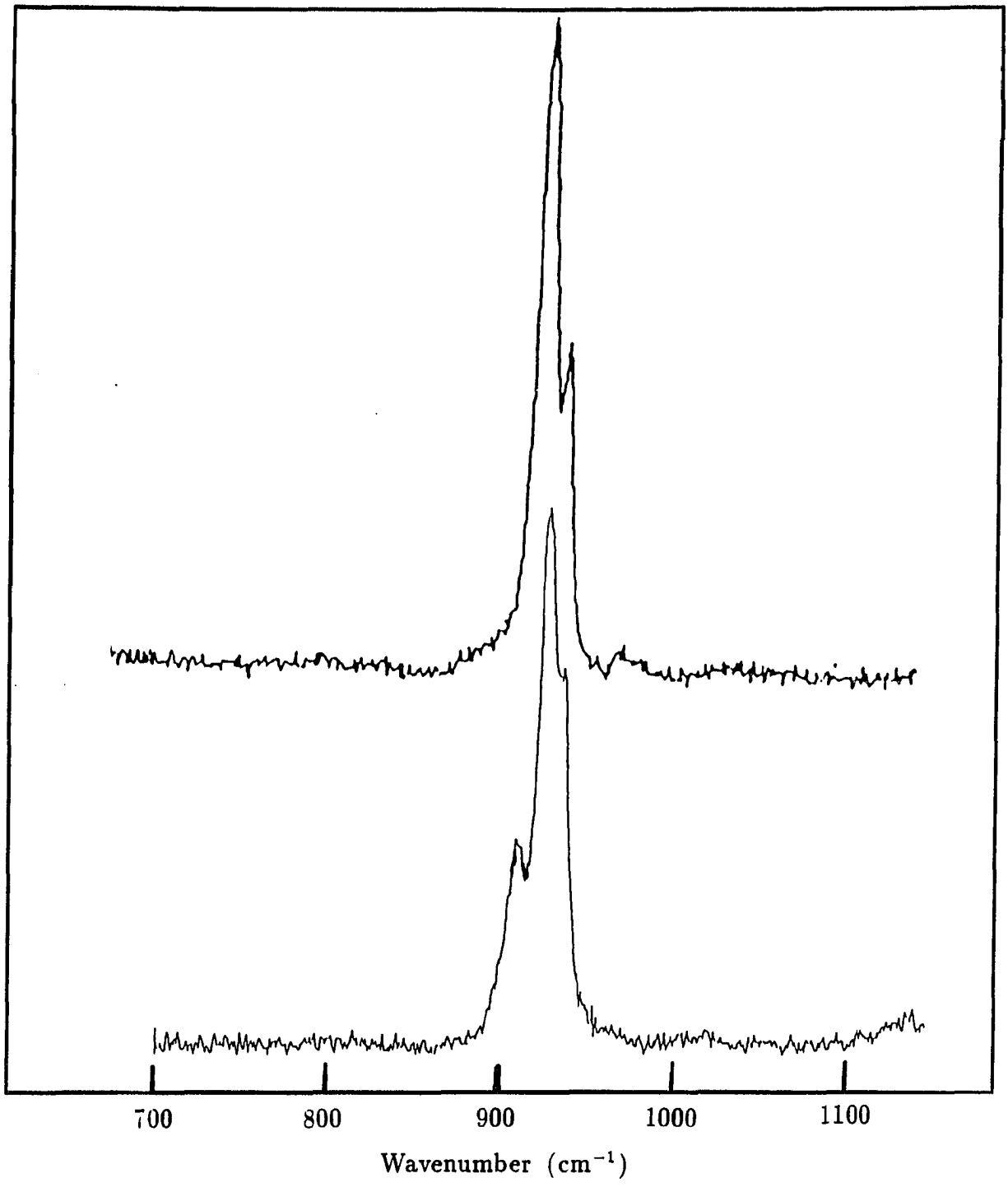

Figure 4: Comparison of Raman spectra of (a)$(VO)_2P_2O_7$ with (b)^{18}O enriched $(VO)_2P_2O_7$

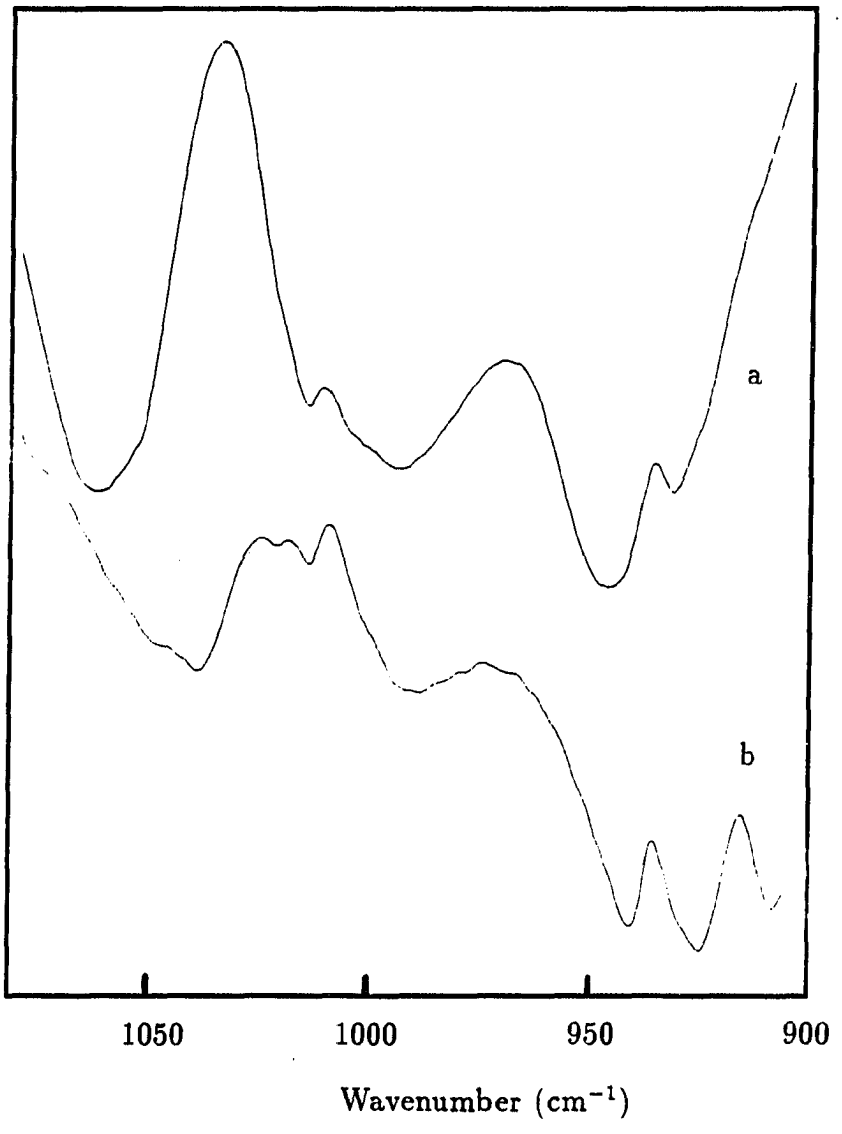

Figure 5: Comparison of FTIR spectra of (a)$(VO)_2P_2O_7$ with (b)^{18}O enriched $(VO)_2P_2O_7$

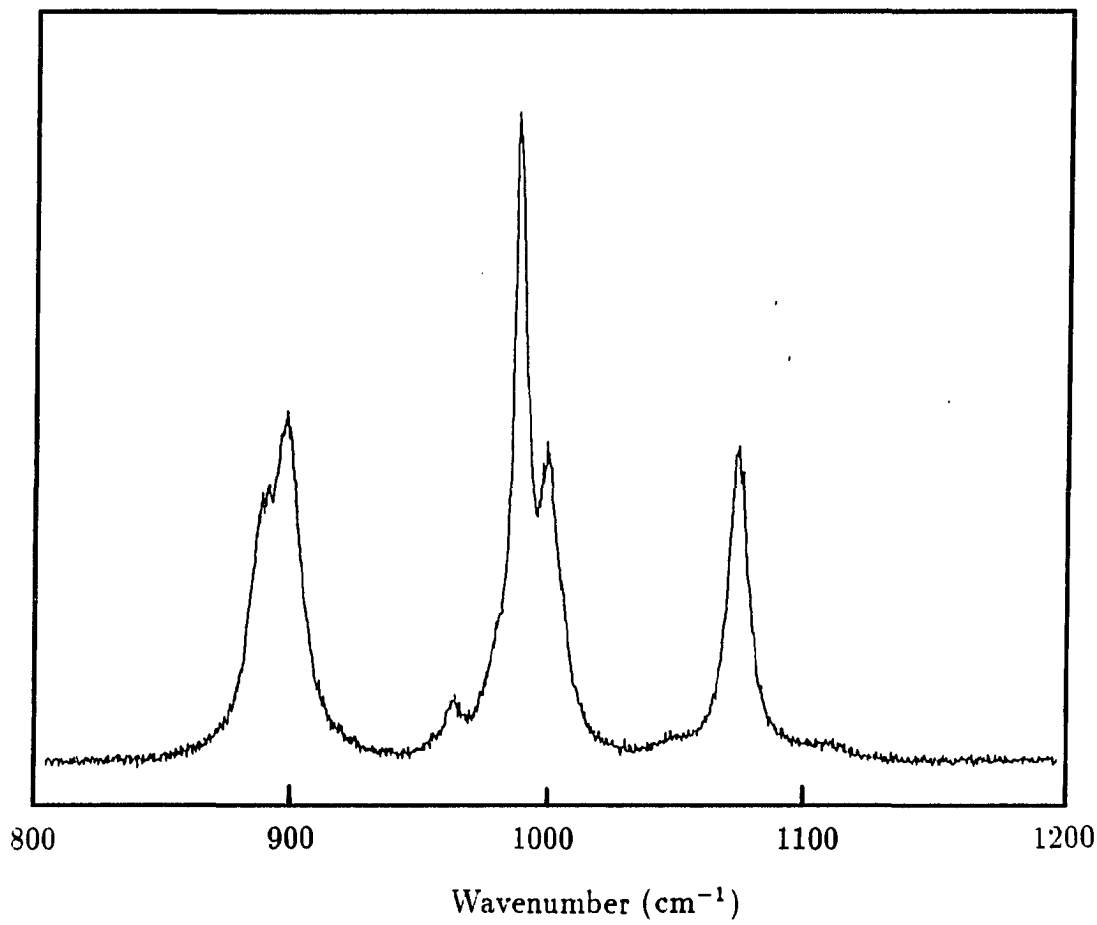

Figure 6: Raman spectrum of β–$VOPO_4$ made by oxidizing ^{18}O enriched $(VO)_2P_2O_7$ with $^{16}O_2$

Characterization of Post Reaction Catalyst

No change in the Raman spectra occurred upon reaction. Post reaction x-ray diffraction also shows no apparent changes in the catalyst bulk structure.

Reactor Studies

^{18}O incorporation into the products of n-butane oxidation

n-Butane pulses Maleic anhydride, furan and CO_2 were produced from all n-butane pulses over ^{18}O enriched $(VO)_2P_2O_7$. Production levels were low (less than 5%), but constant. ^{18}O levels in all products observed remained constant over all pulses, as seen in Figure 7. Five percent of the oxygen in maleic anhydride produced from n-butane over ^{18}O enriched $(VO)_2P_2O_7$ was ^{18}O. Initially about 2% of the oxygen in CO_2 produced in this reaction was ^{18}O. This level dropped to 1% over 75 pulses. Furan produced in this reaction contained no ^{18}O.

Alternating $^{16}O_2$ and n-butane pulses Maleic anhydride, furan and CO_2 were produced from all pulses of n-butane when $^{16}O_2$ and n-butane pulses were alternated over ^{18}O enriched $(VO)_2P_2O_7$. Production levels were similar to those observed when only n-butane was pulsed over the catalyst. The ^{18}O content of all species observed is shown in Figure 8. The ^{18}O content of maleic anhydride produced in this reaction dropped from 5% to 3% over 75 pulses. The ^{18}O content of CO_2 dropped from 2% to 1%, while furan did not incorporate any ^{18}O. Negligible amounts of CO_2 were formed when O_2 was pulsed over the catalyst. No other hydrocarbon species were observed during the O_2 pulses.

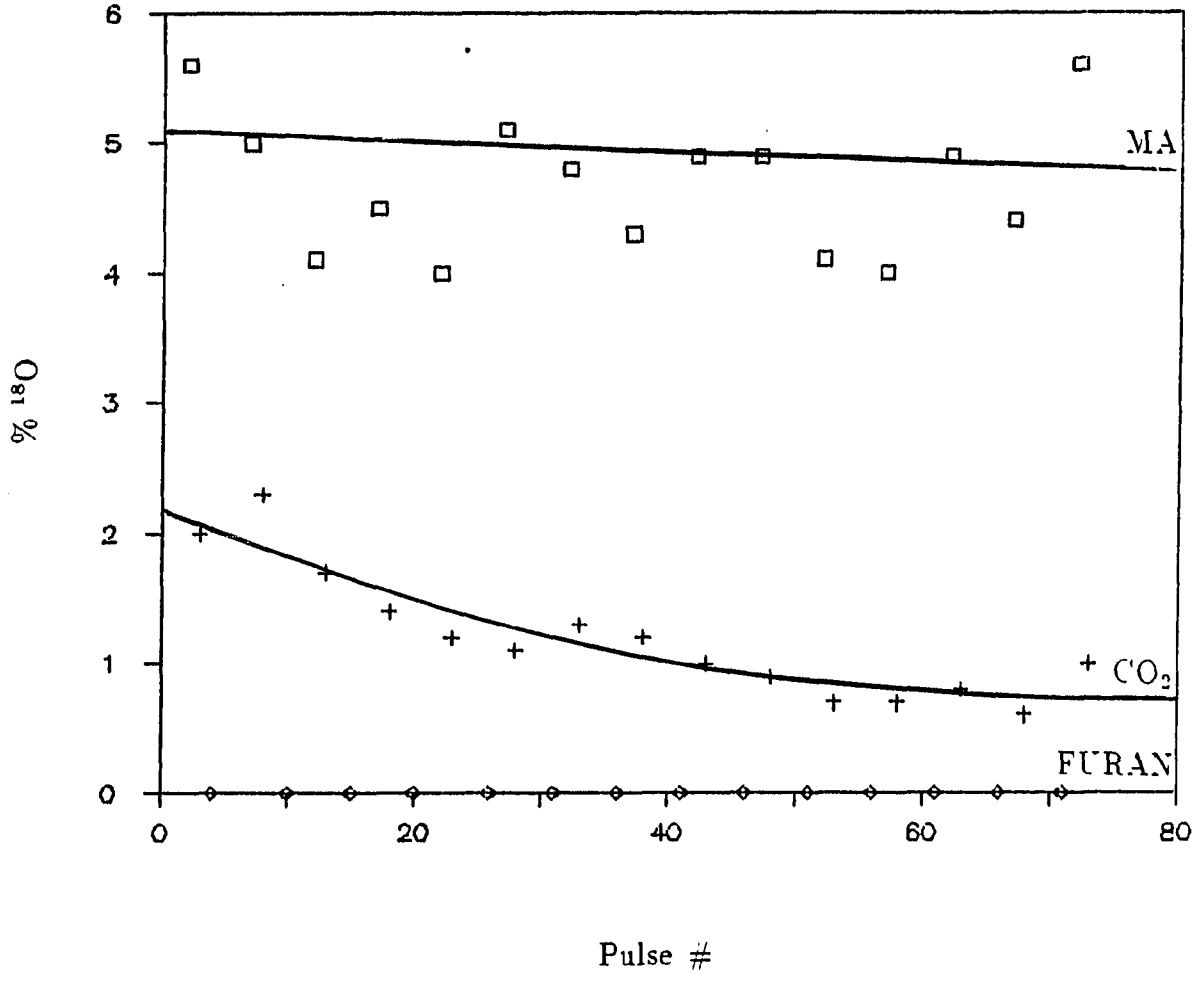

Figure 7: ^{18}O incorporation into products of n-butane oxidation over ^{18}O enriched $(VO)_2P_2O_7$

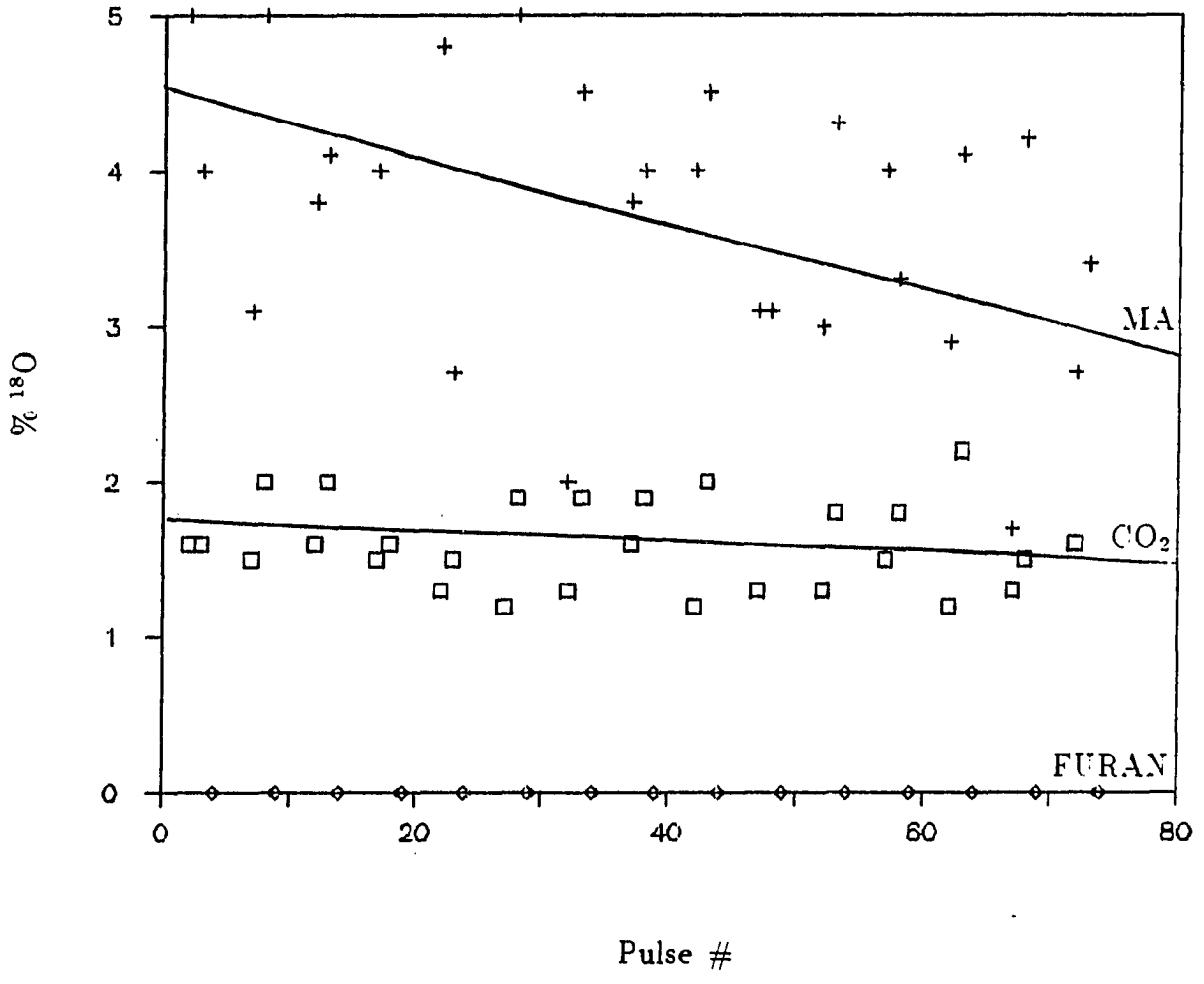

Figure 8: ^{18}O incorporation into products of n-butane oxidation over ^{18}O enriched $(VO)_2P_2O_7$ during $^{16}O_2$ alternating pulse experiments

Alternating $^{18}O_2$ and n-butane pulses Maleic anhydride, furan and CO_2 were produced from all pulses of n-butane when $^{18}O_2$ and n-butane pulses were alternated over ^{18}O enriched $(VO)_2P_2O_7$. Production levels were similar to those observed when only n-butane was pulsed over the catalyst. The ^{18}O content of all species observed is shown in Figure 9. The ^{18}O content of maleic anhydride produced in this reaction increased from 5% to 13% over 75 pulses. The ^{18}O content of CO_2 produced in this reaction increased from 2% to over 24% after 75 pulses. The ^{18}O content of furan produced in this reaction remained near zero, but small amounts (less than 1%) could be detected in later pulses.

^{18}O incorporation into the products of 1-butene oxidation

1-Butene pulses Very little maleic anhydride was produced from 1-butene pulses, while larger amounts of phthalic anhydride and much larger amounts of CO_2(10 times the level observed for n-butane) and furan (200 times more than observed for n-butane) were produced in the reaction of 1-butene over ^{18}O enriched $(VO)_2P_2O_7$. As shown in Figure 10, the oxygen in furan produced in this reaction initially contained nearly 15% ^{18}O. This level dropped with increasing pulse number to a final value of 10%. The ^{18}O content of CO_2 was nearly constant at 1%.

Alternating $^{16}O_2$ and 1-butene pulses Maleic anhydride, furan and CO_2 were produced from all pulses of 1-butene when $^{16}O_2$ and 1-butene pulses were alternated over ^{18}O enriched $(VO)_2P_2O_7$. One hundred times as much maleic anhydride was produced under these conditions than when no O_2 pulses were introduced, while roughly the same amount of furan was observed. The amount of CO_2 produced in this experiment was similar to that observed when no O_2 was

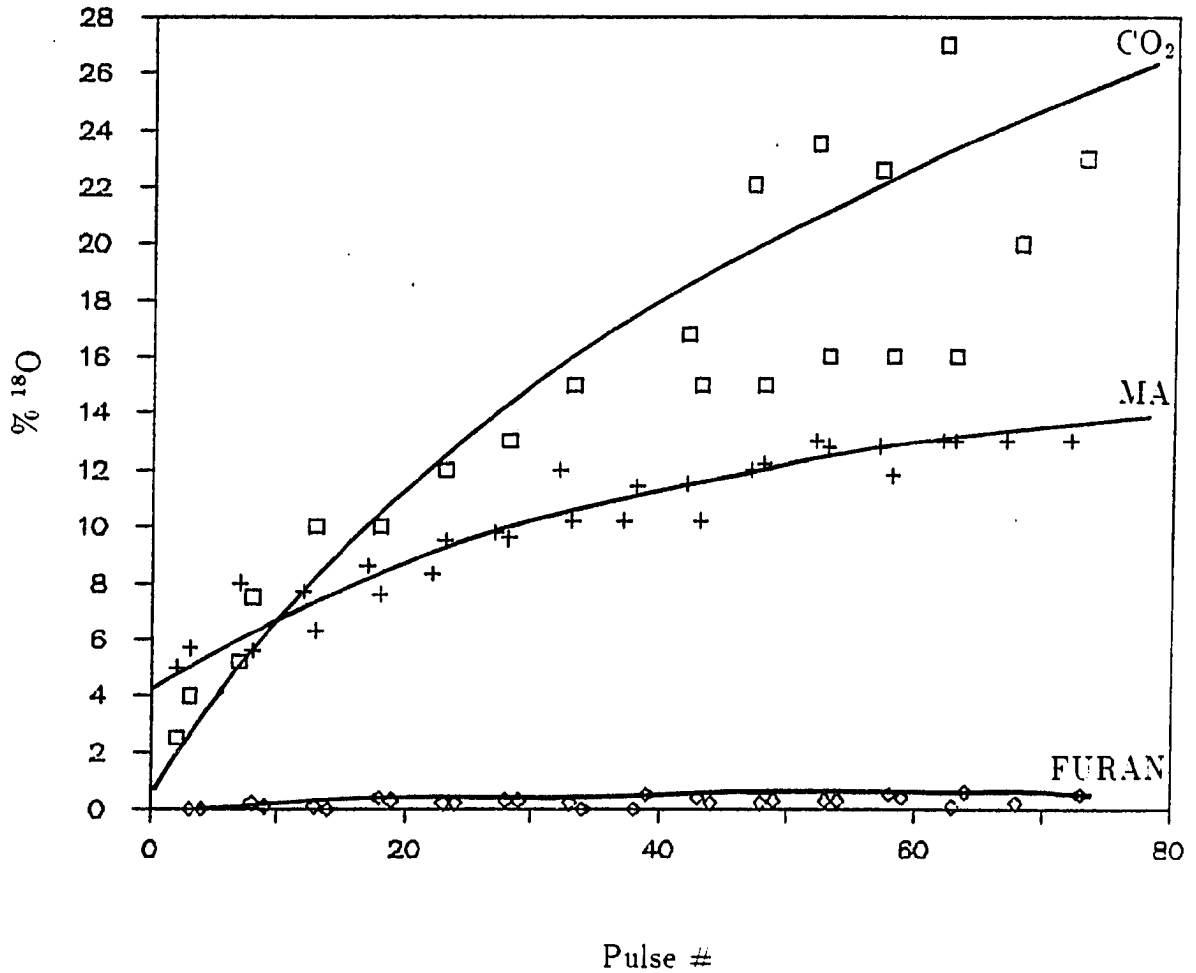

Figure 9: ^{18}O incorporation into products of n-butane oxidation over ^{18}O enriched $(VO)_2P_2O_7$ during $^{18}O_2$ alternating pulse experiments

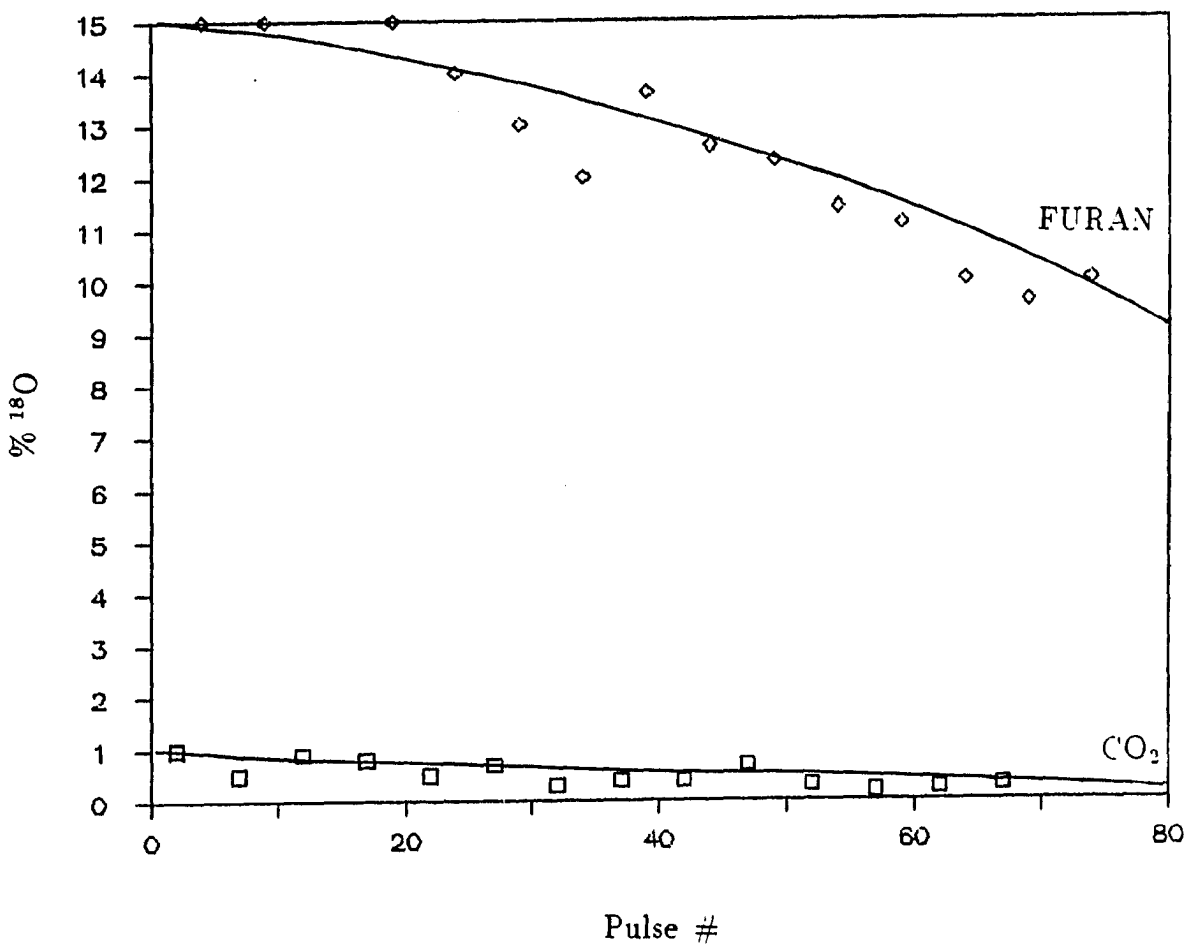

Figure 10: ^{18}O incorporation into products of 1-butene oxidation over ^{18}O enriched $(VO)_2P_2O_7$

introduced, while an additional amount of CO_2 was produced during the O_2 pulses. Trace levels of maleic anhydride and furan were produced during all $^{16}O_2$ pulses, while large amounts of CO_2 were produced from the O_2 pulses. The addition of O_2 pulses suppressed phthalic anhydride formation. The ^{18}O content of all species observed is shown in Figure 11. The ^{18}O content of maleic anhydride fell from 5% to 2% over 75 pulses. The ^{18}O content of furan fell from 12% to 8%, while the ^{18}O content of CO_2 fell from 3% to 0%.

Alternating $^{18}O_2$ and 1-butene pulses Maleic anhydride, furan and CO_2 were produced from all pulses of 1-butene when $^{18}O_2$ and 1-butene pulses were alternated over ^{18}O enriched $(VO)_2P_2O_7$. Production levels were consistent with those observed in the $^{16}O_2$ experiment. The ^{18}O content of the products of this reaction are presented in Figure 12. The ^{18}O content of the maleic anhydride produced in this reaction increased from 5% to 60% in 75 pulses. At the same time, the ^{18}O level observed in furan increased from 13% to over 50% in 75 pulses. The ^{18}O content of CO_2 increased from 2% to 55%. Trace levels of furan and maleic anhydride were detected during $^{18}O_2$ pulses, while significant amounts of CO_2 were produced during the $^{18}O_2$ pulses. The ^{18}O content of the CO_2 produced from $^{18}O_2$ pulses was roughly 40% to 50%.

^{18}O incorporation into products of 1,3-butadiene oxidation

1,3-Butadiene pulses Maleic anhydride, furan and CO_2 were produced from all 1,3-butadiene pulses over ^{18}O enriched $(VO)_2P_2O_7$. Trace levels of phthalic anhydride were detected. Maleic anhydride was produced at 10 times the level observed for n-butane. Furan was produced at 100 times the level observed for

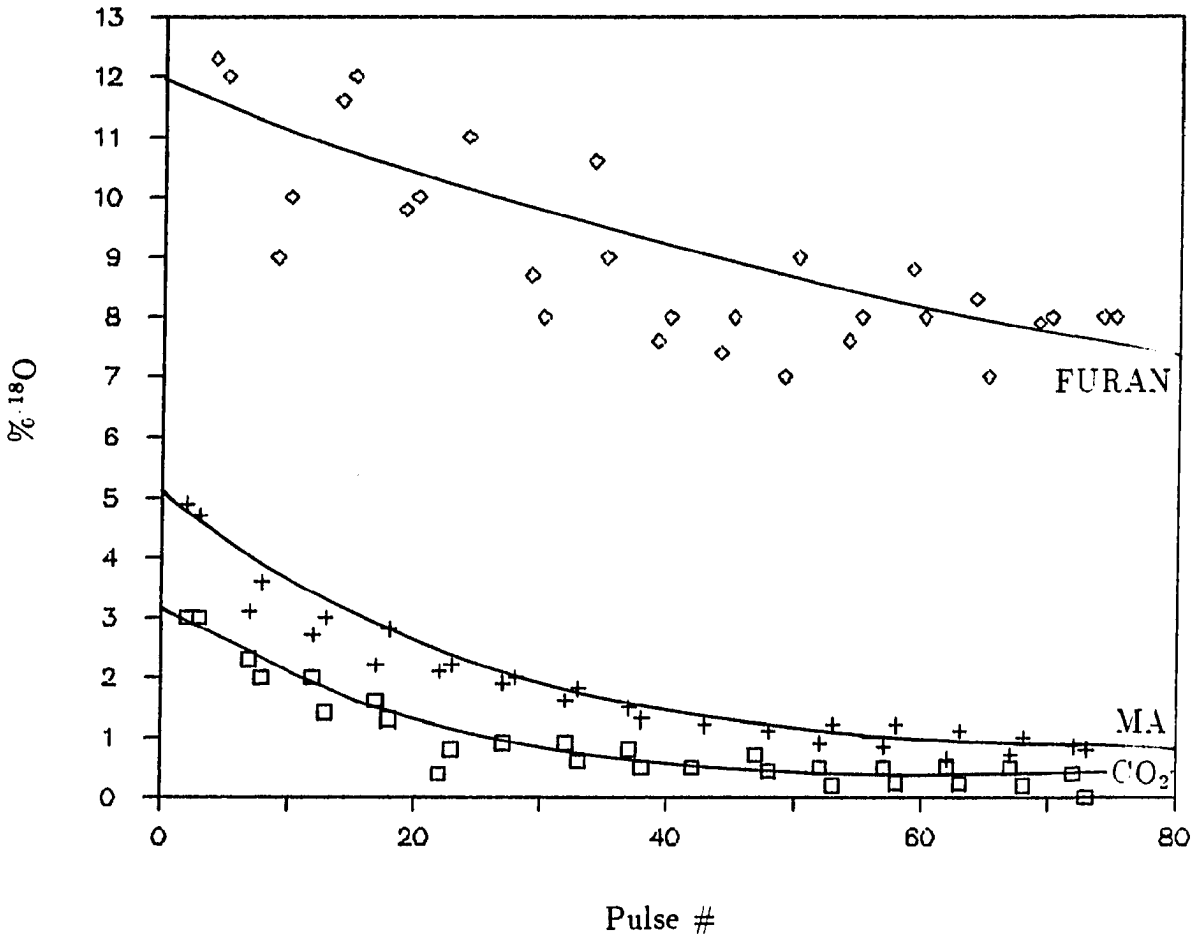

Figure 11: ^{18}O incorporation into products of 1-butene oxidation over ^{18}O enriched $(VO)_2P_2O_7$ during $^{16}O_2$ alternating pulse experiments

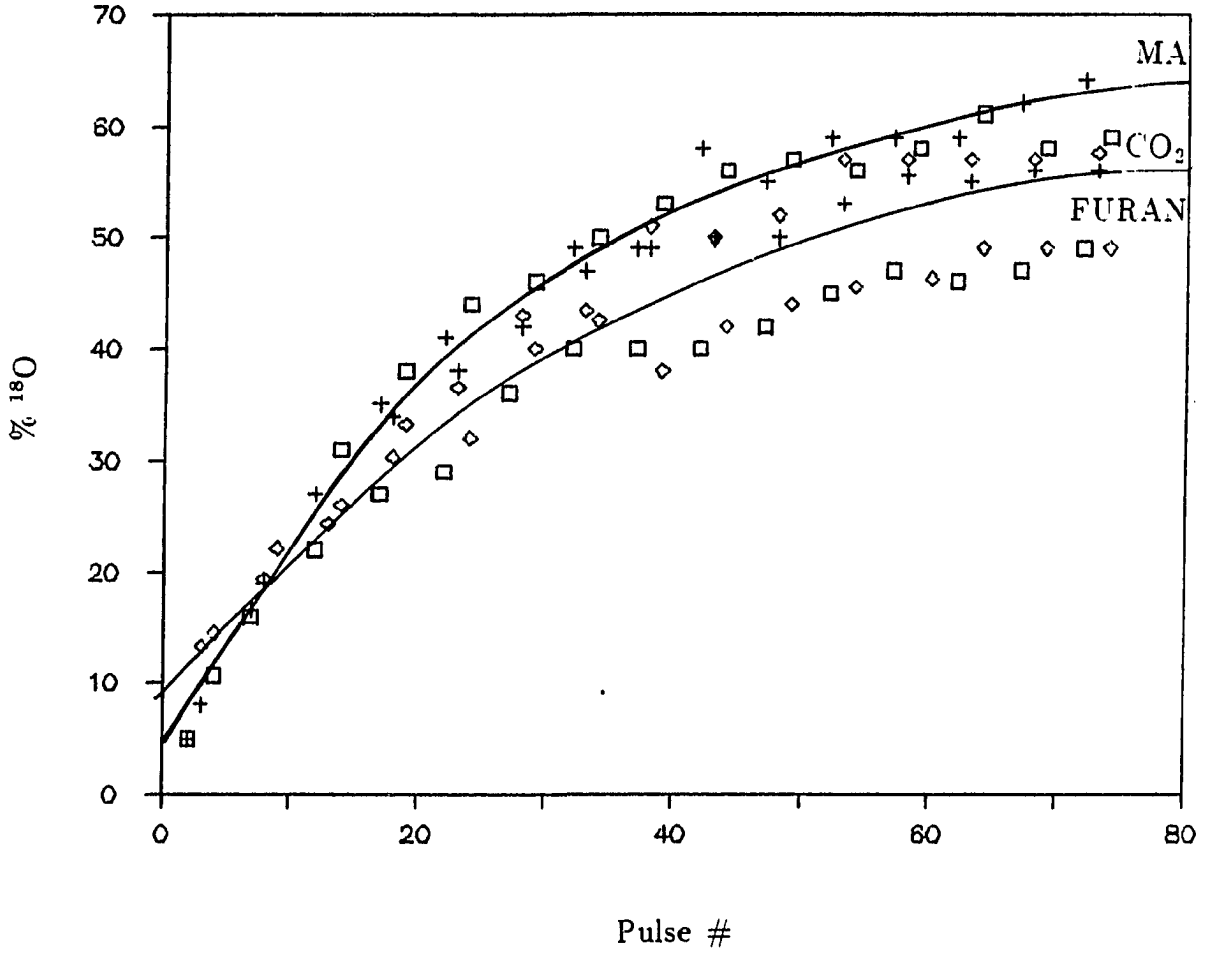

Figure 12: ^{18}O incorporation into products of 1-butene oxidation over ^{18}O enriched $(VO)_2P_2O_7$ during $^{18}O_2$ alternating pulse experiments

n–butane. CO_2 was produced at 200 times the level observed for n–butane. The ^{18}O levels observed in all products are shown in Figure 13. The ^{18}O levels observed for maleic anhydride fell from 5% to 1.5% over the course of the experiment. The ^{18}O levels observed for furan fell from 4.5% to 2.5% over the course of the experiment, while the ^{18}O levels observed for CO_2 fell from 4% to 0%.

Alternating $^{16}O_2$ and 1,3–butadiene pulses Maleic anhydride, furan and CO_2 were produced from all pulses of 1,3–butadiene when $^{16}O_2$ and 1,3–butadiene pulses were alternated over ^{18}O enriched $(VO)_2P_2O_7$. The production levels observed were similar to the production levels observed when only 1,3–butadiene pulses were used. The ^{18}O content of maleic anhydride produced in this reaction fell from 5% to 1.5%, as shown in Figure 14. The ^{18}O content of furan fell from 4% to 2% while that of CO_2 fell from 4% to 0%. Trace levels of maleic anhydride and furan were observed during the O_2 pulses, while large amounts of CO_2 (roughly the same amount as observed during the 1,3–butadiene pulses) were observed during the O_2 pulses.

Alternating $^{18}O_2$ and 1,3–butadiene pulses Maleic anhydride, furan and CO_2 were produced from all pulses of 1,3–butadiene when $^{18}O_2$ and 1,3–butadiene pulses were alternated over ^{18}O enriched $(VO)_2P_2O_7$. Production levels were consistent with those observed in the $^{16}O_2$ experiment. Observed ^{18}O levels are shown in Figure 15. The ^{18}O content of maleic anhydride produced in this manner increased from 5% to 45%, while the levels observed for both furan and CO_2 increased from 4% to 35%. CO_2 produced from $^{18}O_2$ pulses contained roughly 50% ^{18}O.

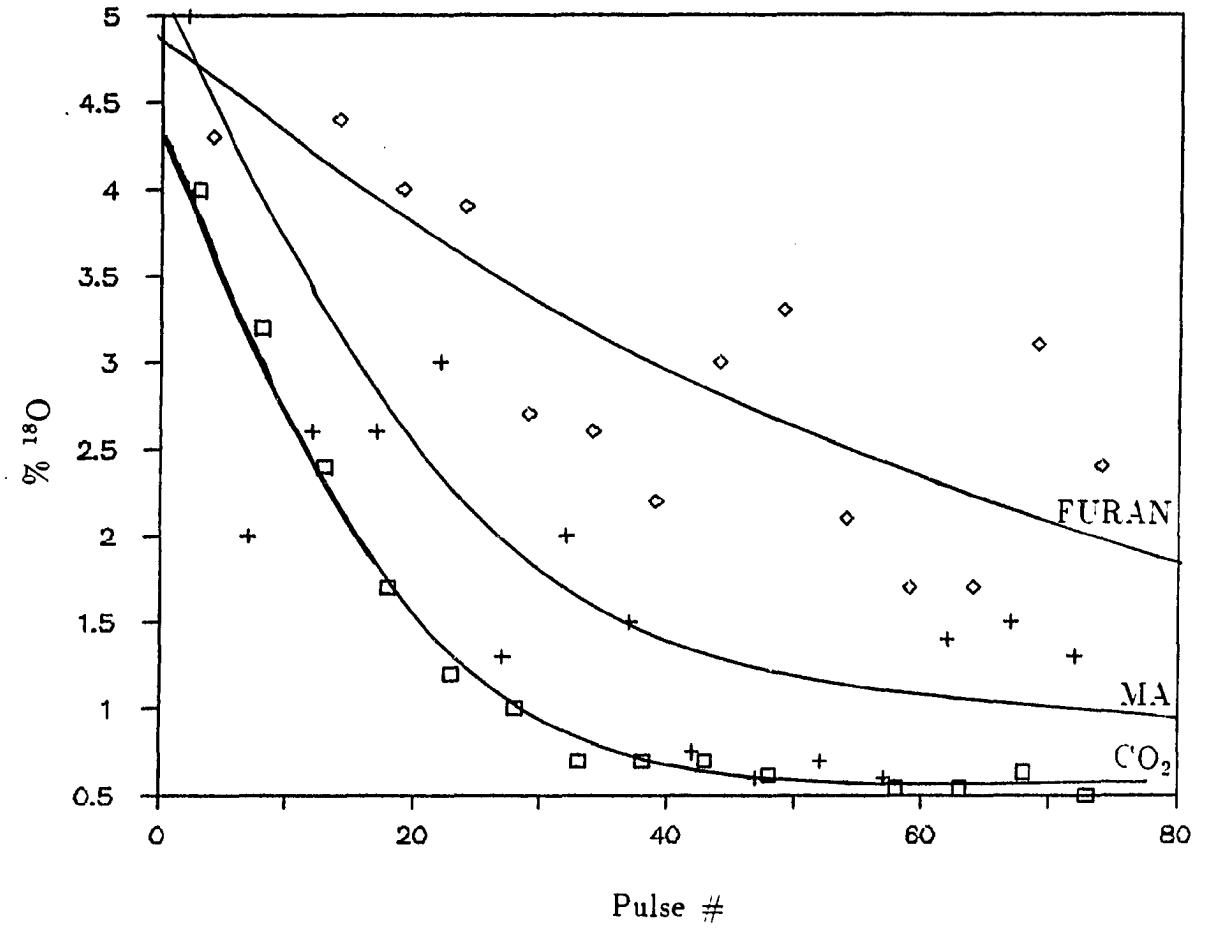

Figure 13: ^{18}O incorporation into products of 1,3-butadiene oxidation over ^{18}O enriched $(VO)_2P_2O_7$

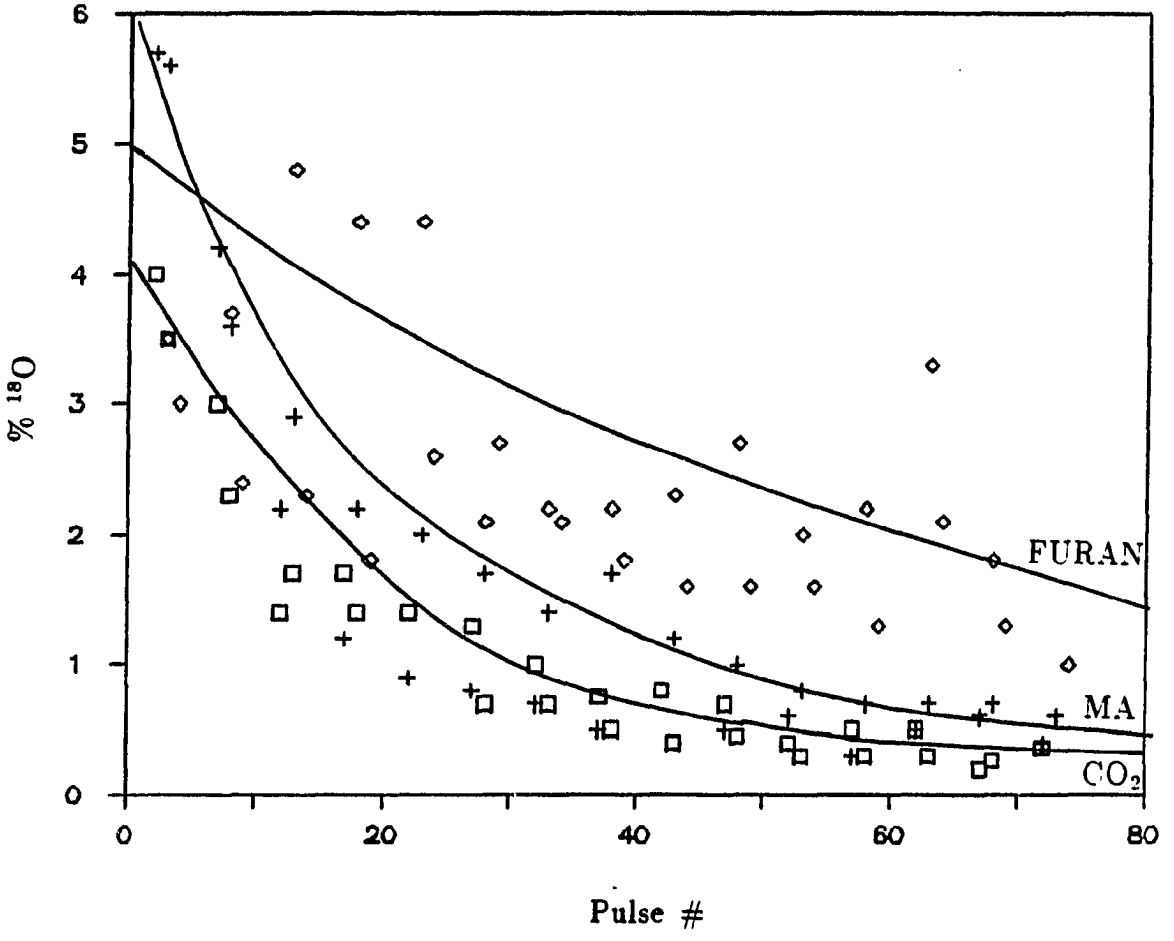

Figure 14: ^{18}O incorporation into products of 1,3-butadiene oxidation over ^{18}O enriched $(VO)_2P_2O_7$ during $^{16}O_2$ alternating pulse experiments

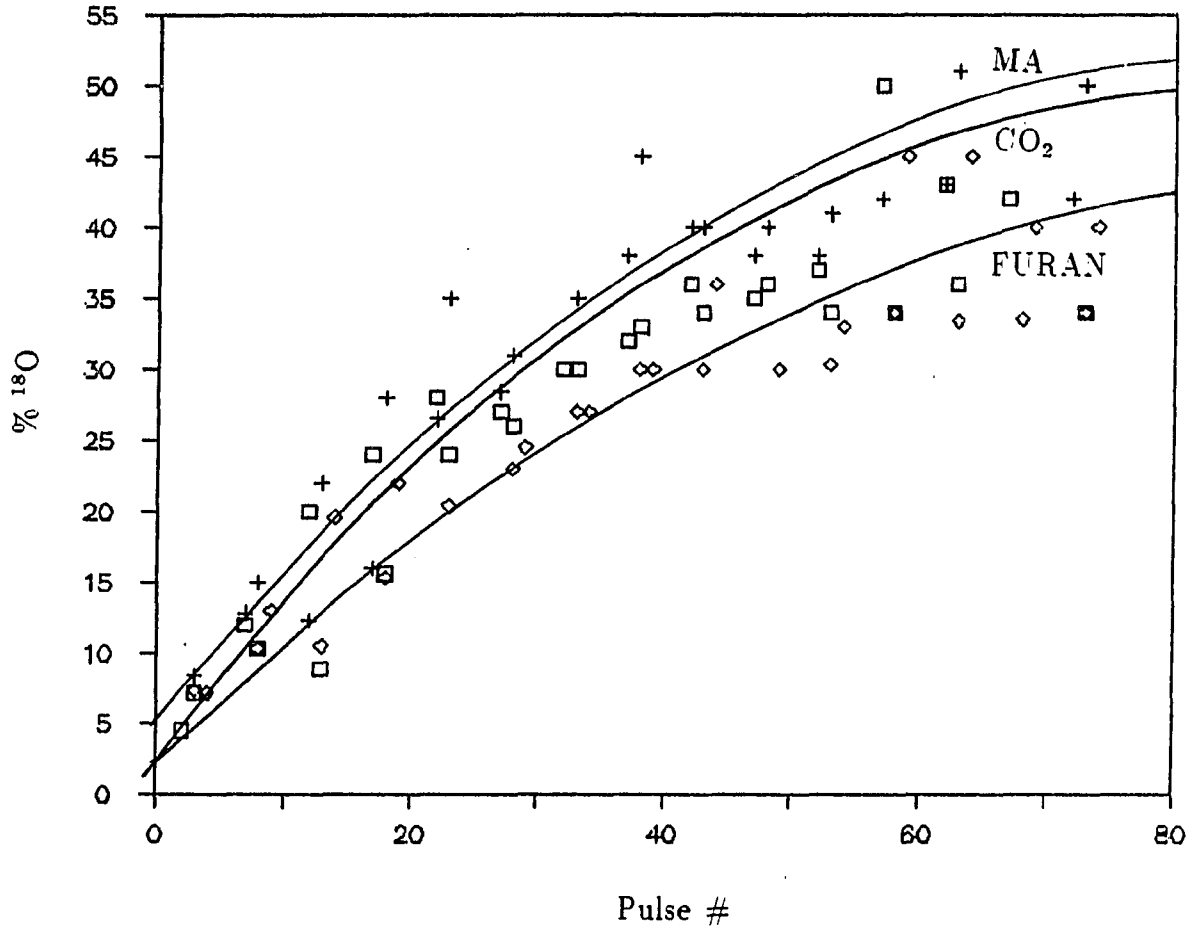

Figure 15: ^{18}O incorporation into products of 1,3-butadiene oxidation over ^{18}O enriched $(VO)_2P_2O_7$ during $^{18}O_2$ alternating pulse experiments

^{18}O incorporation into products of furan oxidation

Furan pulses Maleic anhydride and CO_2 were produced from all furan pulses over ^{18}O enriched $(VO)_2P_2O_7$. Maleic anhydride was produced at 10 times the level observed for n-butane pulses, while CO_2 was produced at roughly 10 times the level observed for n-butane pulses. The ^{18}O levels observed are presented in Figure 16. The ^{18}O level observed in the maleic anhydride 98 m/e range was a nearly constant 4%. The ^{18}O level observed in the maleic anhydride 54 m/e range (terminal oxygens only [36]) was about 2.5%. No ^{18}O was observed in the effluent furan. The ^{18}O level observed in CO_2 produced in this reaction ranged from an initial value of 2% to a final value of 1%.

Alternating $^{16}O_2$ and furan pulses Maleic anhydride and CO_2 were produced from all pulses of furan when $^{16}O_2$ and furan pulses were alternated over ^{18}O enriched $(VO)_2P_2O_7$. The production levels were similar to those observed when only furan pulses were introduced. The resulting ^{18}O levels are presented in Figure 17. The ^{18}O level observed for the m/e 98 range of maleic anhydride fell from 2.5% to less than 2% over the course of the experiment. The ^{18}O level observed for the m/e 54 range of maleic anhydride fell from 4% to slightly greater than 2%. The ^{18}O level observed in CO_2 fell from 2% to 0%. Trace levels of maleic anhydride and furan were observed during O_2 pulses. CO_2 was produced (at levels considerably lower than observed for 1,3-butadiene) during the O_2 pulses.

Alternating $^{18}O_2$ and furan pulses Maleic anhydride and CO_2 were produced from all pulses of furan when $^{18}O_2$ and furan pulses were alternated over ^{18}O enriched $(VO)_2P_2O_7$. Production levels were consistent with those observed in

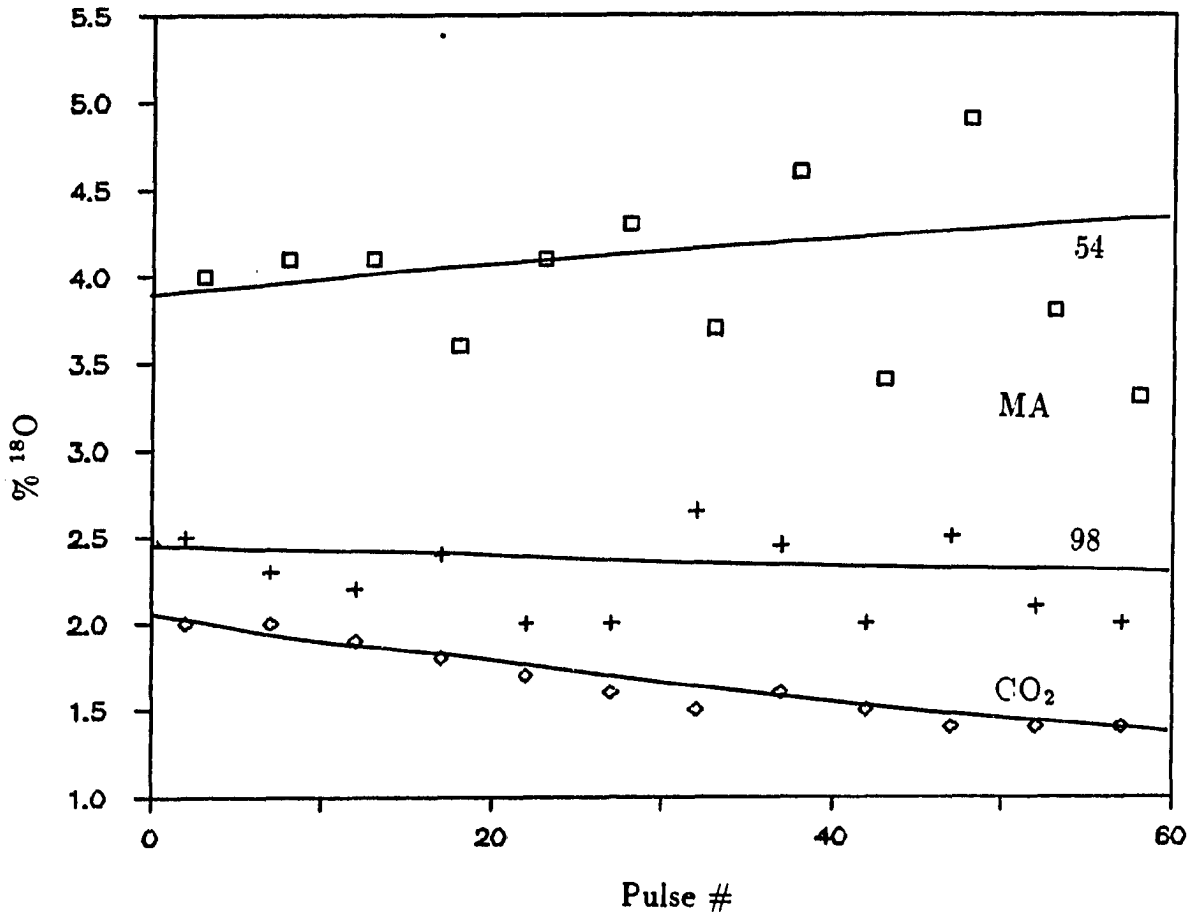

Figure 16: ^{18}O incorporation into products of furan oxidation over ^{18}O enriched $(VO)_2P_2O_7$

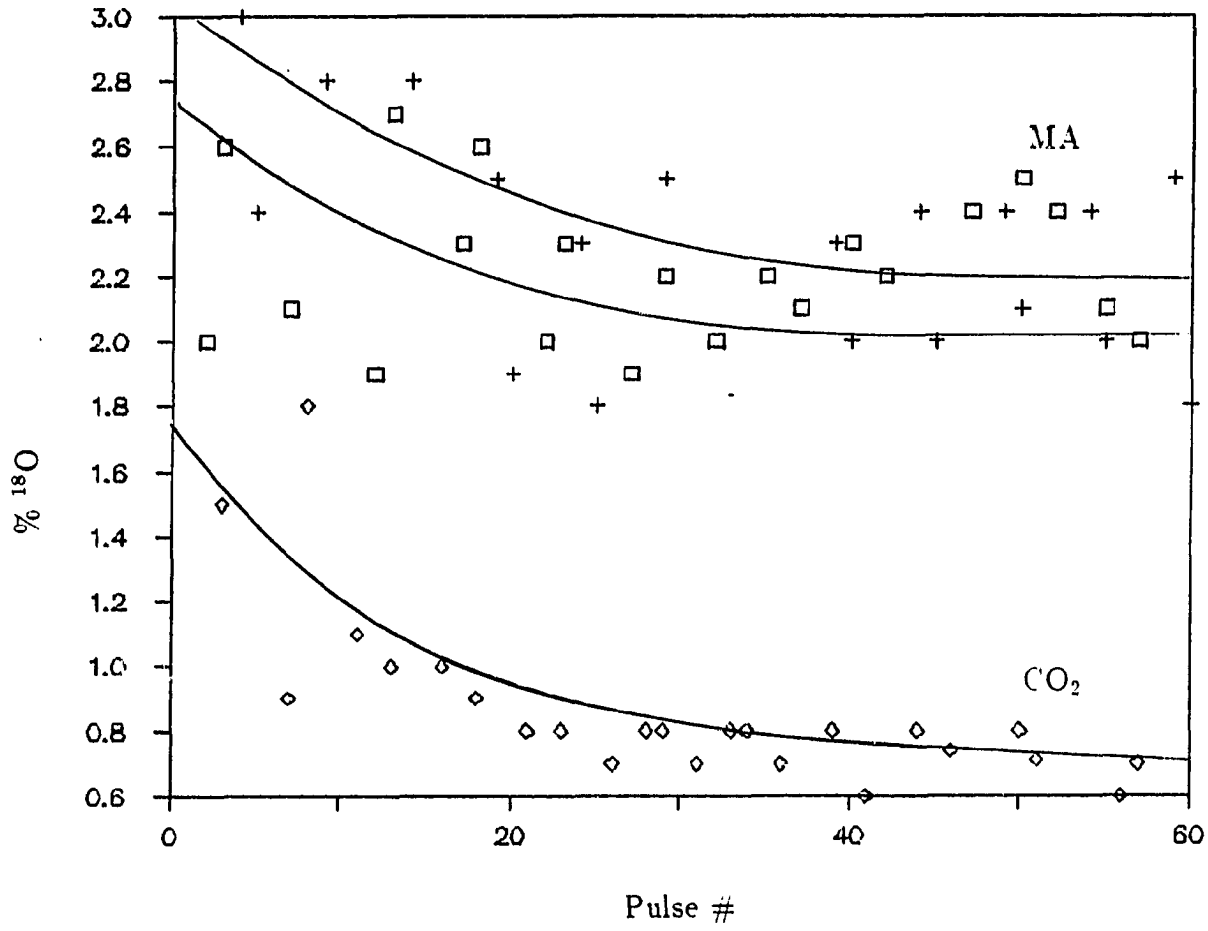

Figure 17: ^{18}O incorporation into products of furan oxidation over ^{18}O enriched $(VO)_2P_2O_7$ during $^{16}O_2$ alternating pulse experiments

the $^{16}O_2$ experiment. The ^{18}O levels observed are presented in Figure 18. The ^{18}O level observed in the m/e 98 range of maleic anhydride increased from 3% to 9% over the course of the experiment. The ^{18}O level observed in the 54 m/e range of maleic anhydride increased from 5% to 12%. The ^{18}O level observed in CO_2 increased from 2% to 18%. CO_2 produced during O_2 pulses contained less than 50% ^{18}O.

^{18}O incorporation into products of γ-butyrolactone oxidation

γ-Butyrolactone pulses Maleic anhydride and CO_2 were produced from all γ-butyrolactone pulses over ^{18}O enriched $(VO)_2P_2O_7$. Maleic anhydride was produced at 10 times the level observed for n-butane, while CO_2 was produced at 50 times the level observed for n-butane pulses. No furan was detected. The level of maleic anhydride production increased 100% from pulse 1 to pulse 75, while the CO_2 production fell 10%. The ^{18}O content of the products is shown in Figure 19. The ^{18}O content of maleic anhydride decreased from 5% to 1.5% from pulse 1 to pulse 75. The ^{18}O content of CO_2 decreased from 1% to 0%. The effluent γ-butyrolactone initially contained 3% ^{18}O. That level dropped to less than 1% by pulse 75.

Alternating $^{16}O_2$ and γ-butyrolactone pulses Maleic anhydride and CO_2 were produced from all γ-butyrolactone pulses when $^{16}O_2$ and γ-butyrolactone pulses were alternated over ^{18}O enriched $(VO)_2P_2O_7$. Production levels were similar to those observed when only γ-butyrolactone pulses were introduced, except that maleic anhydride production decreased by 50% and CO_2 production increased by 50% from pulse 1 to pulse 75. The level of ^{18}O in the products is presented in Figure 20. The ^{18}O level observed in maleic anhydride fell

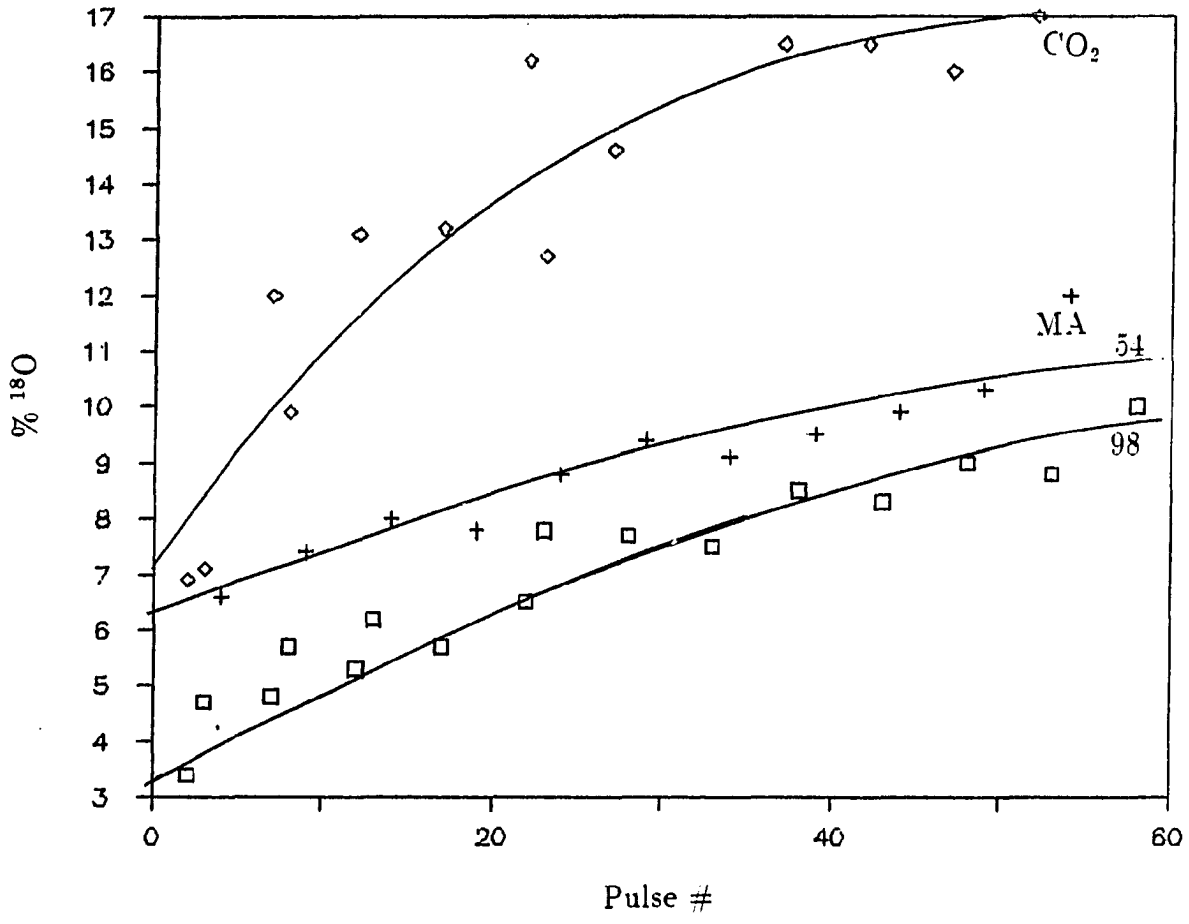

Figure 18: ^{18}O incorporation into products of furan oxidation over ^{18}O enriched $(VO)_2P_2O_7$ during $^{18}O_2$ alternating pulse experiments

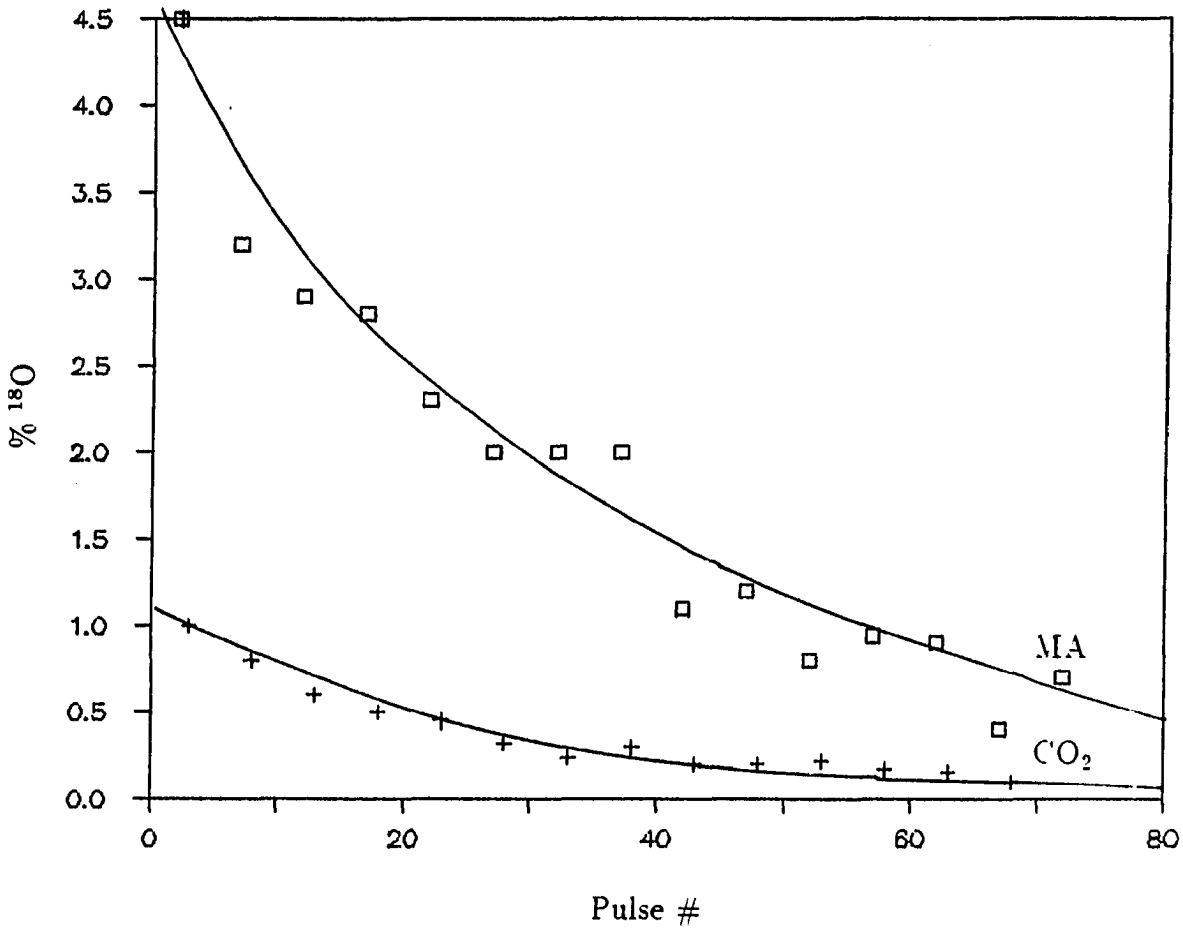

Figure 19: ^{18}O incorporation into products of γ-butyrolactone oxidation over ^{18}O enriched $(VO)_2P_2O_7$

from 4% to 1% from pulse 1 to pulse 75. The ^{18}O level observed in CO_2 fell from 1% to 0%. The ^{18}O level in effluent γ–butyrolactone fell from 3% to less than 1%. Trace levels of maleic anhydride and significant levels of CO_2 were observed during O_2 pulses.

Alternating $^{18}O_2$ and γ–butyrolactone pulses Maleic anhydride and CO_2 were produced from all pulses of γ–butyrolactone when $^{18}O_2$ and γ–butyrolactone pulses were alternated over ^{18}O enriched $(VO)_2P_2O_7$. Production levels were consistent with those observed in the $^{16}O_2$ experiment. The ^{18}O levels observed are presented in Figure 21. The ^{18}O level in maleic anhydride produced in this reaction increased from 4% to 25% from pulse 1 to pulse 75. The ^{18}O level in CO_2 increased from 1% to over 40% while the ^{18}O level in the effluent γ–butyrolactone increased from 4% to 20% from pulse 1 to pulse 75. CO_2 produced from $^{18}O_2$ pulses contained from 0% (pulse 1) to roughly 60% ^{18}O.

^{18}O incorporation into products of maleic anhydride oxidation

Maleic anhydride pulses Maleic anhydride and CO_2 were monitored for all maleic anhydride pulses over ^{18}O enriched $(VO)_2P_2O_7$. No furan was detected. The ^{18}O levels observed are presented in Figure 22. Both maleic anhydride m/e ranges monitored exhibited ^{18}O levels that ranged from about 4% to 2%. The ^{18}O level in CO_2 produced in this reaction contained no ^{18}O.

Alternating $^{16}O_2$ and maleic anhydride pulses Maleic anhydride and CO_2 were monitored for all maleic anhydride pulses when $^{16}O_2$ and maleic anhydride pulses were alternated over ^{18}O enriched $(VO)_2P_2O_7$. No furan was detected. Ninety percent less maleic anhydride survived the reaction when O_2

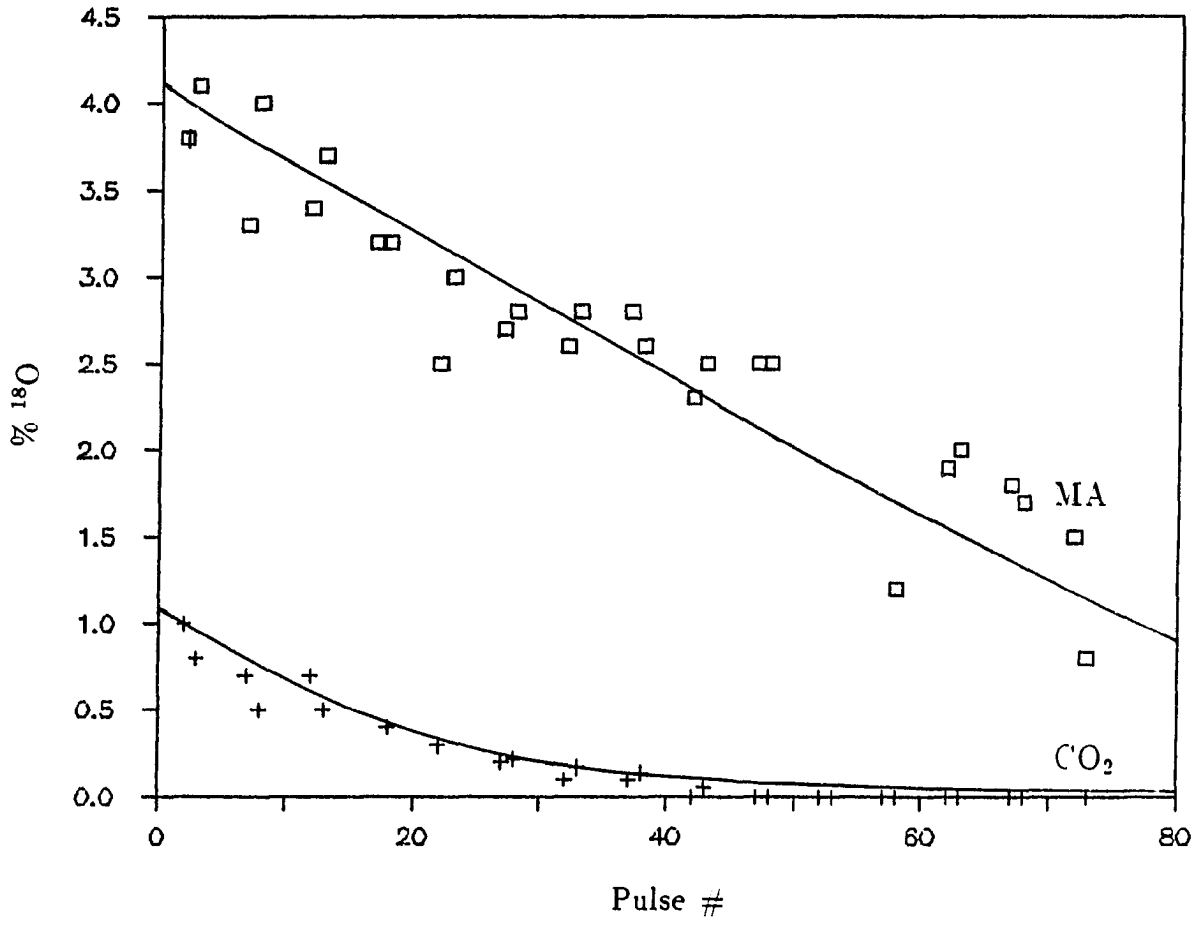

Figure 20: ^{18}O incorporation into products of γ-butyrolactone oxidation over ^{18}O enriched $(VO)_2P_2O_7$ during $^{16}O_2$ alternating pulse experiments

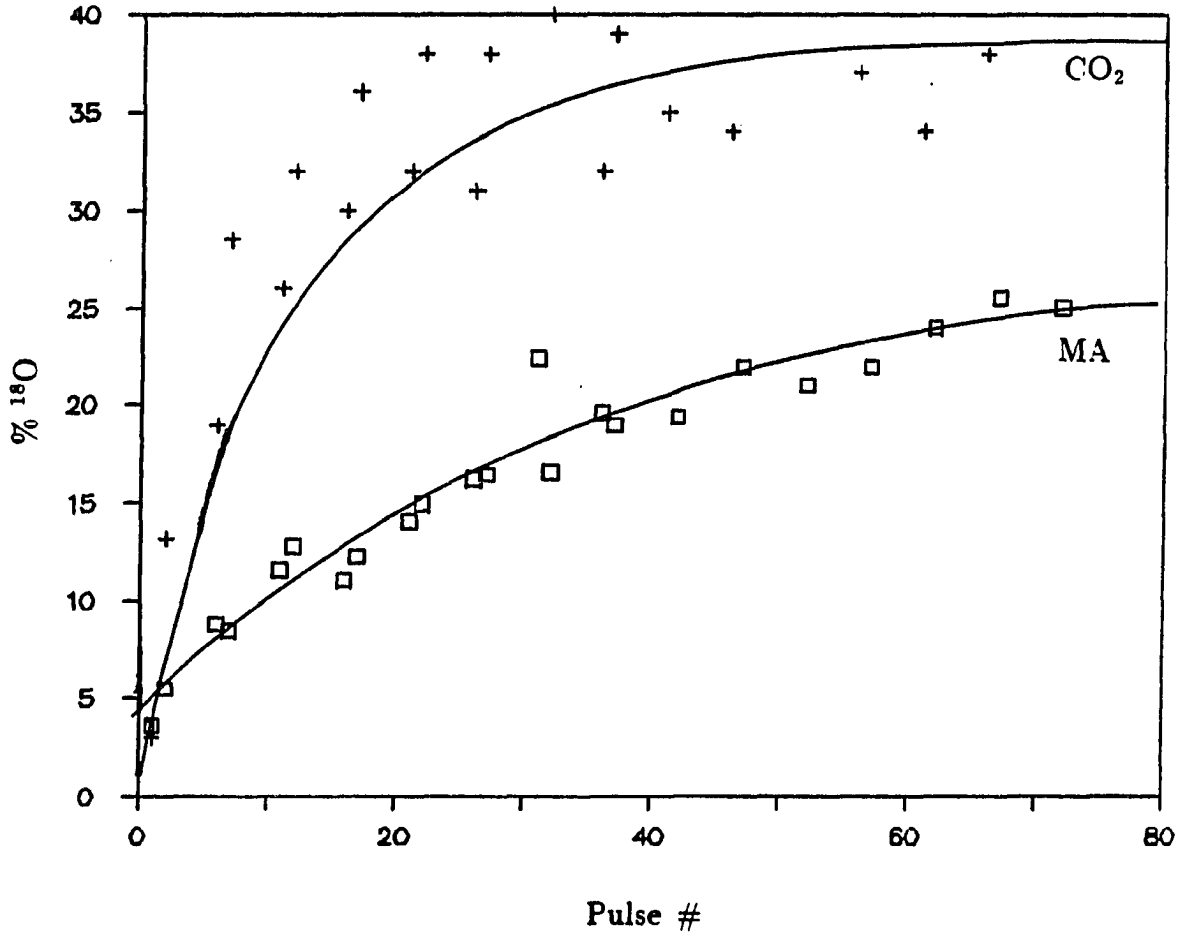

Figure 21: ^{18}O incorporation into products of γ-butyrolactone oxidation over ^{18}O enriched $(VO)_2P_2O_7$ during $^{18}O_2$ alternating pulse experiments

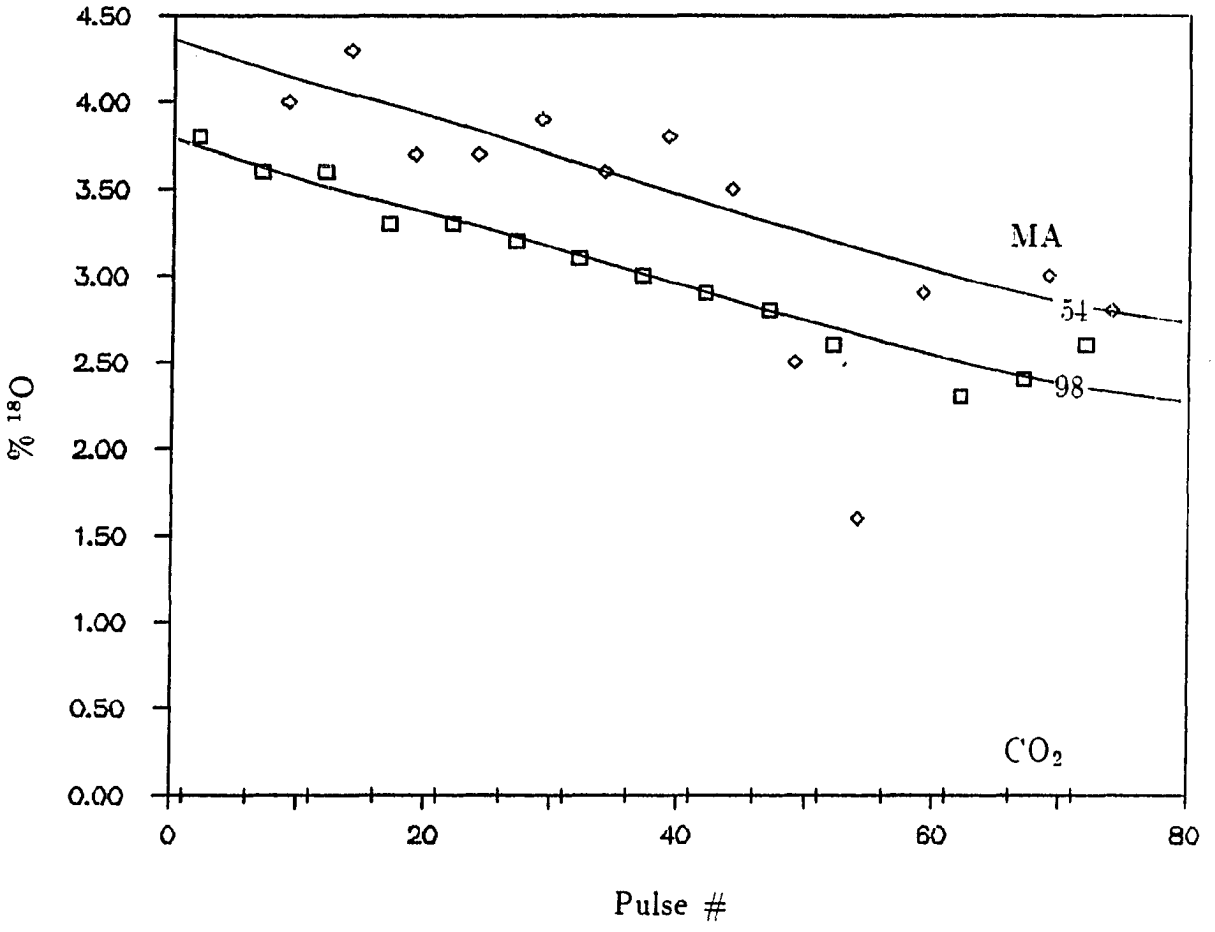

Figure 22: ^{18}O incorporation into products of maleic anhydride oxidation over ^{18}O enriched $(VO)_2P_2O_7$

pulses were alternated with the maleic anhydride pulses than when no O_2 was introduced. CO_2 production increased with pulse number and was 75% greater than that observed in the O_2 free experiment. The resulting ^{18}O levels are presented in Figure 23. The ^{18}O level in maleic anhydride (both fragment ranges) decreased from 3% to 0% in less than 50 pulses. CO_2 contained no detectable ^{18}O. CO_2 was also produced during the O_2 pulses at about 10% of the level observed during the maleic anhydride pulses.

Alternating $^{18}O_2$ and maleic anhydride pulses Maleic anhydride and CO_2 were monitored for all maleic anhydride pulses when $^{18}O_2$ and maleic anhydride pulses were alternated over ^{18}O enriched $(VO)_2P_2O_7$. No furan was detected. CO_2 production and maleic anhydride conversion were consistent with that observed in the ^{16}O experiment. ^{18}O observed in effluent maleic anhydride and CO_2 are presented in Figure 24. ^{18}O levels in effluent maleic anhydride increased from 4% to 13% after 20 pulses. The ^{18}O level remained near this level for the duration of the experiment (50 pulses). The ^{18}O level observed in CO_2 increased from 0% to greater than 32% after 50 pulses. CO_2 produced during the $^{18}O_2$ pulses contained less than 50% ^{18}O.

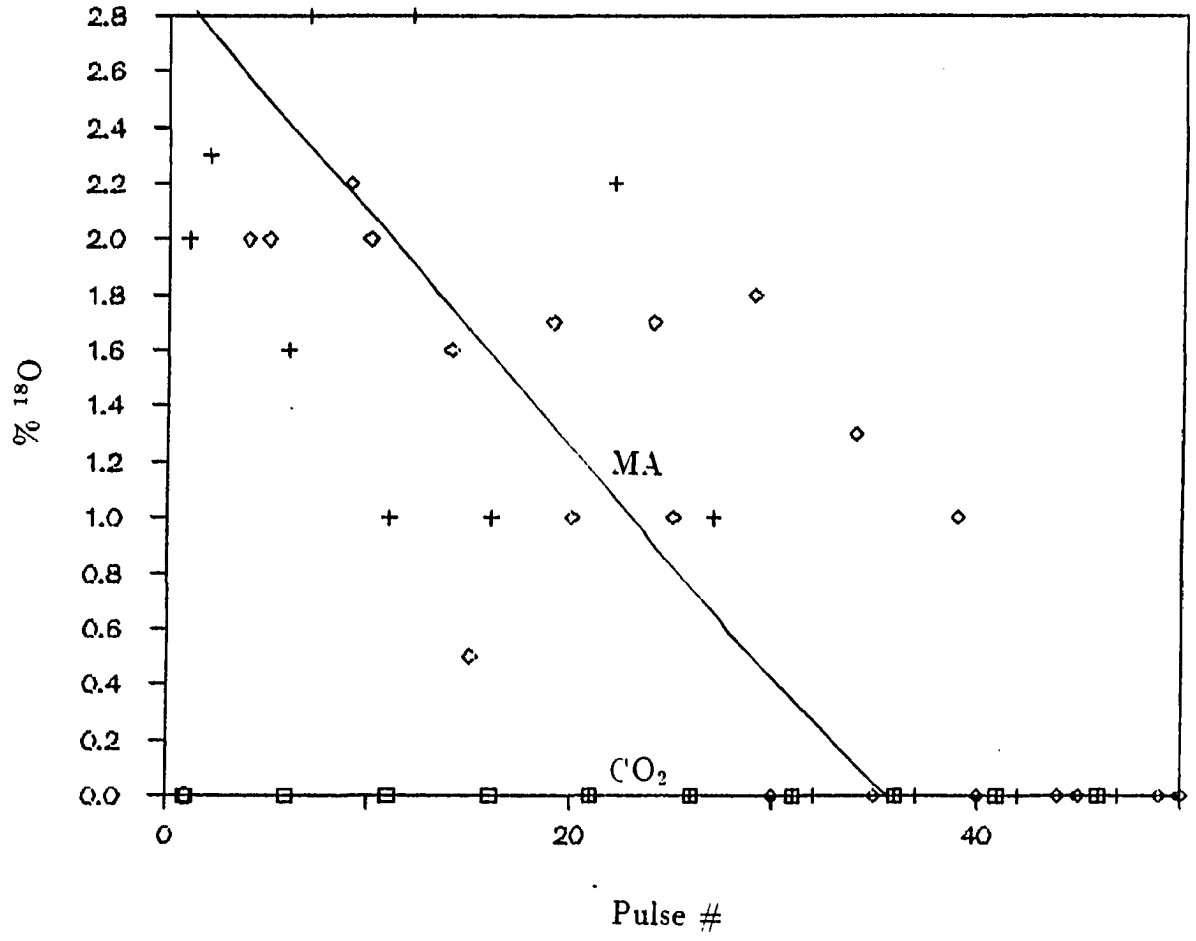

Figure 23: ^{18}O incorporation into products of maleic anhydride oxidation over ^{18}O enriched $(VO)_2P_2O_7$ during $^{16}O_2$ alternating pulse experiments

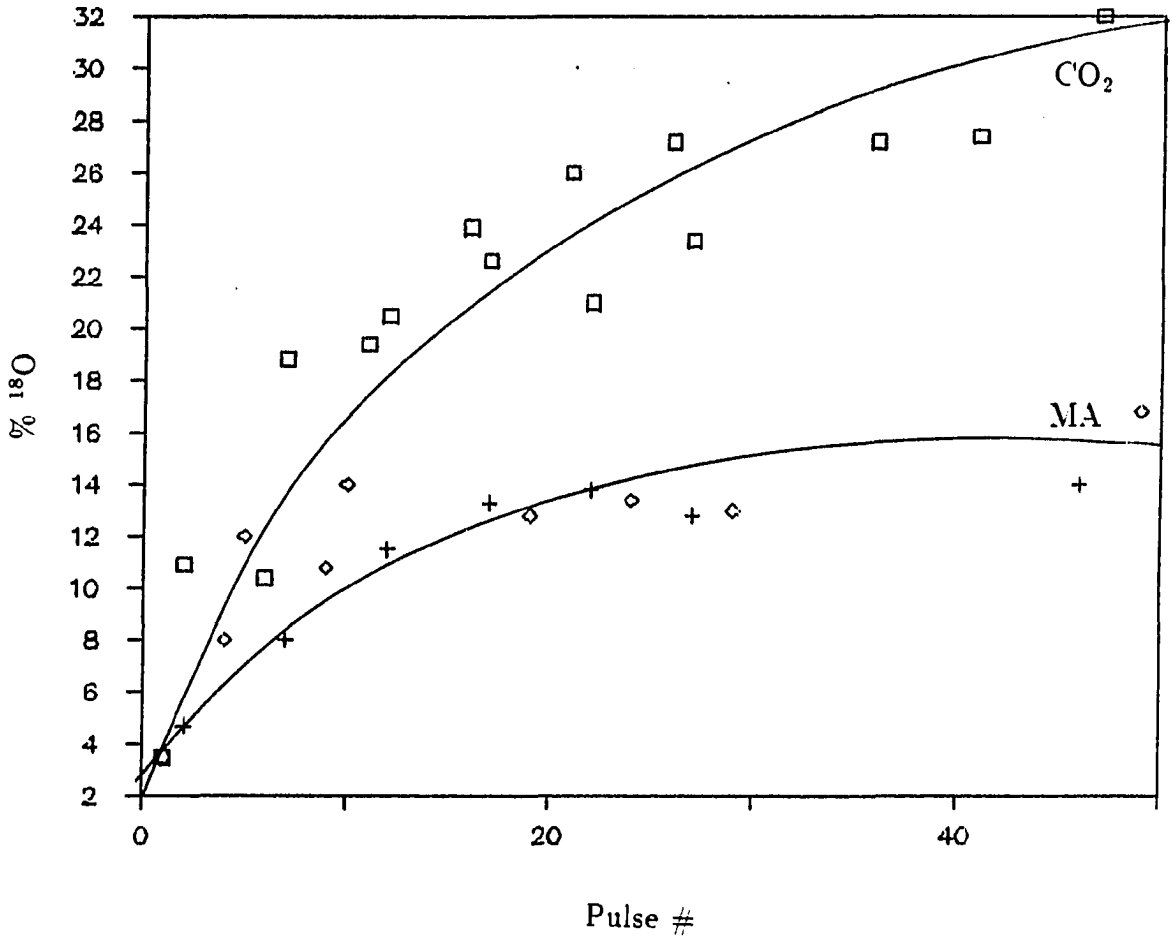

Figure 24: ^{18}O incorporation into products of maleic anhydride oxidation over ^{18}O enriched $(VO)_2P_2O_7$ during $^{18}O_2$ alternating pulse experiments

DISCUSSION

Structural Considerations

The $(VO)_2P_2O_7$ structure consists of irregular edge sharing octahedral pairs which form infinite chains through V=O–V bonding. Pyrophosphate groups (P_2O_7) form two tridentate oxygen bridges with three separate chains, forming 4 P–O–V bonds, 2 V–O/^{P}–V bonds and 1 P–O–P bond, as shown in Figure 25. Only equatorial oxygens in the V polyhedra are shared with the pyrophosphate groups. As a result, at least 3 distinct P–O oxygen groups exist in this structure [35].

Raman and FTIR spectra indicate that upon thermal reduction of β–$VOPO_{7/2}{}^{18}O_{1/2}$, ^{18}O remains in the $(VO)_2P_2O_7$ which is formed, and in fact, this ^{18}O can be found only in specific sites. The P–^{18}O–P and P–^{16}O–P Raman bands at 910 cm^{-1} and 925^{-1} clearly show that 30% of the P–O–P oxygen is ^{18}O. The labeling of this site is confirmed by the FTIR spectra. Additionally, the FTIR spectra show that the P–O groups which from the tridentate bridges are enriched to some extent with ^{18}O, while the FTIR band for V=O shows no signs of isotopic labeling.

The amount of ^{18}O in the $(VO)_2P_2O_7$ catalyst is determined by the ^{18}O content of the β–$VOPO_4$ from which it is made and the ^{18}O content of the oxygen released in the reduction process. Ten percent of the oxygen in the original

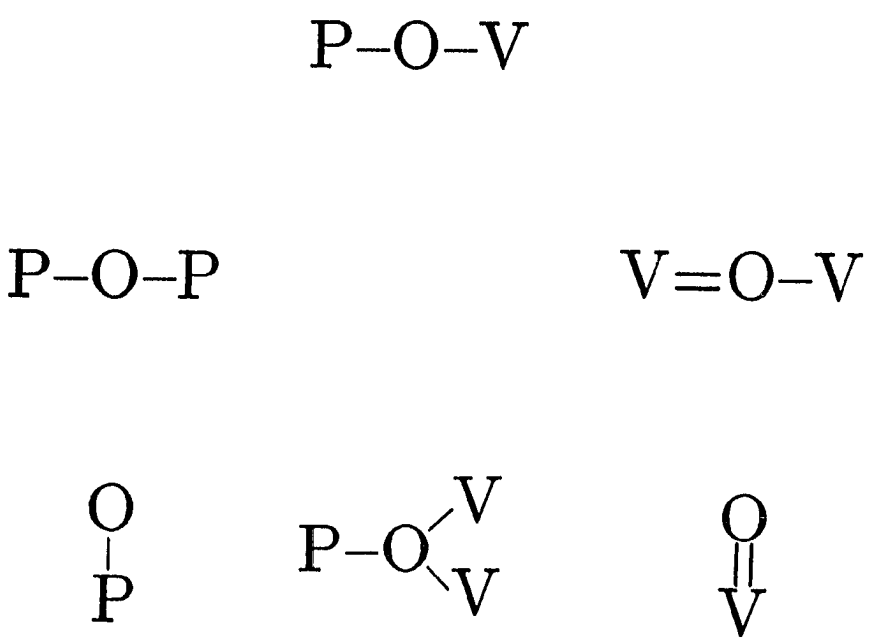

Figure 25: P-O bonds in $(VO)_2P_2O_7$

β-$VOPO_{7/2}{}^{18}O_{1/2}$ is ^{18}O. The ^{18}O is distributed in a very specific fashion in β-$VOPO_{7/2}{}^{18}O_{1/2}$ [31]. The PO_4 groups in β-$VOPO_4$ contain three crystallographically distinct P–O–V species. One of the P–Os is enriched to around the 40% level, two of the four P–O–Vs are identical and contain about 5% ^{18}O each while the fourth P–O–V contains no ^{18}O as indicated in Figure 26. The V=O and V=O–V sites contain no ^{18}O. This accounts for all of the ^{18}O in β-$VOPO_{7/2}{}^{18}O_{1/2}$.

Thermal reduction experiments show that the O_2 released in the reduction of β-$VOPO_{7/2}{}^{18}O_{1/2}$ to ^{18}O enriched $(VO)_2P_2O_7$ is 14–15% ^{18}O. By ^{18}O balance, this results in an overall ^{18}O content in the $(VO)_2P_2O_7$ of about 9.5%. The FTIR spectra indicate that no ^{18}O appears in the V=O sites. All the ^{18}O is in the pyrophosphate groups. Therefore, the ^{18}O content of the pyrophosphate group is about 12%. The Raman spectra indicate that the P–O–P oxygen is about 30% ^{18}O. This means that, again by ^{18}O balance, the remaining PO_3 groups contain about 9% ^{18}O.

Raman spectra of β-$VOPO_4$ made by reoxidizing ^{18}O enriched $(VO)_2P_2O_7$ with ^{16}O at high temperatures (850 K) indicate that the P–O–V which contained no ^{18}O in the original β-$VOPO_{7/2}{}^{18}O_{1/2}$ remains ^{18}O free. Thus, no scrambling of ^{18}O among the various sites occurs, providing evidence that this particular P–O–V maintains its integrity throughout this type of oxidation and reduction and remains unlabeled in the ^{18}O enriched $(VO)_2P_2O_7$.

The pyrophosphate groups are formed from pairs of PO_4 groups which collapse when one of the eight oxygens is removed in the reduction process. Based on the ^{18}O labeling in β-$VOPO_{7/2}{}^{18}O_{1/2}$, the reduction data and the sites labeled in $(VO)_2P_2O_7$, the reduction mechanism and resulting ^{18}O distribution in

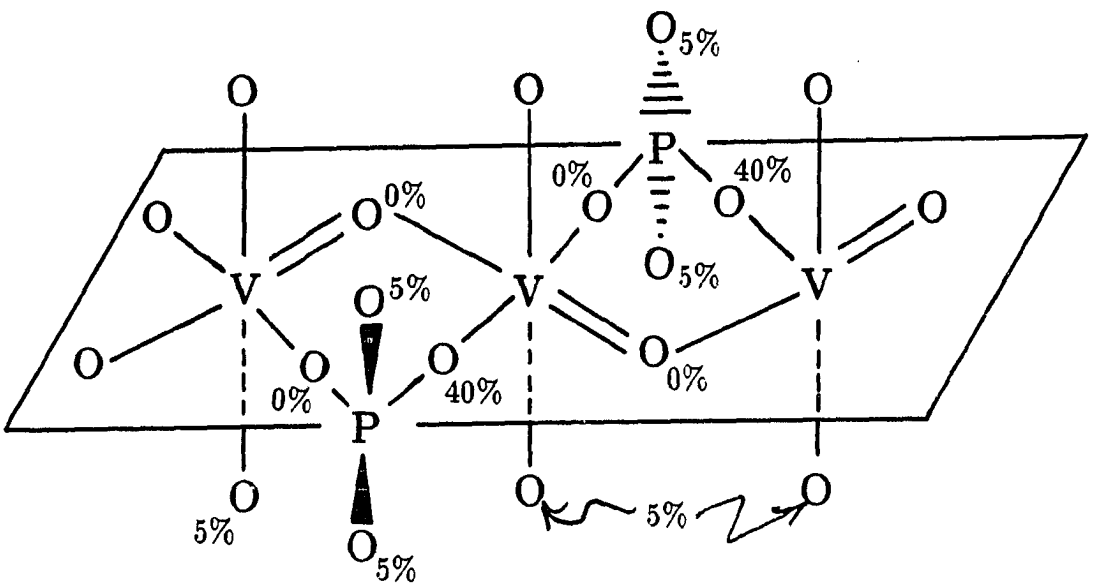

Figure 26: ^{18}O enriched sites in β-$VOPO_{7/2}{}^{18}O_{1/2}$

$(VO)_2P_2O_7$ shown in Figure 27 is proposed.

This mechanism satisfies the observed ^{18}O balance and the observed vibrational spectroscopic information. Thirty percent of the oxygen removed in the thermal reduction is from the 40% ^{18}O P-O-V site in β-$VOPO_{7/2}{}^{18}O_{1/2}$, while the remaining 70% is from the 5% P-O-V site. Conversely, 30% of the P-O-P oxygen originates in the 5% P-O-V site of β-$VOPO_{7/2}{}^{18}O_{1/2}$, while the remaining 70% comes from the 40% P-O-V site. The remaining 5% and 40% sites occupy P-O-V tridentate bridging sites in $(VO)_2P_2O_7$.

The result is a $(VO)_2P_2O_7$ catalyst with specifically labeled P-O sites. In the context of the entire $(VO)_2P_2O_7$ structure, the spectroscopic and thermal reduction data suggest that the two unlabeled P-Os are the two 2 V-O-P-V groups present in each pyrophosphate entity, while the 4 P-O-V oxygens are the labeled sites, in addition to the P-O-P sites labeled at the 30% level. The stoichiometry of the reduction is indicated below:

$$2\ \beta\text{-}VOPO_{7/2}{}^{18}O_{1/2} \longrightarrow (VO)_2P_2{}^{16}O_{6.15}{}^{18}O_{0.85} + 1/2\ {}^{16}O_{1.7}{}^{18}O_{0.3}$$

The bulk distribution of ^{18}O in labeled $(VO)_2P_2O_7$ is shown in Figure 28.

Hydrocarbon Oxidation

n-Butane

In the absence of gas phase oxygen, n-butane reacts over ^{18}O labeled $(VO)_2P_2O_7$ to form maleic anhydride containing 5% ^{18}O, while combustion results in CO_2 with low levels of ^{18}O (1% to 2%). The furan produced in this reaction contains no ^{18}O. This indicates that n-butane interacts with the surface in a very

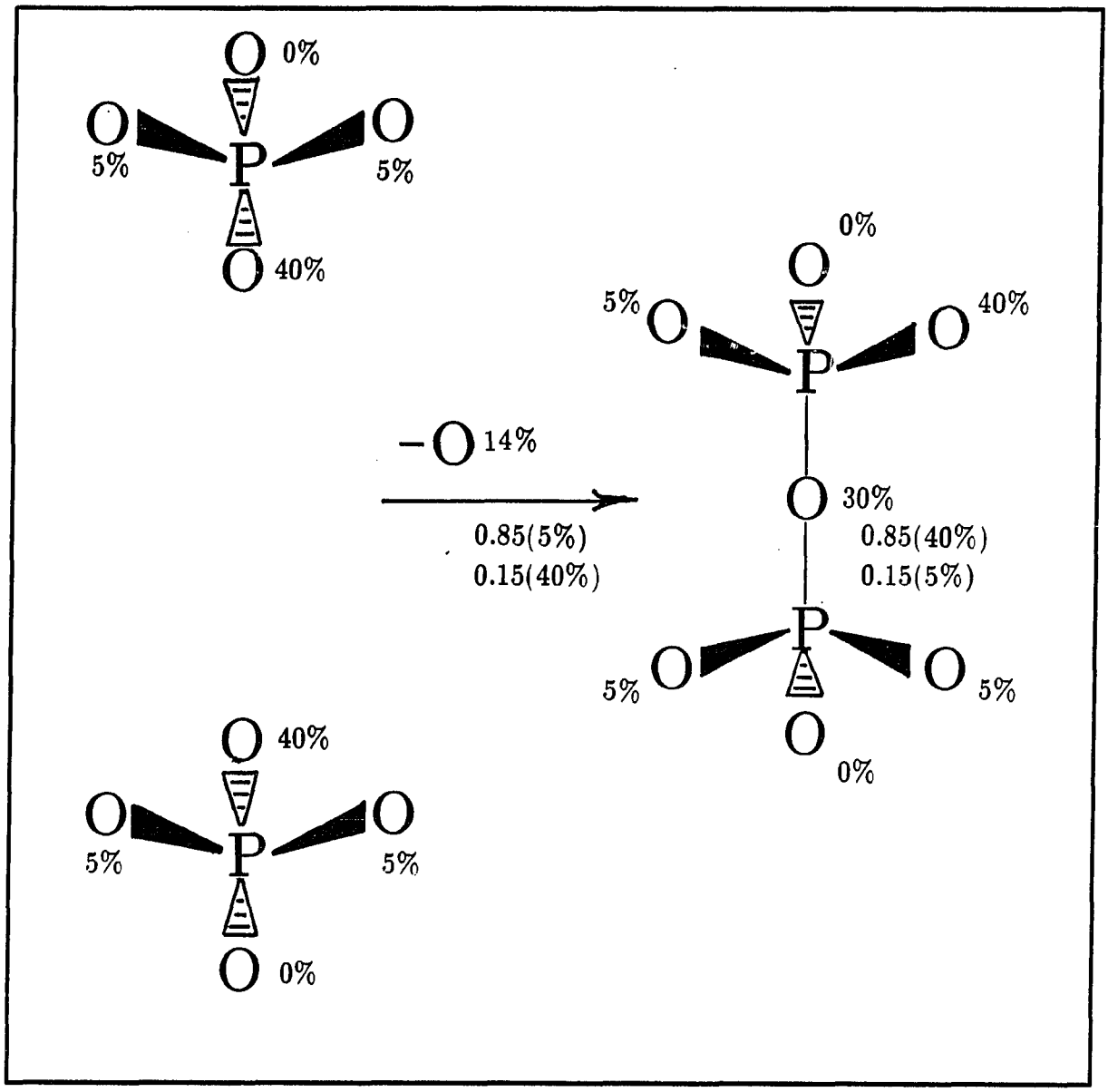

Figure 27: Possible reduction mechanism: β-$VOPO_{7/2}{}^{18}O_{1/2}$ to ^{18}O enriched $(VO)_2P_2O_7$ and the resulting ^{18}O labeled sites in $(VO)_2P_2O_7$

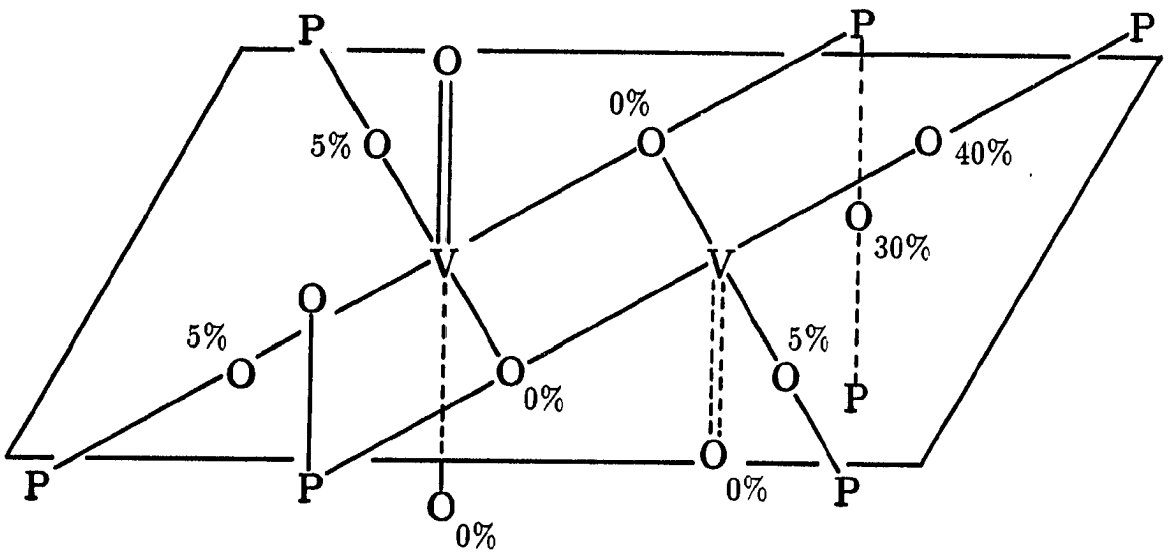

Figure 28: ^{18}O labels in $(VO)_2P_2O_7$ bulk structure

selective manner such that the process is constrained to form this adsorbed species at only one type of site. The unlabeled V-O-P-V site could provide this function. In turn, this adsorbed intermediate is constrained to react only with nearby oxygen sites. The ^{18}O levels observed indicate that this second type of oxygen must contain about 7.5% ^{18}O. This indicates that the P-O-V oxygens are involved, with the 5% ^{18}O site being utilized most frequently. There is no indication that the P-O-P (30% ^{18}O) is involved in any catalytic reactions. ^{18}O levels in CO_2 are slightly higher than would be expected for the consecutive combustion of maleic anhydride on unlabeled sites. This was also observed in the reaction of maleic anhydride over labeled β-$VOPO_4$ [31].

Alternating pulses of O_2 (^{16}O or ^{18}O) between pulses of n-butane does not alter the role of specific sites in the reaction. While the ^{18}O levels observed in the products change, the catalytic sites maintain their original identity and continue to perform the same catalytic functions observed in the oxygen free experiments. This is most evident in the $^{18}O_2$ experiments. The ^{18}O content in CO_2 increased from less than half the level observed in maleic anhydride to nearly twice that observed in maleic anhydride, while the level in maleic anhydride increased from 5% to 13%. The furan formation site shows very limited ^{18}O incorporation. This is probably a result of the low conversion (and hence low number of sites addressed) and the limited reactivity of this site. The nearly negligible amount of CO_2 formed during O_2 pulses indicates that very small amounts of combustible adsorbed species exist on the surface between n-butane pulses. The incorporation of O atoms from gas phase O_2 occurs more rapidly into CO_2 than that observed for maleic anhydride.

1–Butene

The behavior of 1–butene is markedly different than that of n–butane. When 1–butene pulses were fed to the ^{18}O labeled $(VO)_2P_2O_7$, very little maleic anhydride was formed while a much greater amount of furan was formed. The ^{18}O content in the furan formed was high (15% to 10%), while that observed for CO_2 was very low (1%). This indicates that CO_2 and furan are formed at very different sites. Additionally, furan formed from 1–butene is not formed in the same manner as from n–butane. In the absence of gas phase oxygen or replenishing oxygen pulses, 1–butene utilizes the surface lattice oxygens to form mainly furan and small amounts of phthalic anhydride. The initial interaction of 1–butene with the surface overwhelms the available sites, and, as a result, not enough selective sites remain in close enough proximity to allow the formation of maleic anhydride. Another possibility is that upon contact with the surface, 1–butene is either burned or constrained in such a fashion so that it can form only furan and not continue on to maleic anhydride.

The alternate pulse experiments shed light on this problem. The data indicate that, upon introducing gas phase O_2 between 1–butene pulses, selective and nonselective sites maintain their identity and continue to perform the same catalytic function as was observed in the O_2 free experiment. But, the formation of phthalic anhydride is suppressed and the formation of maleic anhydride is enhanced. Additionally, while the furan formed still contains high levels of ^{18}O (12% dropping to 8%), the maleic anhydride formed contains considerably less ^{18}O (5% dropping to 2%). These figures indicate that the two oxygens added to the furan intermediate come originally from the $^{16}O_2$ pulses. Additional ^{16}O is introduced through reoxidation of the reduced furan formation sites. The ^{18}O pulse data confirm these

observations. In summary, 1-butene forms furan at sites which contain 10% to 15% ^{18}O (combination of all P-O-V sites) and cannot form large quantities of maleic anhydride unless an additional surface oxygens species is provided by introduction of gas phase O_2 pulses. The initial interaction of 1-butene is occurs in a particular fashion, but not as particular and constrained as that of n-butane. Again, there is no sign of P-O-P site involvement in either selective or nonselective oxidation.

The formation of large amounts of CO_2 during O_2 pulses indicates that large amounts of strongly adsorbed hydrocarbon remain on the surface between hydrocarbon pulses. ^{18}O pulses indicate that at least 50% of the combustion oxygen comes from the original lattice oxygen. Therefore, the strongly adsorbed hydrocarbon may be in a highly oxidized state.

1,3-Butadiene

The oxidation of 1,3-butadiene over ^{18}O labeled $(VO)_2P_2O_7$ is much less site specific than either n-butane or 1-butene. In all three 1,3-butadiene experiments, maleic anhydride, furan and CO_2 are formed containing ^{18}O at much the same levels. The addition of O_2 pulses increases the production of both furan and maleic anhydride (at the expense of phthalic anhydride), but the ^{18}O levels in all products remain similar.

CO_2 is produced during oxygen pulses at nearly the same quantity as the hydrocarbon pulses. This indicates the presence of adsorbed, combustible hydrocarbon on the catalyst surface between hydrocarbon pulses. The $^{18}O_2$ pulse experiment shows that much (over 50%) of the oxygen utilized to form CO_2 during $^{18}O_2$ pulses is ^{16}O and thus, comes from the original catalyst lattice. Therefore, as with 1-butene, the strongly adsorbed combustion precursor is highly oxidized.

Furan

The ^{18}O levels observed in the products of furan oxidation over ^{18}O enriched $(VO)_2P_2O_7$ show that selective and nonselective oxidation of furan occur at different sites. This site identity is maintained upon introduction of oxygen pulses. The mass spectrometry data show no evidence of furan exchanging oxygen with labeled sites. Comparison of the m/e 98 thru 104 (all three maleic anhydride oxygens) range and the m/e 54 thru 56 (only one of two terminal oxygens) [36] shows that the ring oxygen contains no ^{18}O. All ^{18}O is concentrated into the 2 terminal C=O oxygens of maleic anhydride. When no O_2 pulses are introduced, the overall ^{18}O content of maleic anhydride from furan is about 2.5%, while that of just the terminal oxygens is about 4%. This confirms that the two terminal oxygens come from lattice sites enriched at about the 4% level.

When O_2 pulses (either ^{16}O or ^{18}O) are introduced, selective verses nonselective site identity is maintained, while the ring oxygen in maleic anhydride remains unlabeled, even as the overall ^{18}O incorporation into maleic anhydride during $^{18}O_2$ experiments approaches 12%. Thus, the selective oxidation sites for furan conversion to maleic anhydride are the 4% to 5% enriched P–O–V sites. Once again, P–O–P sites are not involved in any catalytic reaction.

Incorporation of O atoms originally from the gas phase into CO_2 occurs more rapidly than into maleic anhydride.

γ–Butyrolactone

The oxidation of γ–butyrolactone over ^{18}O enriched $(VO)_2P_2O_7$ is another example of a unique interaction of a molecule with this catalyst. The large amount of exchange exhibited by γ–butyrolactone, especially when $^{18}O_2$ pulses are

introduced, is evidence that this species interacts with the catalytic surface in a way not not closely related to the other hydrocarbons studied. In contrast to other species fed, the production of maleic anhydride from γ–butyrolactone increases as oxygen is removed from the catalyst surface, while it decreases with [illegible] number when oxygen pulses are introduced. The one similarity observed is the identity of selective and nonselective sites. In all three γ–butyrolactone experiments, CO_2 and maleic anhydride incorporate distinctly different amounts of ^{18}O. Incorporation of O atoms originally from the gas phase into CO_2 occurs much more rapidly than for maleic anhydride.

Maleic anhydride

Finally, when maleic anhydride is pulsed over ^{18}O enriched $(VO)_2P_2O_7$, significant exchange occurs with oxygens at ^{18}O enriched sites. The ^{18}O is introduced at random positions in the maleic anhydride. This indicates that the mechanism of exchange involves opening of the maleic anhydride ring, possibly forming adsorbed maleic acid, followed by dehydration to maleic anhydride.

The observed mass spectra for CO_2 indicate no incorporation of ^{18}O. When oxygen pulses are introduced, 90% more of the maleic anhydride is combusted. The remaining maleic anhydride exhibits exchange with the selective sites. The incorporation of O atoms originally from gas phase O_2 into CO_2 occurs much more rapidly than into maleic anhydride.

CONCLUSIONS

By labeling specific lattice oxygen sites in $(VO)_2P_2O_7$ with ^{18}O, it is possible to resolve the existence of selective and nonselective lattice oxygen sites in this catalyst. The selectivity of a particular site depends upon the hydrocarbon fed. For n-butane, combustion occurs mainly at V=O sites, with the consecutive combustion of all intermediates possible. Maleic anhydride combusts only at V=O sites, as observed by Centi *et al.* [29].

These studies support the assertion by Centi and Trifiro [37] that the initial activation of n-butane occurs on a pair of vanadyl octahedra. Then, as postulated by Pepera *et al.* [38], the selectivity is controlled by the consecutive reactions of the reactive intermediate(s). If properly orientated, the intermediate reacts with a $V\text{-}O\text{-}\overset{P}{}\text{-}V$ oxygen and forms a strongly adsorbed furan like intermediate, which may react with neighboring P-O-V oxygens to form maleic anhydride, or in the presence of V=O oxygens, combust. If the activation results in an intermediate oriented such that these reactions cannot take place, it may result in a highly oxygenated, strongly adsorbed intermediate which results in combustion products as the surface is reoxidized by gas phase oxygen.

This two oxygen site pathway is depicted in Figure 29. Gleaves and Ebner also propose that at least two different oxygen species are responsible for the selective oxidation of n-butane on $(VO)_2P_2O_7$, but they postulate that one oxygen, O^*,

may not be a surface lattice oxygen [28]. While a chemisorbed highly reactive oxygen species may enhance the activation of n-butane, the terminal oxygens of maleic anhydride are formed from P-O-V oxygens. This reaction is enhanced, however, by the reoxidation of the surface by gas phase oxygen. This fact is not evident in experiments not utilizing specifically labeled catalysts.

The diverging reaction pathways evidenced by the ^{18}O content of the products formed during the oxidation of the various hydrocarbons fed demonstrates the importance and uniqueness of the initial interaction and stabilization of each species on the catalyst surface. After that initial interaction, each species is constrained to follow certain pathways to the final products, and, while the final products may be the same, the path can be very different.

This work also provides evidence concerning the nature of the catalytic surface of $(VO)_2P_2O_7$ under reaction conditions. While selective oxidation occurs on β-$VOPO_4$, and selective and nonselective sites can be distinguished on this phase [31], this phase is not present on the surface of $(VO)_2P_2O_7$ under reaction conditions. The P-O-P bond in $(VO)_2P_2O_7$ is not utilized in either selective or nonselective reactions, as it would be if $(VO)_2P_2O_7$ were converted to β-$VOPO_4$. Therefore, the V(V) species present on the reactive surface of $(VO)_2P_2O_7$ is not any form of β-$VOPO_4$.

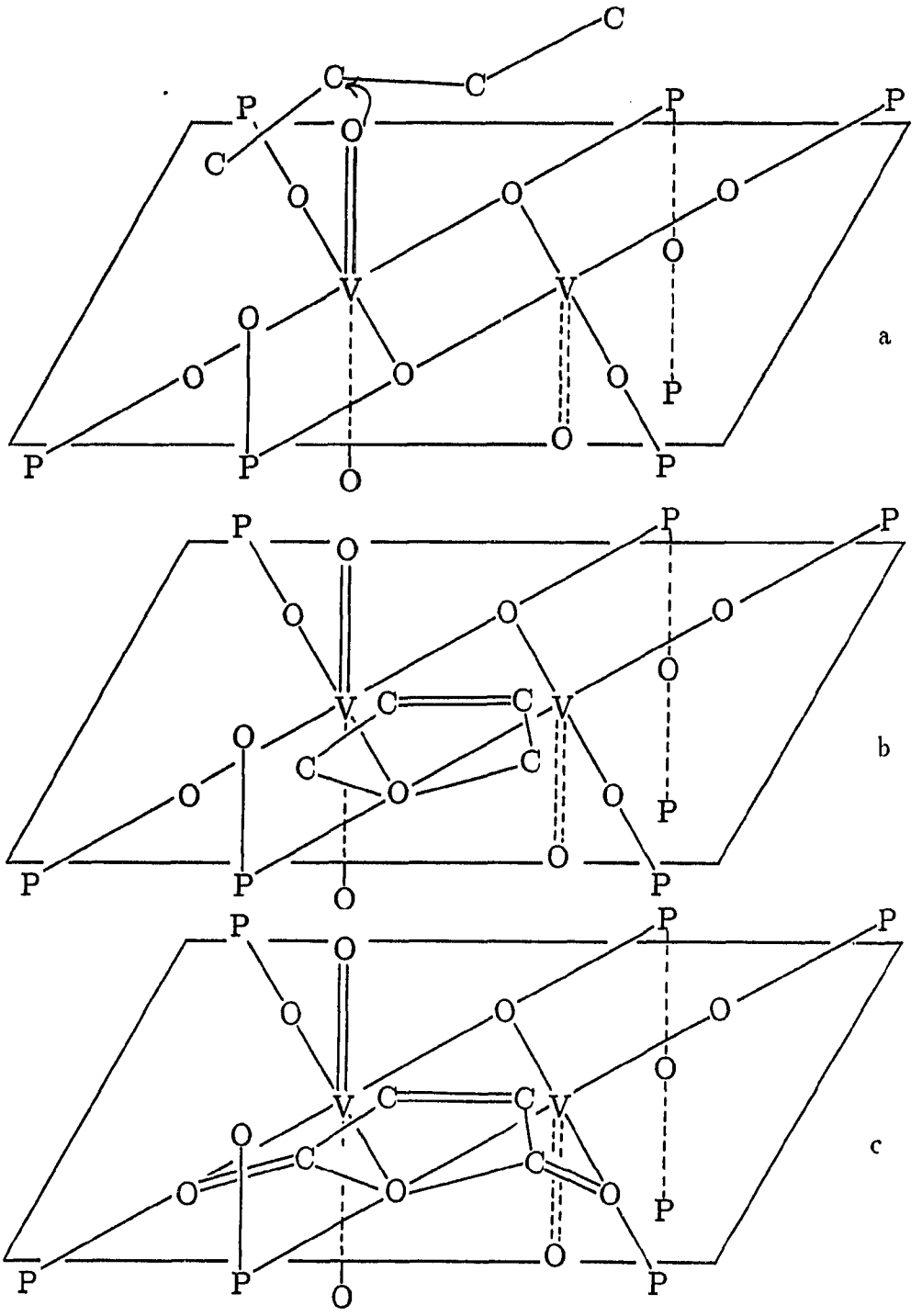

Figure 29: Selective oxidation of n-butane on ^{18}O labeled $(VO)_2P_2O_7$: (a) Activation [37, 38], (b) formation of adsorbed furan-like species, (c) formation of maleic anhydride

ACKNOWLEDGMENT

This work was performed at Ames Laboratory under contract No. W-7405-eng-82 with the U. S. Department of Energy. The United States government has assigned the DOE Report number IS-T 1411 to this thesis.

REFERENCES CITED

1. Busca, G.; Centi, C.; Journal of the American Chemical Society (1989) **111**, 46.
2. Moser, T. P.; Schrader, G. L. Journal of Catalysis (1985) **92**, 216.
3. Wenig, R. W.; Schrader, G. L. Journal of Physical Chemistry (1986) **90**, 6480.
4. Ostroushko, V. I.; Kernos, Yu. D.; Ioffe, I. I. Neftekhimiya (1972) **12(3)**, 95.
5. Morselli, L.; Riva, A.; Trifiro, F.; Emig, G. La Chimica E L'Industria (1978) **60(10)**, 791.
6. Ai, M.; Bountry, P.; Montarnal, R. Bulletin de la Societe Chimique de France (1970) **8–9**, 2775.
7. Ai, M. Bulletin of the Chemical Society of Japan (1970) **43(1)**, 3490.
8. Varma, R. L.; Saraf, D. N. Journal of Catalysis (1978) **55**, 361.
9. Escardino, A.; Sola, C.; Ruiz, F. Aneles de Quimica (1973) **69**, 385.
10. Wohlfhart, K.; Hofmann, H. Chemie Ingenieur Technik (1980) **52(10)**, 811.
11. Hodnett, B. K.; Permanne, Ph.; Delmon, B. Applied Catalysis (1983) **6**, 231.
12. Wustneck, N.; Wolf, H.; Seeboth, H. Reaction Kinetics and Catalysis Letters (1982) **21(4)**, 497.
13. Centi, G.; Fornasari, G.; Trifiro, F. Journal of Catalysis (1984) **89**, 44.
14. Hodnett, B. K.; Delmon, B. Applied Catalysis (1985) **15**, 141.
15. Centi, G.; Manenti, I.; Riva, A.; Trifiro, F. Applied Catalysis (1984) **9**, 177.
16. Morselli, L.; Trifiro, F.; Urban, L. Journal of Catalysis (1982) **75**, 112.
17. Ai, M. Journal of Catalysis (1981) **67**, 110.

18. Puttock, S. J.; Rochester, C. H. Journal of the Chemical Society Faraday Transactions 1 (1986) **82**, 3033.

19. Busca, G.; Centi, G.; Trifiro, F.; Lorenzelli, V. Journal of Physical Chemistry (1986) **90**, 1337.

20. Puttock, S. J.; Rochester, C. H. Journal of the Chemical Society Faraday Transactions 1 (1986) **82**, 2773.

21. Centi, G.; Golinelli, G.; Trifiro, F. Bicentenary Catalysis (1988), 191.

22. Bordes, E.; Courtine, P. Journal of the Chemical Society, Chemical Communications (1985), 294.

23. Bordes, E.; Courtine, P. Journal of Catalysis (1979) **57**, 236.

24. Wenig, R. W.; Schrader, G. L. Industrial Engineering Chemistry Fundamentals (1986) **25**, 612.

25. Garbassi, F.; Bart, B.; Tassinari, R.; Vlaic, G.; and Lagarde; P. Journal of Catalysis (1986) **98**, 317.

26. Hodnett, B.; Delmon, B. Journal of Catalysis (1984) **88**, 43.

27. Busca, G.; Centi, G.; Trifiro, .F. Journal of the American Chemical Society (1985) **107**, 7758.

28. Gleaves, J. T.; Ebner, J. R.; Kuechler, T. C. Catalysis Reviews, Science and Engineering (1988) **30(1)**, 49.

29. Centi, G.; Golinelli, G.; Trifiro, F. Applied Catalysis (1989) **48**, 13.

30. Contractor, R. M.; Sleight, A. W. Catalysis Today (1988) **3**, 175.

31. Lashier, M. E.; Moser, T.P.; Schrader, G.L.; In *Studies in Surface Science and Catalysis: New Developments in Selective Oxidation*; Centi, G., Trifiro, F., eds. (Elsevier:Amsterdam 1990).

32. Bordes, E. Catalysis Today (1988) **3**, 163.

33. Moser, T.P.; Wenig, R.W.; Schrader, G.L. Applied Catalysis (1987) **34**, 39.

34. McCarty, K.F. Dissertation, Iowa State University, Ames, IA (1985).

35. Gorbunova, Yu.E.; Linde, S.A. Soviet Physics-Doklady (1979) **24(3)**, 138.

36. Stenhagen, E.; Abrahamson, S.; McLafferty, F.W.; eds. *Atlas of Mass Spectral Data* (Interscience Publishers, New York, 1969).

37. Centi, G.; Trifiro, F. Catalysis Today (1988) **3**, 151.

38. Pepera, M. A.; Callahan, J. L.; Desmond, M. J.; Milberger, E. C.; Blum, P. R.; Bremer, N. J. Journal of the American Chemical Society (1985) **107**, 4883.

SUMMARY AND RECOMMENDATIONS

Overall Summary

Labeling specific active sites in both β-$VOPO_4$ and $(VO)_2P_2O_7$ model catalysts provided the opportunity to probe the role of lattice oxygens in the selective and nonselective oxidation of C_4 hydrocarbons over these catalysts as never before. As these catalysts and their vibrational spectra have been well characterized by other workers, the reliability of the labeling assignments made based on this information is high. This information was exploited to not only resolve selectivity and nonselectivity of specific lattice oxygens for the conversion of n-butane to maleic anhydride, but also to associate specific lattice oxygens with mechanistic steps. While the specific sites and the role of those sites involved varied from β-$VOPO_4$ to $(VO)_2P_2O_7$, this was accomplished for both catalysts.

For β-$VOPO_4$, it was found that, once properly activated, n-butane (actually a reactive activated form of n-butane) is constrained to react with a P-O-V associated with the equitorial plane of the vanadyl octahedra, forming an adsorbed furan like species. This species can then react with two adjacent P-O-V sites which bridge two parallel infinite vanadyl octahedral chains. This species can then desorb as maleic anhydride.

For $(VO)_2P_2O_7$, it was found that similar, yet quite different phenomenon

occur. n-Butane is activated on a pair of vanadyl octahedra and, if the activation is selective (perhaps resulting in a particular "selective" orientation), the resulting adsorbed species is constrained in such a manner that it then reacts with one of two V-O/^{P}-V sites associated with the vanadyl octahedral pair. This adsorbed furan like species then reacts with neighboring P-O-V sites to form a species which desorbs as maleic anhydride. The P-O-P pyrophosphate bond is never disturbed.

The initial interaction of the other species studied with the catalytic surface is quite different than that of n-butane. Different lattice oxygens have different functions from species to species. As a result, conclusions drawn about the mechanism of n-butane conversion to maleic anhydride on these catalysts based simply on the observation of the interaction of these other species with the catalyst may not be valid. These conclusions may be based on reactions the activated n-butane species is constrained from participating in, even though the resulting adsorbed species may be closely related to the gaseous species being used. This definite difference must be taken into consideration.

Nonselective oxidation occurs by several paths, and may be simply the result of a statistical probability. Maleic anhydride combusts mainly at V=O sites, yet all other "intermediates" utilize a wide variety of lattice oxygens, not to mention the possibility of highly reactive adsorbed oxygens, in the formation of carbon oxides.

Finally, evidence was presented that clearly shows that β-$VOPO_4$ is not the V(V) species formed in the V(IV) $\rightarrow$ V(V) oxidation/reduction couple on the surface of $(VO)_2P_2O_7$. Formation of β-$VOPO_4$ domains on the surface of $(VO)_2P_2O_7$ would require the disruption of the P-O-P species in $(VO)_2P_2O_7$, and this is never observed.

Recommendations for Future Work

The information provided by this investigation coupled with a thorough knowledge of the recent VPO related literature provides fertile ground for the development of future investigations. Particularly, any aspect of the reactive surface of $(VO)_2P_2O_7$ that can be investigated should be investigated by any means possible. The following is a list of specific suggestions along those lines.

1. Evidence exists in the literature that active and selective oxygens on the surface of $(VO)_2P_2O_7$ may be associated with hydroxyl groups. The concentration and type of surface hydroxyl may depend on the reaction atmosphere and catalyst history, specifically the partial pressure of H_2O the catalyst has been exposed to. Surface hydroxyls on zeolite catalysts have been characterized and quantified by solid state ^1H NMR techniques. A similar approach could be taken with VPO catalysts, although several factors may complicate the spectra. The paramagnetic nature of V(IV) species, low surface area and the existence of strongly adsorbed hydrocarbons, which could also contain protons, are the major challenges to be overcome. These complications do not necessarily preclude the observation of surface hydroxyls though. The type and quantity of surface hydroxyls should be correlated (if possible) to catalyst history, and catalytic activity and selectivity. Steam treatments could be used to force additional hydroxyls onto the catalytic surface. Also, deuterated species could be used to determine the origin of different hydroxyls.

2. It has been suggested throughout the literature that strongly adsorbed carbonaceous species exist on the surface of working VPO catalysts. These species may alter the catalytic properties of the surface, or may simply be a

precursor to carbon oxides. This species, along with other adsorbed intermediates, may be best characterized by solid state ^{13}C NMR techniques. Also, the present investigation shows that the adsorbed reactive intermediate produced from n-butane is much different than those produced by other C_4 hydrocarbons. These differences could also be explored with solid state NMR.

3. Selective and nonselective lattice oxygen species have been identified in the present work. Industrial catalysts quite often contain dopants or supports which could alter these sites. These effects should be investigated using techniques developed in this work.

4. The selective oxidation of n-butane to maleic anhydride on VPO catalysts is limited to the near surface region of the catalyst. Thin films of these catalysts should then exhibit behavior similar to the bulk catalyst. Additionally, thin film work would allow better characterization of the near surface layers, such as ^{18}O labels in surface lattice sites. Thin films could be characterized by x-ray diffraction, laser Raman spectroscopy and FTIR. The surface sensitive technique of pulse modulated Fourier transform infrared reflection adsorbtion spectroscopy (PM-FTIRRAS) holds particular promise as a probe of the catalytic surface. Information on the nature and orientation of adsorbed species, as well as the nature of the working catalyst can be obtained by utilizing this technique. Additionally, by putting a thin film of VPO catalyst over a thin film of support, such as TiO_2 or SiO_2, support/catalyst interactions can be investigated. The thin films could be made either by sputtering vanadium and phosphorus in the presence of oxygen or by chemical vapor deposition using $VOCl_3$ and $POCl_3$.

5. Once the characteristics of VPO thin films are understood, the difference in paraffin verses olefin interaction with this catalyst surface could be exploited and the possibility of using these materials as thin film gas sensors could be explored.

ADDITIONAL REFERENCES CITED

1. Centi, G.; Trifiro, F. Catalysis Today (1988) **3**, 151.
2. Malow, M. Hydrocarbon Processing (1980) **11**, 149.
3. Mars, P.; van Krevelen, D. W. Chemical Engineering Science: Special Supplement (1954), 41.
4. Pepera, M. A.; Callahan, J. L.; Desmond, M. J.; Milberger, E. C.; Blum, P. R.; Bremer, N. J. Journal of the American Chemical Society (1985) **107**, 4883.
5. Centi, G.; Trifiro, F.; Ebner, J. R.; Franchetti, V. M. Chemical Reviews (1988) **88(1)**, 55.
6. Cavani, F.; Centi, G.; Trifiro, F. Journal of the Chemical Society, Chemical Communications (1985), 492.
7. Gleaves, J. T.; Ebner, J. R.; Kuechler, T. C. Catalysis Reviews, Science and Engineering (1988) **30(1)**, 49.
8. Moser, T. P.; Schrader, G. L. Journal of Catalysis (1985) **92**, 216.
9. Wenig, R. W.; Schrader, G. L. Journal of Physical Chemistry (1986) **90**, 6480.
10. Ostroushko, V. I.; Kernos, Yu. D.; Ioffe, I. I. Neftekhimiya (1972) **12(3)**, 95.
11. Morselli, L.; Riva, A.; Trifiro, F.; Emig, G. La Chimica E L'Industria (1978) **60(10)**, 791.
12. Ai, M.; Bountry, P.; Montarnal, R. Bulletin de la Societe Chimique de France (1970) **8–9**, 2775.
13. Ai, M. Bulletin of the Chemical Society of Japan (1970) **43(1)**, 3490.
14. Varma, R. L.; Saraf, D. N. Journal of Catalysis (1978) **55**, 361.
15. Escardino, A.; Sola, C.; Ruiz, F. Aneles de Quimica (1973) **69**, 385.
16. Wohlfhart, K.; Hofmann, H. Chemie Ingenieur Technik (1980) **52(10)**, 811.

17. Hodnett, B. K.; Permanne, Ph.; Delmon, B. Applied Catalysis (1983) **6**, 231.

18. Wustneck, N.; Wolf, H.; Seeboth, H. Reaction Kinetics and Catalysis Letters (1982) **21(4)**, 497.

19. Centi, G.; Fornasari, G.; Trifiro, F. Journal of Catalysis (1984) **89**, 44.

20. Hodnett, B. K.; Delmon, B. Applied Catalysis (1985) **15**, 141.

21. Centi, G.; Manenti, I.; Riva, A.; Trifiro, F. Applied Catalysis (1984) **9**, 177.

22. Morselli, L.; Trifiro, F.; Urban, L. Journal of Catalysis (1982) **75**, 112.

23. Ai, M. Journal of Catalysis (1981) **67**, 110.

24. Wenig, R. W.; Schrader, G. L. Journal of Physical Chemistry (1987) **97 (1)**, 1911.

25. Wenig, R. W.; Schrader, G. L. Journal of Physical Chemistry (1987) **91 (22)**, 5674.

26. Centi, G.; Trifiro, F.; Busca, G.; Ebner, J. R.; Gleaves, J. T. In *Proceedings of the Ninth International Congress on Catalysis*, Calgary, 1988 (The Chemical Institute of Canada: Ottawa, Ontario, Canada, 1988) **4**, 1538.

27. Puttock, S. J.; Rochester, C. H. Journal of the Chemical Society Faraday Transactions 1 (1986) **82**, 3033.

28. Szakacs, S.; Wolf, H.; Mink, G.; Bertoti, I.; Wustneck, N.; Lucke, B.; Seeboth, H. Catalysis Today (1987) **1**, 27.

29. Kruchinin, Y. A.; Mishchenko, Y. A.; Nechiporuk, P.P.; Gel'bshtein, A. I. Kinetica i Kataliz (1984) **25(2)**, 369.

30. Busca, G.; Centi, G.; Trifiro, F.; Lorenzelli, V. Journal of Physical Chemistry (1986) **90**, 1337.

31. Puttock, S. J.; Rochester, C. H. Journal of the Chemical Society Faraday Transactions 1 (1986) **82**, 2773.

32. Centi, G.; Golinelli, G.; Trifiro, F. Bicentenary Catalysis (1988), 191.

33. Wenig, R. W.; Schrader, G. L. Industrial Engineering Chemistry Fundamentals (1986) **25**, 612.

34. Haber, J. Serwicka, E. M. Reaction Kinetics and Catalysis Letters (1987) **35(1-2)**, 369.

35. Hodnett, B. K.; Delmon, B. Industrial Engineering Chemistry Fundamentals (1984) **23**, 465.

36. Martini, G.; Trifiro, F.; Vaccari, A. Journal of Physical Chemistry (1982) **86**, 1573.

37. Cavani, F.; Trifiro, F.; Vaccari, A. In *Adsorption and Catalysis on Oxide Surfaces*; Che, M., Bond, G. C., Eds. (Elsevier:Amsterdam, 1985), 287.

38. Zazhigalov, V. A.; Zaitsev, Y. P.; Belousov, V. M.; Wustneck, N.; Wolf, H. Reaction Kinetics and Catalysis Letters (1984) **24(3–4)**, 375.

39. Kung, H. H. Industrial Engineering Chemical Product Research and Development (1986) **25**, 171.

40. Matsuura, I. In *Proceedings, Eighth International Congress on Catalysis* (Berlin, 1984), Dechema: Frankfurt au Main, 1984; **IV**, 473.

41. Haber, J. In *Proceedings, Eighth International Congress on Catalysis* (Berlin, 1984), Dechema: Frankfurt au Main, 1984; **IV**, 276.

42. Fricke, R.; Jerchekewitz, H. G.; Lischke, G.; Ohlmann, G. Zeitscrift fuer Anorganische und Allgemeine Chemie (1979) **448**, 23.

43. Centi, G.; Trifiro, F. Journal of Molecular Catalysis (1986) **35**, 255.

44. Contractor, R. M.; Sleight, A. W. Catalysis Today (1988) **3**, 175.

ACKNOWLEDGMENTS

I would like to thank Dr. Glenn Schrader for his guidance in this challenging area of research. His timely advice often provided the inspiration required to complete such an endeavor. I would also like to thank the E. I. duPont de Nemours Corporation for providing me with personal financial support for the past four years.

Additionally, I would like to thank the various coworkers that have put up with me over the last four years and two months. MEE, SJF, KAO, CGO, RPT, JSC, YNC, and SNK – I've learned more from you guys than you will probably ever realize. I'm particularly indebted to Mark Ekman (MEE) for keeping my entropy production under control these last few months. I wish you all the best of luck in your future endeavors.

I would like to thank my parents–in–law, Bob and Myrna Schneller, for the support they have given Laurie and me these past four years.

I would like to give special thanks to my parents, Neil and Vivian Lashier for their unconditional love and support. They made me realize that when things get tough, giving up is not an option.

Although she will not be able to read this for a few years, I would like to thank my daughter Chelsea. She came along just in time to help me maintain my sanity and keep things in proper perspective.

Finally and most of all, I would like to thank my wife Laurie. In addition to typing most of this dissertation, you helped me gain the confidence I needed to achieve this and many other goals. Putting it simply, you are the best.